OIL SPILL PROCESSES AND MODELS

EE-8

Oil Spill Processes and Models

by

D. Mackay
I. Buist
R. Mascarenhas
S. Paterson
Department of Chemical Engineering
University of Toronto
Toronto, Ontario

This report is the result of a contract let under a research and development program of the Environmental Impact Control Directorate. This unedited version is undergoing a limited distribution to transfer the results to people working in related research.

It has not undergone rigorous technical review by the Environmental Impact Control Directorate and it does not necessarily reflect the views and policies of Environment Canada.

Any comments concerning its content should be directed to:

Research and Development Division
Environmental Emergency Branch
Environmental Impact Control Directorate
Environmental Protection Service
Environment Canada
Ottawa, Ontario
K1A 1C8

December, 1980

ABSTRACT

The results of an experimental and theoretical research program into the behaviour of oil spills are presented. A novel set of equations has been assembled to describe the kinetics of oil spreading into thin and thick slicks with ultimate area stabilisation. Agreement with reported spill area-time data is satisfactory. A computational procedure has been devised to permit the degree of evaporation of a given oil (characterised by its API gravity or ASTM D86 temperature-volume distillation curve) to be calculated for any evaporative exposure expressed in terms of temperature, area, time and wind speed. The procedure also permits oil property changes such as viscosity, density, solubility and volatility to be quantified. An equation is proposed to describe the kinetics, stability and viscosity of water-in-oil emulsion formation on the sea surface as a function of sea state and oil slick properties. Experimental work on emulsion formation in a small-scale, variable turbulence apparatus is described. A brief review of natural dispersion processes is presented and equations are derived to quantify this process as a function of sea state and oil-slick thickness. Experimental results from a 6 metre long wind wave tank are described.

The results of this and other work are capable of being combined into an oil spill behaviour model, the structure of which is described.

FOREWORD

This study was carried out at the University of Toronto under contract from the Environmental Emergency Branch of the Department of Fisheries and Environment, Ottawa. Dr. S.L. Ross was the scientific authority.

RESUME

TABLE OF CONTENTS PAGE

1. INTRODUCTION

This report describes work which has been undertaken in 1978 at the University of Toronto as part of the Arctic Marine Oil Spill Program. The general objective has been to undertake experimental and theoretical studies with a view to understanding more fully the various processes which occur when oil is spilled on water, particularly in the colder waters of the Canadian Arctic. It is believed that the successful development and deployment of oil spill countermeasures is predicated on having available in advance a satisfactory understanding of oil behaviour in the arctic marine environment. The abilities to burn, boom, disperse or pick up oil are very dependent on properties such as the oil density, viscosity, thickness and volatility and it is only by being able to predict the rates of processes such as evaporation or dispersion that these properties can be estimated.

Oil spills are subject to a complex array of physical, chemical and biological processes as is illustrated in Figure 1.1. These processes alter the oil and partition it between the atmosphere, water surface, ice, water column, sediment and shore in an only partially predictable manner. Figure 1.2 is a speculative attempt to assemble a mass balance for oil over a period of 1000 days on a logarithmic time scale. Obviously, spills vary considerably depending on oil type and prevailing weather conditions, but Figure 2 is regarded as representing a reasonably typical spill. It should be emphasised that some of the values are quite speculative - particularly those for sedimentation.

Those seeking to understand oil spills thus face two problems. First is quantification of the various individual spill processes such as evaporation or dispersion. In many cases, our present predictive ability is inadequate and proven equations which can express rates are not available. Second, the various processes occur simultaneously and often interact in an only partially predictable manner. For example, a thick oil spill which rapidly forms stable water-in-oil emulsions (mousse) may evaporate, spread, or disperse very slowly. A thin spill will evaporate faster and may be subject to faster dispersion into the water column with little opportunity to form emulsions. The only satisfactory approach to elucidating and quantifying such interacting processes is to assemble an oil spill model in which all processes are considered. Such a "behaviour" model is different in character from oil spill "trajectory" models which seek to identify the location of the oil versus time for a given geographical setting and which may only treat oil alteration processes in a cursory manner.

The approach taken in this work has been to undertake a number of spill process studies and then assemble the resultant findings into a spill behaviour model. The processes which have been examined are as follows.

Spreading

A literature review has demonstrated the inadequacy of existing models, particularly in their ability to quantify oil spreading into thick and thin patches. A new set of spreading equations has been assembled which satisfactorily describe the behaviour of a number of actual spills in this respect. It is based on Fay's surface tension-viscous equation for thin slick spreading and on a viscous-inertial equation for thick slick spreading within the thin slick. Allowance is made for the thick slick to "feed" the expanding thin slick up to the point at which the thick slick has insufficient volume to support the feeding process. The spill then tends to stabilise in area. Provision is made to permit the slick to adopt an ellipsoidal shape rather than just circular, the degree of elongation being wind speed dependent. The equations are presented in finite difference form and are solved numerically rather than in analytical form. Comparisons of predicted (fitted) and actual spill areas are presented. No experimental work on spreading was undertaken.

Evaporation and Oil Property Changes

Previous work in our group has been extended to devise a procedure in which an oil, characterised by its ASTM D86 distillation temperature-versus-volume curve (which is usually available or can be estimated from its API gravity using published data) is assigned a simulated ten-component composition which will yield the same (computed) distillation curve. A curve of fraction of oil mass remaining versus "evaporative exposure" (a combination of time, area per unit oil volume and mass transfer rate) is then computed enabling the evaporative characteristics to be quantified for any time, temperature, spill area and wind conditions. In addition, the oil property changes with time can be calculated, including density, solubility, volatility and viscosity. It is believed that these property changes will be of considerable relevance to the success of countermeasures efforts.

This work has been largely computational in nature. Computer plotted graphical outputs are provided.

Water-in-Oil Emulsion (Mousse) Formation

To our knowledge, there are no equations available for predicting the rate of mousse formation or for characterising the stability of the mousse. From a consideration of the likely mechanism of the process, we have suggested a suitable equation which appears to have the correct properties. There are two parameters, one which quantifies the rate of water incorporation into the oil and a second which determines the stability. Using these two parameters, it is believed that most oils can be characterised with respect to mousse formation. In addition, a quantitative expression is derived and fitted to available data to give viscosity as a function of water content.

Some experimental work has been undertaken in a small-scale variable turbulence apparatus and in a 6 metre long wind wave tank in an attempt to verify this approach.

Natural Dispersion of Oil in Water

No quantitative expressions for this process are available. By observing the mechanism of natural and chemically induced dispersion in the small-scale test apparatus and in the wind-wave tank,we have suggested a suitable equation in which "permanent" and "temporary" dispersions are quantified in terms of oil droplet particle size. A brief literature review is presented which draws heavily on work contracted by the U.S. Coast Guard The equations purporting to quantify the process are derived and experimental data presented in support of the findings. It is suggested that the dispersion rate is very dependent on slick thickness, thin slicks being very rapidly dispersed compared to thick slicks.

Oil Spill Model

These individual processes can be combined into an overall oil - spill behaviour model which is similar in character to that published previously by Mackay and Leinonen (1977) (EPS-3-EC-77-19). The structure of the model is described.

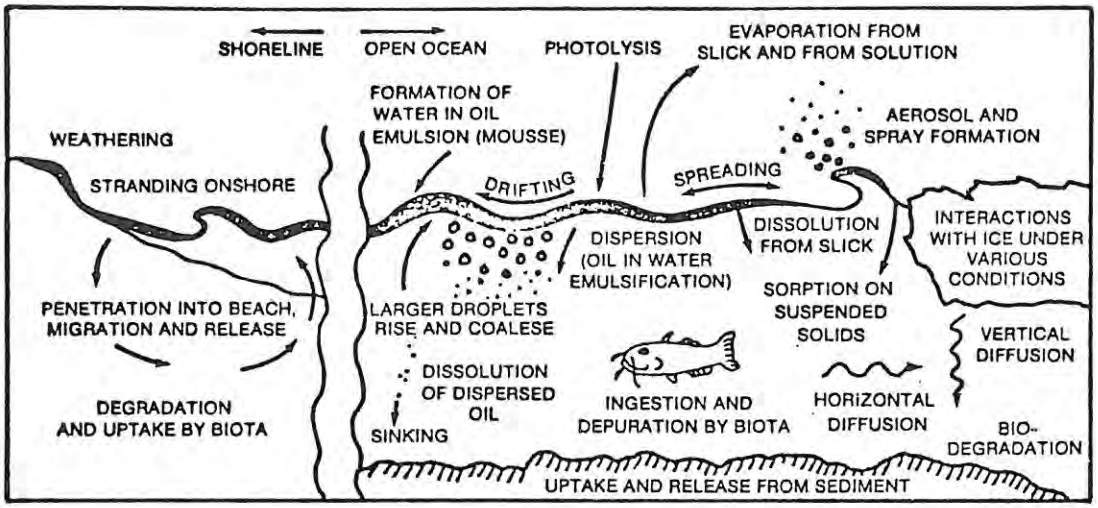

Figure 1.

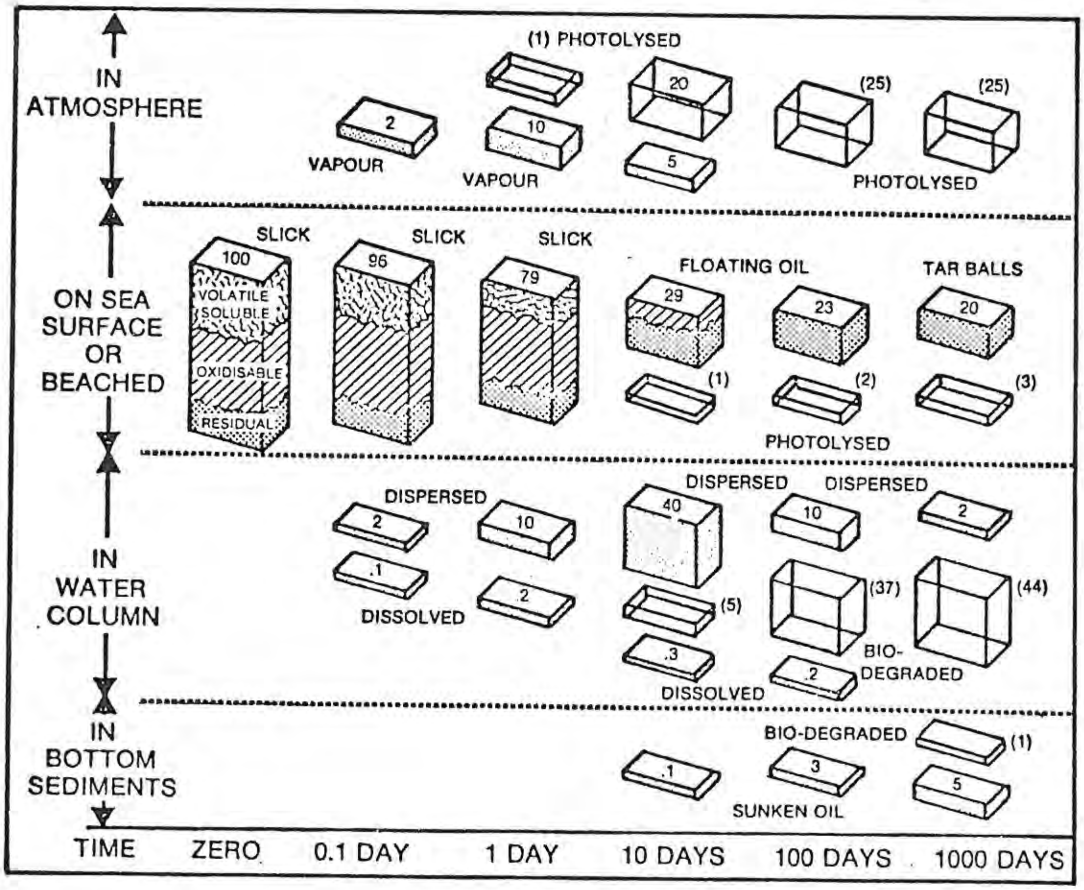

Figure 2.

2. SPREADING

When oil is discharged on a water surface, it spreads as a result of gravitational (hydrostatic) and surface forces, against which are exerted inertial, viscous (and occasionally surface) forces. The balance between these forces determines the oil behaviour. Actual spreading behaviour is difficult to predict accurately since oils vary in composition, there may be composition changes during spreading, the water surface is rarely calm, wind may drive the oil across the surface and there is an observed tendency for the oil to separate into thin and thick patches which behave differently.

The usual approach to quantifying oil spreading is to postulate an equation which expresses area as a function of time, with oil volume and properties inserted as constants. The studies by Fay (1971) of laboratory spreading led to postulation of three "spreading laws" applicable to inertial, viscous and surface-tension regimes. These laws or equations give a satisfactory representation of real spill data when fitted with appropriate coefficients. In addition, Fay (1971) suggested a maximum slick area (as a function of volume) to account for cessation of spreading. Fay's equations have been widely used in spill models.

In this work, we take a slightly different approach by suggesting that equations in finite difference form, solved numerically are fundamentally more suitable for incorporation in oil-spill models. This introduces a greater degree of complexity but there is no doubt that this complexity is necessary to accomodate the actual complex behaviour of oil spills. In particular, in this work we attempt to quantify the spreading into thick and thin patches, make provision for evaporation and natural dispersion (oil-in-water emulsion formation) and allow for discharges over variable time periods.

Derivation of the Equations

It is suggested that a volume of oil is discharged (either continuously or instantaneously) on to the water surface into a "thick" patch of oil, that is typically 1 mm to 1 cm deep. This patch spreads and is surrounded by a "thin" patch of oil, that is typically 1 to 10 μm thick which is spreading under the influence of surface forces. Generally, the thick patches are 10 to 20% of the thin patch area, as observed by Jeffrey (1973) and JBF (1976).

Spreading of the thin patch is quantified by a power relationship to area rather than time. Observations of total spill area as a function of time suggest relationships of the form

$$\text{area} \propto \text{time}^n$$

where n is 3/2 according to Fay (1973) or 2/3 according to Blokker (1964). The JBF (1976) and Cormack (1978) data suggest a value close to unity. It seems likely that very large spills will exhibit behaviour consistent with the 3/2 power because of their large perimeters. It may not be possible to ascertain the power accurately because of dispersion and evaporation processes and the inherent difficulties of measuring areas. Adopting the 3/2 power and converting to finite difference form yields the area (A m^2) and time (t s) equations

If $\quad A = Kt^{1.5}$

then $\quad dA/dt = 1.5Kt^{0.5} = 1.5K(A/K)^{0.33} = K'A^{0.33}$

or $\quad \Delta A = K A^{0.33}\Delta t$

This form is more convenient since the area change is calculated as a function of actual area, rather than time.

It is assumed that the thin slick is of constant thickness (1 μm) and as it spreads it "draws" oil from the thick patches. This continues until the thick patches reach a critical thickness below which they are unable to "feed" the thin slick. This effect is included by inserting a factor in the above equation of the form exp(-C/Z) where C is a constant (m) and Z is the thickness (m) of the thick slick. For example, if C is set at 0.0001 m this factor has a value of 0.9 when Z is 0.001 m (thus having little effect), a value of 0.37 when Z is 0.001 m (thus having a significant effect on spreading, and a value of 0.01 (thus essentially stopping spreading) when Z is 0.000022m. The constant C thus stops spreading of the thin slick when the thick slick decreases to approximately C m in depth. The final equation is then (in computed form with constants AK and CK)

$$\Delta A_{TN} = (AK)A_{TN}^{0.33}\exp(-CK/Z)\Delta t$$

The volume in the thin slick is calculated as area (A_{TN}) times thickness (1 μm)

For spreading of the thick slick, Fay's (1971) gravity-viscous equation is modified to give and an equation for area as a function of thickness and area rather than volume (V m^3) and time as follows

If $\quad A = KV^{0.67}t^{0.5}$

then $\quad dA/dt = 0.5KV^{0.67}t^{-0.5} = 0.5KV^{0.67}(KV^{0.67}/A)$

$\quad\quad = K'V^{1.33}A^{-1} = K'Z^{1.33}A^{0.33}$

where Z is the thickness (m) and equals V/A. In finite difference form this is written in terms of a constant BK giving the change in area A_{TK} as

$$\Delta A_{TK} = (BK)Z^{1.33}A_{TK}^{0.33}\Delta t$$

Allowance must also be made for the loss in volume (and area) from the thick slick as a result of the oil drawn into the thin slick. This volume is (A_{TN} x 0.000001) m^3, resulting in an area decrease of the thick slick of (0.000001 A_{TN}/Z) m^2. THe final equation for thick slick area change is thus

$$\Delta A_{TK} = BKZ^{1.33}A_{TK}^{0.33}\Delta t - (0.000001\Delta A_{TN}/Z)$$

The area of the thick slicks will thus tend to increase initially, level off as the feeding process drains more oil from the thick slick then it falls until Z reaches a value close to CK when spreading tends to cease. At this time natural dispersion will have a dominating effect.

The calculation is started by taking an initial volume of oil (during the first time increment) and arbitrarily assuming that it adopts a "thick" area equivalent to an oil depth of 2 cm and a thin area eight times this value. Fortunately, subsequent areas are not sensitive to this assumption except if very large volumes are discharged instantaneously, a condition which rarely if ever occurs.

Allowance can be made for continuous discharges by adding to the thick patch a volume increment at each appropriate time increment, thus increasing the thickness rather than the area. In addition, volumes of oil can be removed from each slick as a result of evaporation, dissolution and dispersion. These losses cause a decrease in volume in both thick and thin slicks and it is assumed that the areas shrink accordingly. This shrinkage is usually less than the spreading area increase early in the spill; thus there is still net growth but later it may actually cause both slicks to shrink. This does not imply that the spill occupies a smaller overall area but rather that it breaks up into several isolated patches, distributed over an area and separated by water. This is consistent with actual spill observations in which the slick "breaks up" before finally disappearing.

The final spreading equations are given in computer form in Appendix 1.

Simulation of Actual Spill Data

Data in the form of spill volumes discharge times, areas and times were gathered from a number of sources as listed in Table 2.1 and the area-time plot in Figure 2.1 was prepared. Various values of AK, BK and CK were tested and optimum values were selected as follows

AK = 1.0
BK = 150
CK = 0.0015

It is emphasised that this selection does not represent a precise regression since the area data are very variable, with some obvious inconsistencies such as large volume spills giving smaller areas. It is believed that oil type, wind and currents may play significant roles in determining spreading areas and these variables are not presently included. Provision could be made to include them as follows. AK presumably depends linearly on the oil-water spreading coefficient. Data obtained by Hollinger (1974) suggests the spreading rate is dependent on wind speed and he introduced a factor to account for this effect. BK is probably inversely related to oil viscosity. It may also be desirable to include an estimate of slick shape, i.e. allowing it to be ellipsoidal rather than circular, the ratio of the dimensions being wind speed dependent.

The general area-time behaviour as predicted by the equations is illustrated in Figure 2.1, on which is presented the JBF (1976) data. The equations predict a steady increase in area of both slicks with a tendency for the thin slick area to "level off" as the thick slick reaches CK in thickness.

To illustrate the effect of varying the constants AK, BK, and CK and the spill discharge time, a series of computations was undertaken for a discharge volume of 100 m^3.

Figure 2.2 shows that the effect of varying AK is (as expected) to alter the thin slick area, the thick slick area being little affected. Figure 2.3 shows that BK affects both areas and in particular their ratio. High values of BK tend to give larger thick slicks and smaller thin slicks. Figure 2.4 shows that decreasing CK reduces the slope of the area-time curve and effectively determines the upper limit to thin spill area. As expected when CK is zero, the spill increases indefinitely in area at a slope of approximately 1.33 on a log-log plot. Figure 2.5 shows the effect of discharging the oil over various time periods. This dependence can not be included in the simple area-time equations such as those of Fay.

Figure 2.6 is a composite prediction of the behaviour of a series of spills ranging in volume from 1 m^3 to 10^5 m^3. The discharge times were arbitrarily selected using the equation below. Plotted on this figure are data compiled by Hoult (1972) and the line corresponding to the simple area-time relationship presented in that paper.

$$\text{Spill Duration (s)} = 1000\ (\text{Volume Spilled } (m^3))^{0.5}$$

It is apparent that this three constant set of equations has the capacity to describe oil-spill behaviour with acceptable accuracy. The abilities to discriminate between thick and thin spills and to simulate cessation of spreading are particularly useful. Approximate values of the constants have been obtained but more accurate determination must await the provision of more area-time-volume-oil property data (particularly viscosity and spreading coefficient) with measurement of wind and water surface conditions. Data as produced recently by JBF (1976) are particularly valuable in this regard and it is hoped that more such data will be forthcoming. It should also be noted that the spreading phenomena can not be adequately quantified unless the simultaneous processes of evaporation, dissolution, water-in-oil and oil-in-water emulsion formation can be quantified simultaneously. The proposed equations have sufficient flexibility that these processes could be included in an overall oil-spill mathematical description or model.

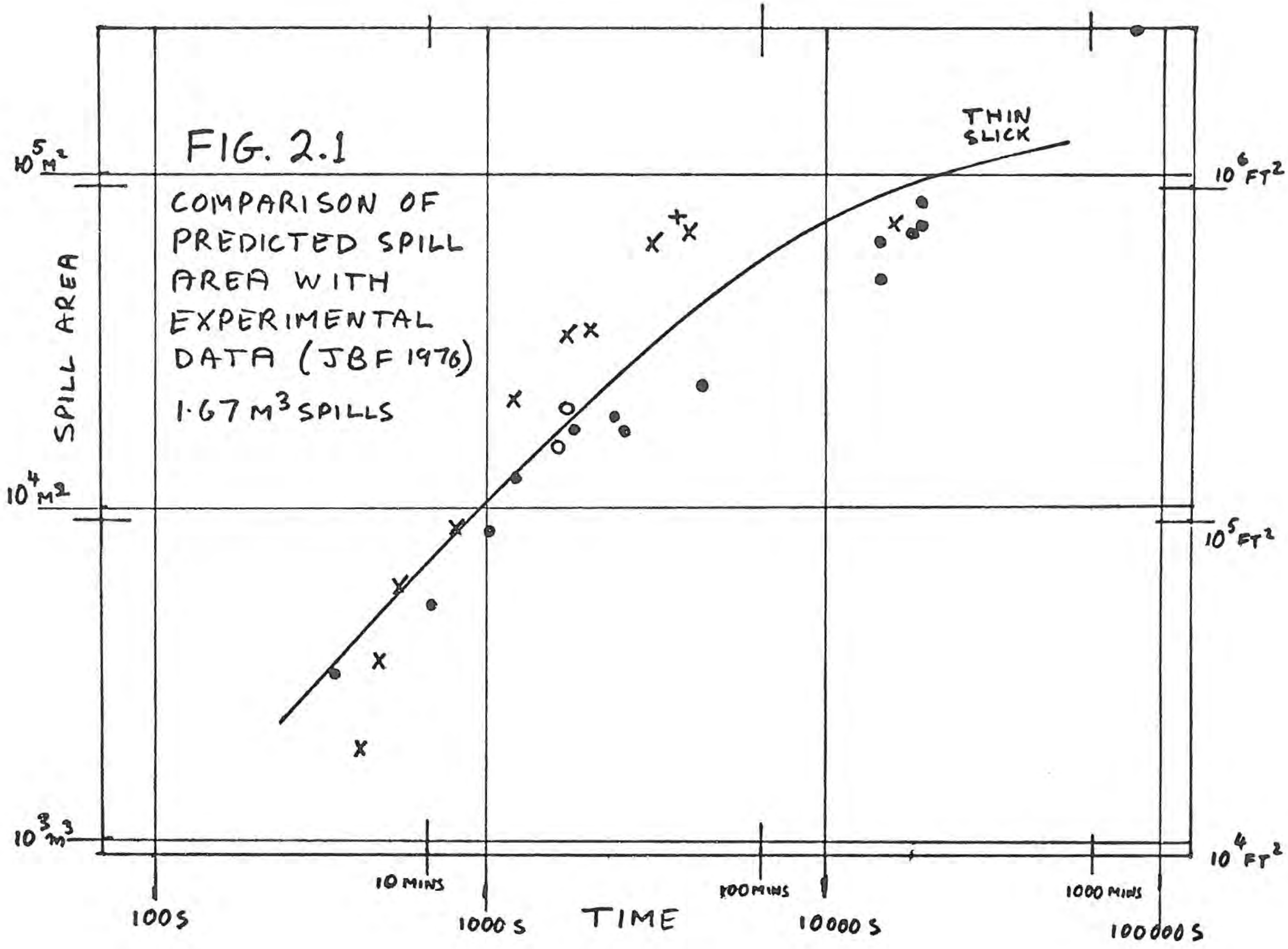

FIG. 2.1

COMPARISON OF PREDICTED SPILL AREA WITH EXPERIMENTAL DATA (JBF 1976)

1·67 M^3 SPILLS

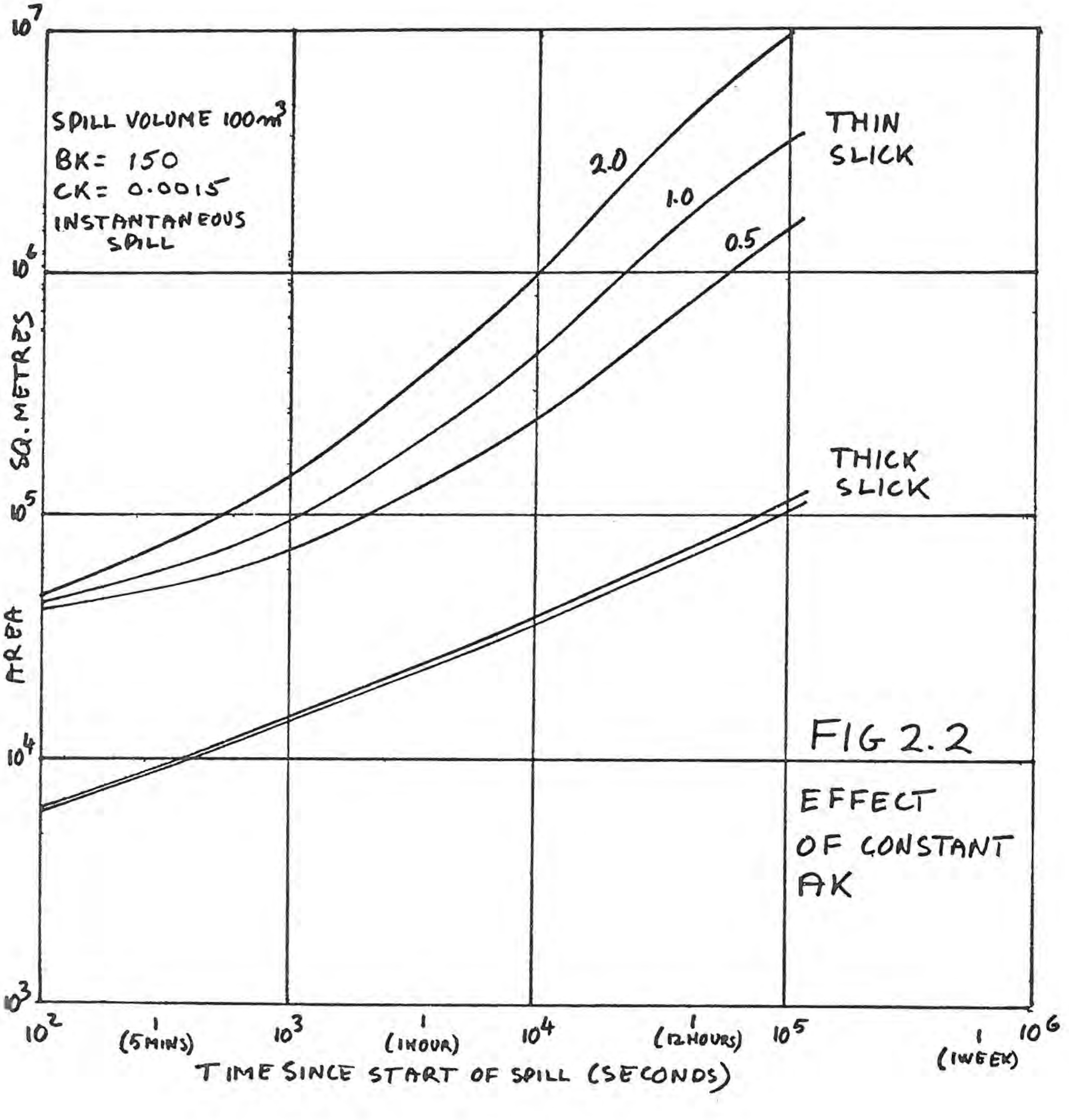

FIG 2.2

EFFECT OF CONSTANT AK

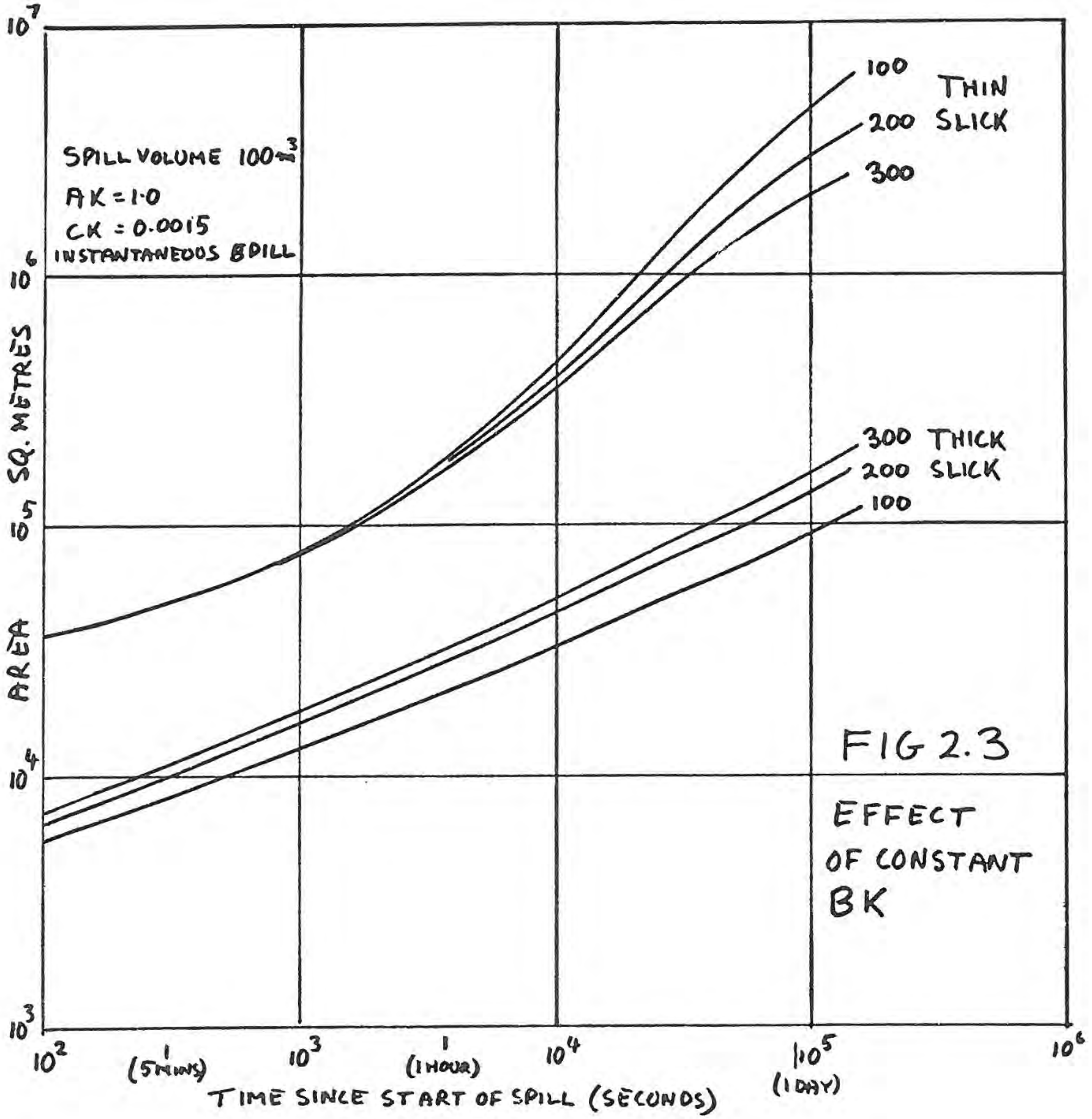

FIG 2.3

EFFECT OF CONSTANT BK

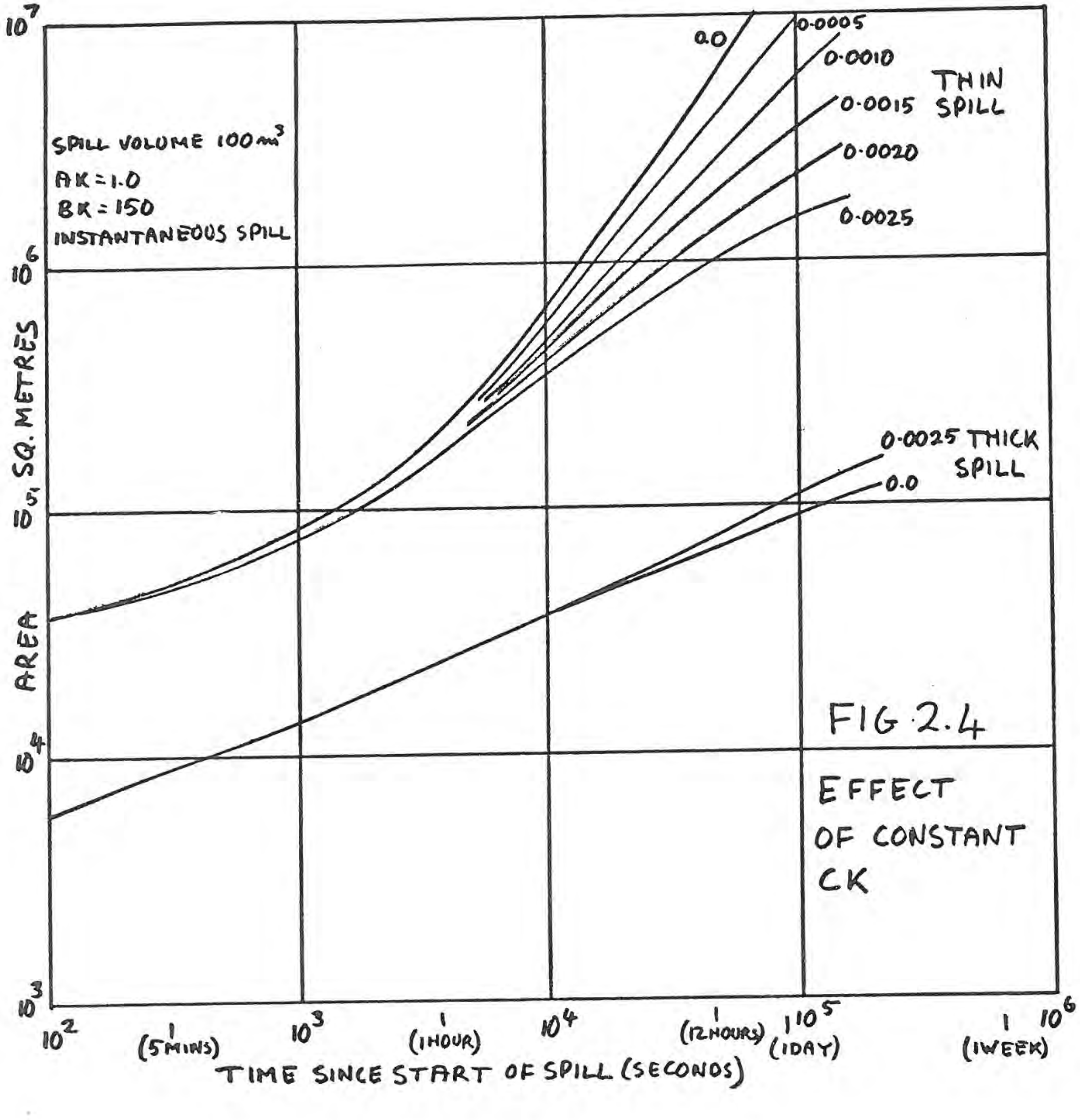

FIG 2.4

EFFECT OF CONSTANT CK

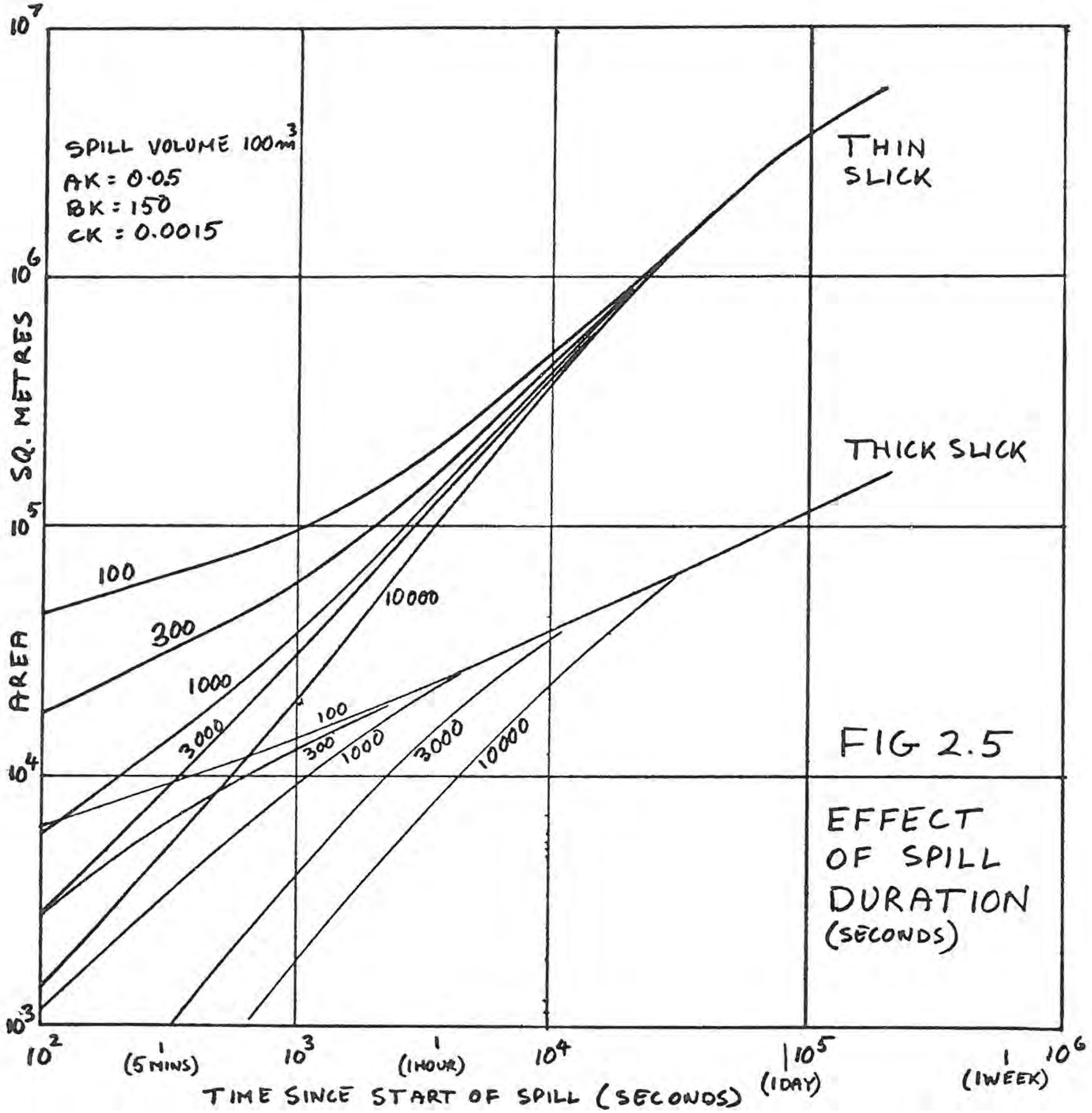

FIG 2.5

EFFECT OF SPILL DURATION (SECONDS)

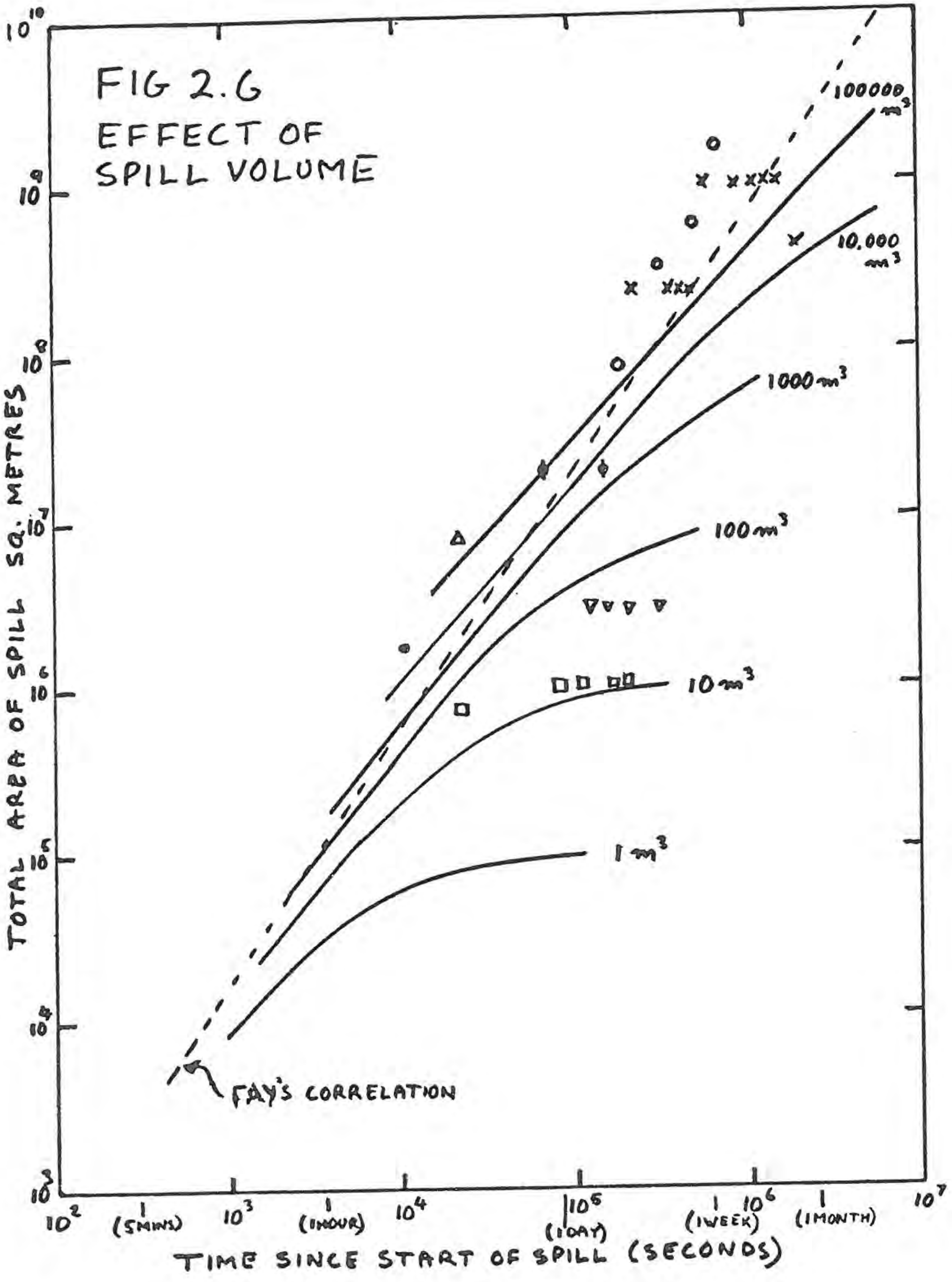

FIG 2.6
EFFECT OF SPILL VOLUME

3. Evaporation and Oil Property Changes*

Mathematical models of the behaviour of spills of crude oil and petroleum products must include quantitative expressions for the major physical processes which occur during weathering such as evaporation, dissolution, dispersion, water-in-oil emulsion (chocolate mousse) formation, spreading and even in some cases, sinking. The rates of these processes depend on the oil's physical properties such as volatility, aqueous solubility, density, viscosity and surface tension, all of which change as the oil weathers. Quantification of these physical processes can be accomplished by defining a multi-component hydrocarbon mixture with physical properties similar to that of a crude oil or product and allowing the mixtures's composition to change with time as a result of the weathering process, for example, the loss of volatiles as a result of evaporation. The use of the actual oil composition is unlikely to be feasible since most oils are exceedingly complex and rarely can a high proportion of the compounds present be identified and quantified.

An oil or petroleum product is usually characterized by a set of physical property measurements including density (often as API gravity), volatility (usually as a standard distillation curve of temperature vs. volume fraction distilled), viscosity at a standard temperature, aqueous solubility and pour point. These properties vary with the fraction of the oil evaporated and with temperature.

For oil evaporation calculations, Goodwin et al.(1976) have suggested using a plot of the mass fraction of the oil remaining as a function of the total volume of oil vapour evaporated during differential evaporation. Nadeau and Mackay (1977) compiled graphs of this type to permit easy and fast evaporation calculations. Mackay et al. (1975) have also discussed the characterization of northern crude oils and Mackay and Shiu (1975) have discussed the solubility of oil as a function of weathering.

The approach used here is that described by Leinonen and Mackay (1977) and Yang and Wang (1977) who postulated a mixture of hydrocarbons of known physical properties which can be adjusted to give an oil of predictable behaviour similar to that of a crude oil or petroleum product.

In this work, we postulate the 10 component mixture given in Figure 3.1. The hydrocarbons selected are representative of a group of hydrocarbons of similar properties. For example, n-decane represents C_9 - C_{11} alkanes, phenanthrene represents the polynuclear aromatic hydrocarbons and the inert hydrocarbon represents asphaltenes. Physical property data were obtained as follows:

Vapour pressures were obtained in the form of Antoine equation constants from Zwolinski and Wilhoit (1971) for all hydrocarbons except naphthalene and phenanthrene for which the appropriate vapour pressure is that of the sub-cooled liquid. This vapour pressure is estimated from the vapour pressure, enthalpy of vapourization and triple point of these hydrocarbons. By assuming the enthalpy of vapourization to be independent of

---

* Subsequent work in this area has been described in two reports "The Physical Properties of Fresh and Weathered Crude Oils" which is in press with Environment Canada, Arctic Marine Oilspill Program and "Calculation of the Evaporation Rate of Volatile Liquids" presented to the 1980 National Conference on Control of Hazardous Material Spills, Louisville, Kentucky, published in the proceedings, p. 361. It should be noted that this latter publication was not proof read and thus contains some errors. A correct version is available from the author.

temperature, the vapour pressure of the sub-cooled liquid at temperatures lower than the triple point can be estimated using a 2 constant Antoine equation which is essentially the integrated Clapeyron Clausius equation. Fortunately, accurate vapour pressures are not necessary since these hydrocarbons are quite involatile. For the inert hydrocarbon, zero volatility was assumed.

For mixtures, the total vapour pressure and the equilibrium vapour composition were calculated assuming Raoult's Law to hold, i.e.,

$$P_i = x_i P^S i, \quad P_T = \Sigma P_i \quad \text{and} \quad y_i = P_i / P_T$$

where P_i is the partial pressure, x_i is the liquid mole fraction, y_i is the vapour mole fraction, $P^S i$ is the saturation vapour pressure (all of component i) and P_T is the total pressure.

Densities were obtained from the API Technical Data Book and their temperature dependence correlated using the equation below.

$$\rho = a - bt$$

Here ρ is density (g/cm^3), t is temperature (^oC) and a and b are constants. A common value of b was assumed for all hydrocarbons. For mixtures, the density was calculated by assuming additive volumes with zero volume mixing. For the inert component, a density of 1.0 g/cm^3 was assumed as a reasonable value for highly weathered crude oils. This density is, however, adjustable in the program by applying a variable factor.

Viscosities were obtained from the API Technical Data Book as a function of temperature using the equation below:

$$\mu = \mu_o \exp(K(1/T - 1/273))$$

where μ is viscosity (cP) at T (K) and μ_o is viscosity at 0^oC. K is a constant for all hydrocarbons.

This viscosity does not include the effect of water-in-oil emulsion formation nor is any allowance made for non-Newtonian behaviour. The viscosity of mixtures was calculated as recommended by Reed et al. (1977) using the equation below:

$$\ln \mu = \Sigma x_i \ln \mu_i$$

The pour point was arbitrarily assigned as being the temperature at which viscosity reached 1,000 cP based on the work of Wood (1971) on the viscosity and pour point of Prudhoe Bay and Norman Wells crude oil in which the pour points of -10°C and -40°C corresponded to viscosities of 4000 and 6000 cP extrapolated from higher temperature data using the above equation.

For aqueous solubilities, the data of Leinonen (1977) and Mackay and Shiu (1977) were used for the individual hydrocarbons. Mixture solubilities were calculated by assuming that the solubility is proportional to the mole fraction with a correction factor in the solubility of enhancement factor ε as discussed by Leinonen (1977) who showed that this enhancement factor is necessary in order to predict realistic solubilities. The ε_E values were obtained experimentally were as follows:

alkanes and cycloalkanes	$\varepsilon_E = 1.4$
aromatics	$\varepsilon_E = 2.2$
olefins	$\varepsilon_E = 1.8$

In order that the equations are consistent in predicting the true solubility of a pure hydrocarbon, it is necessary to force the enhancement factor ε to adopt a value of unity when the mole fraction is unity. This was done arbitrarily by expressing the factor as a function of component mole fraction x_i using the equation below.

$$\varepsilon = \varepsilon_E (1 - x_i) + x_i$$

The component solubilities S_i (g/m^3) were calculated from the pure component solubility using

$$S_i = S_o x_i \varepsilon$$

For sea water, the solubilities were reduced by a factor of 0.77 (Mackay and Shiu, 1975).

May, Wasik and Freeman (1975) have reported enthalpies of solution for aromatic hydrocarbons of approximately 6 to 10 kcal/mol. Using a value of 6.3 (for naphthalene), the effect of temperature on total solubility can be deduced as

$$S_T = S_{25} \exp(3150(1/298 - 1/T)$$

where S_{25} is the solubility at 25°C (298K) and S_T is the solubility at T K.

The program receives as input a temperature and the ten numbers of moles (one for each component) assigned by the user, and normalizes them such that the total mole fraction is unity. This permits the user to arbitrarily adjust one component concentration without adjusting the others. It then calculates the component properties at this temperature, calculates the volume and mass fractions of the oil, and calculates the mixture properties as illustrated in Figure 3.1.

It then calculates the isobaric distillation curve (ASTM D84) of temperature versus volume fraction, prints out the results and it can also plot the graph, if requested, and if plotting facilities are available. It is thus possible to match the computed distillation curve with an experimental curve and obtain better agreement by adjusting the number of moles of each component. This is particularly useful since it enables the user to compile a composition which will yield the same distillation curve and which will thus display the same general evaporation behaviour.

To facilitate the use of the program, a set of compositions was obtained which will reproduce the distillation curves presented as being typical of various gravity crude oils by Nelson et al. (1951, 1952). Figure 3.2 is a reproduction of Nelson's graph and Table 3.1 is a listing of the compositions which yield these curves.

Figure 3.3, 3.4 and 3.5 are isobaric distillation curves for three crude oils with the computed isobaric curves superimposed. Agreement is clearly satisfactory.

At this stage, the program has characterised the original oil properties. Some further adjustment is possible to obtain better agreement with physical properties as follows.

Oil density and viscosity are best adjusted by altering the inert component (10) density and viscosity. Total solubility depends primarily on the butane and toluene contents which can be adjusted. Since toluene and octane have similar vapour pressures "trading" one for the other alters solubility but not volatility. Pour point can be adjusted independently of viscosity by selecting a different pour point viscosity.

The next stage is to calculate the evaporation behaviour and the physical property changes which result from evaporation, for example, viscosity and density increase.

During oil spill evaporation, the conditions are nearly isothermal, rather than isobaric, thus it is necessary to calculate the isothermal (constant temperature, variable hydrocarbon partial pressure) characteristics. The most convenient form of this data is a plot of fraction of the oil remaining against "exposure to evaporation" which is essentially a combination of time, spill area and mass transfer rate, as controlled by wind speed. The program proceeds to undertake this distillation, which is essentially a mathematical description of evaporation from a pan of constant area and temperature. It calculates the mass, mole and volume fractions remaining and the oil physical properties.

These evaporation and physical property calculations are necessarily complex and time and space consuming. It is believed that, for modelling purposes, it is more efficient to de-couple evaporation from the rest of the program by calculating, in the actual spill, only the fraction of the oil remaining as a function of time and not the detailed compositions. This requires only the isobaric evaporation-exposure data at the system temperature, which is, of course, only one line or its equation. It is, therefore, useful to devise a correlation of that line from the evaporation program and include it in the separate oil spill program and that the incremental evaporation during a time step be calculated from that correlation. The new "fraction of oil remaining" can then be calculated and, if desired, the properties and composition of this oil can be calculated separately by consulting the evaporation program. The disadvantage of this approach is that it assumes that only evaporation causes oil composition changes. This is, however, a good assumption since dispersion does not affect the oil composition and dissolution is so slow that it has a negligible effect on composition.

The next section presents a detailed discussion of the concept of isothermal evaporation exposure.

Isothermal Evaporation Characteristics

An understanding of the physical significance of the isothermal, fraction remaining-exposure curve is essential for the successful use of the program. The plot illustrated in Figure 3.6 is of mass, mole or volume fraction remaining (as ordinate) against the total volume of oil vapour evaporated under differential evaporation conditions (as abscissa). This latter quantity is difficult to grasp conceptually but fortunately it has been shown to be identical to a more easily grasped concept, namely that of evaporation "exposure". This exposure is a product of three factors, time, area and evaporation mass transfer coefficient (Goodwin et al.(1976)).

The time variable t (s) is obvious, long times corresponding to long exposure. The area term A is defined as area per unit initial oil mass (m^2/kg). Obviously, for a given oil mass, larger areas cause faster evaporation and the change in oil mass is proportional to the area exposed to evaporation. The oil composition thus changes more rapidly. The mass transfer coefficient K has units of velocity (m/s) and can be regarded as the velocity with which molecules of evaporated oil move vertically away from the oil surface. In practice, it is controlled by the velocity and nature of turbulent eddies at the oil surface and by the rate of diffusion of oil vapour through a thin film of near stagnant gas in the boundary layer close to the interface. It can also be regarded as a diffusivity (m^2/s) divided by a diffusion path length (m).

Correlations are available for K as a function of wind speed, for example, Mackay and Matsugu (1973). Typical values range from 0.001 to 0.05 m/s. The product of these quantities, the group KAt has thus units of m^3/kg consistent with a vapour volume removed per unit mass of oil. It is referred to here as the evaporation exposure E.

If a real or simulated oil composition is available, it is relatively easy to calculate the rate of isothermal evaporation and prepare a curve of fraction remaining versus E. This is most easily done by taking an initial mass of 1 kg with a corresponding composition, assuming that a small fraction of the total (say 0.001 or n moles) is evaporated, calculating the composition of the vapour formed by a conventional Raoult's Law vapour-liquid equilibrium calculation as follows.

If the compositions and individual vapour pressures are x_i and $P^s{}_i$, then the individual partial pressures P_i, the vapour mole fraction y_i, and the total hydrocarbon partial pressure P_T are given by

$$P_i = x_i P^s{}_i, \quad P_T = \Sigma P_i, \quad \text{and } y_i = P_i/P_T$$

The composition of the evaporated increment and the new composition of the remaining oil can be calculated. Thus at one atmosphere total pressure (air and hydrocarbon), the vapour volume ΔV is nRT/P_T.

This calculation can be repeated, the volumes of vapour formed being summed to give the total volume differentially evaporated. This total volume is the "exposure" and has a unique value for every mass, mole, or volume fraction of oil remaining.

The relationship of this volume to the group KAt is apparent if one writes the mass evaporation equation for the same increment. If n moles are evaporated from a mass of 1 kg (initially) of area A (m^2), the mass flux equation is

$$n = KAP_T\Delta t/RT \quad \text{(moles)}$$

But the vapour volume formed ΔV is given by

$$\Delta V = nRT/P_T = KA\Delta t \quad (m^3)$$

If K and A are constant, the total volume obtained by summing the ΔV values must equal KAt where t is the sum of the Δt values.

If the desired plot is of mass fraction remaining versus KAt, it is necessary to include the additional factor (1000/molecular weight) to scale the volume up to that which would cause the same composition change in 1 kg of oil. This convention is more convenient since A is easily expressed as m^2 per kg of oil and in wind tunnel evaporation experiments mass is easily measured as a function of time as exposure.

A plot of fraction of mass remaining versus V or KAt thus contains the essential isothermal evaporation information about the oil. The curve can be readily deduced by a numerical integration (repetitive Raoult's Law) calculation Plots of this type are given in Figures 3.7, 3.8 and 3.9 for the three oils.

It may be useful to be able to calculate the oil vapour pressure P_T at any given degree of evaporation from this curve. Considering an initial mass of 1 kg with evaporation of n moles, the change in mass fraction remaining F, i.e. ΔF is nM where M is the molecular weight of the evaporating material. The corresponding change in V, i.e. ΔV is nRT/P_T thus $\Delta F/\Delta V$ or dF/dV is MP_T/RT. THe slope of the F,V line is thus proportional to the vapour pressure. Involatile oils such as heavy fuel oils or weathered crude oils will have very "flat" or near horizontal curves corresponding to very low vapour pressures, whereas lighter fuel oils will have steeper curves.

Mass Transfer Coefficient Correlation

It is suggested that the correlation developed by Mackay and Matsugu (1973) be used. This gives the mass transfer coefficient K_H (m/hr) as a function of wind speed U (m/hr), slick diameter X (m) and the dimensionless oil vapour Schmidt Number Sc as follows

$$K_H = 0.0292\, U^{0.78} X^{-0.11} Sc^{-0.67}$$

Sc is 2.7 for cumene evaporation, which gives a reasonable value. A typical slick diameter X is 100 m, but a precise value is not necessary since the power on X is small, a tenfold increase in X giving a reduction in K_H by a factor of only 1.29. Inserting these values for Sc and X gives

$$K_H = 0.0090\, U^{0.78} \text{ m/hr}$$

converting U to km/hr and K_H to m/s gives

$$K = 0.0055\, (U \text{ km/hr})^{0.78} \text{ m/s}$$

$$\text{or } K = 0.0015\, (U \text{ m/s})^{0.78} \text{ m/s}$$

Correlation of Exposure Data

It is useful to have the exposure/fraction remaining data in correlated form in order to enable it to be inserted into the spill model program. In postulating a correlating equation, it is noteworthy that a plot of fraction remaining versus log (exposure) is quite linear. It is thus desirable that the equation meets three criteria.

(i) the fraction remaining should be linearly or nearly linearly related to log (exposure).

(ii) at zero exposure (i.e. zero time), the fraction remaining should be unity,

(iii) at infinite exposure the fraction remaining should become the inert or non-volatile fraction.

An equation with these properties is

$$F_{vol} = (F - F_I)/(1 - F_I) = 1 - C \ln((E + B)/B)$$

where F_{vol} is the fraction of volatile hydrocarbons remaining, F is the fraction remaining, F_I is the fraction of inert hydrocarbons, E is the exposure (m^3/kg), C is a constant which is essentially the slope of the F_{vol} ln E curve, and B is a constant which corresponds to a very small exposure (approximately one minute evaporation) at which it is arbitrarily assumed that F is unity. A typical value of B is 0.02; however B depends on temperature and on the oil type.

This equation can be defined for mass, volume or mole fraction remaining, F_I and C changing accordingly.

It should be noted that initially when E is zero the log term becomes zero and F and F_{vol} become unity. When E is large, the right hand side passes through zero, F_{vol} becomes zero and F becomes F_I, i.e. evaporation is complete. This actually occurs when

$$E = B\{\exp(1/C) - 1\}$$

For a medium crude oil, a typical value of C is 0.060 for mass fraction, and 0.065 for volume fraction, and B is typically 0.02. The exposure for complete evaporation is thus typically 10^6 m^3/kg which is equivalent to 10 to 100 years and is thus outside the present range of interest.

For some oil mixtures, this simple equation may be inadequate and it is suggested that more complex versions may be devised of the form

$$F_{vol} = 1 - C_1 \ln((E + B)/B) - C_2\{\ln((E + B)/B)\}^2 \text{ etc.}$$

This equation provides a convenient method of including evaporation in an oil spill model. If at some time t after the spill the fraction remaining is F, it is necessary to calculate the new (smaller) fraction remaining $(F + \Delta F)$ at a time $(t + \Delta t)$. Differentiation of the F - E equation above and conversion into finite difference form yields

$$\Delta F = -\Delta E C(1 - F_I)/(E + B)$$

where $\Delta E = KA\Delta t$

The calculation of the spill specific area presents a slight problem in that the correct value is the area (m^2) per kilogram of original oil, not the existing partially weathered oil. For example, an oil of density 800 kg/m^3, if initially 1 cm thick would have a specific area of 0.125 m^2/kg when half the oil volume is evaporated under the constant area conditions (which apply to the F - E equation), the oil thickness will be reduced to 0.5 cm but the specific area is unchanged. It is thus necessary to calculate what the original oil thickness would have been at the prevailing area. This is the prevailing thickness divided by the volume fraction remaining (F_v).

In summary, the specific area A kg/m^2 can be calculated as either

F_v/{(Prevailing spill thickness (m))(Original oil density(kg/m^3))

or F_v/(Prevailing spill area (m^2))(Prevailing spill volume (m^3))(Original oil density (kg/m^2))

Another complication arises from the water content of the oil which is assumed to be zero in the evaporation equations. In an actual spill, the oil may absorb up to three times its volume of water as water-in-oil emulsion.

It is thus possible to incorporate into the model changing values of the mass transfer coefficient and the spill area. In summary, the procedure is as follows:

The state of the oil F is known from the previous iteration.

The corresponding value of E is calculated from a rearrangement of the F - E equation, namely

$$E = B\{\exp((1 - F)/(1 - F_I)C) - 1\}$$

ΔE is then calculated as the product of mass transfer coefficient, spill specific area and time increment.

ΔF is then calculated using

$$\Delta F = -\Delta EC(1 - F_I)/(E + B)$$

The new value of F is then $(F + \Delta F)$.

Separate evaporation calculations may be necessary for thick and thin oil slicks.

The program accepts an initial value of spill thickness (m) from which it calculates A, and a mass transfer coefficient K, which can be obtained from the correlation, and from the calculated exposure E estimates for each fraction of oil remaining the corresponding time t(s) as

$$t = E/KA$$

This evaporation time is printed out for each increment of evaporation. Also printed out is an "exposure function" which is useful for estimating the constant C. It is defined as EF where

$$EF = \ln((E + B)/B)$$

The slope of the F, EF line is thus the constant C.

Example

After a spill of 10000 m^3 of crude oil of original density 828 kg/m^3, it occupies an area of 10^6 m^2. From evaporation correlations C is 0.065 and B is 0.02 on a fraction volume remaining basis. The non-volatile fraction F_I is 0.238 (volume). The water content of the oil is 50% (volume). Evaporation has resulted in 19.5% (volume) loss, i.e. F_V the volume fraction remaining is 0.805. The prevailing mass transfer coefficient is 0.003 m/s. How much oil will evaporate in the next 277 seconds?

$$E = B\{\exp(1 - F)/(1 - F_I)C) - 1\} = 1.005\ m^3/kg\}$$

The spill volume is 8050 m^3 of oil plus 8050 m^3 water, i.e. 16100 m^3. The actual thickness is thus 1.61×10^{-2} or 1.61 cm but only 0.8 cm of this is oil.

The specific area A is thus either

$$0.805/(0.00805)(828) = 0.1207\ m^2/kg$$

or

$$0.805 \times 10^{-6}/(8050)(828) = 0.1207\ m^2/kg$$

the mass transfer coefficient is 0.003 and Δt is 277 thus

$$\Delta E = 0.003 \times 0.1207 \times 277 = 0.100$$

ΔF can thus be calculated as

$$\Delta F = -\Delta EC(1 - F_I)/(E + B) = 0.0048$$

and the new value of F is thus (0.8050 - 0.0048) or 0.8002 and the new oil volume is 8002 m^3, 48 m^3 having evaporated during the time increment.

If the molecular weight of the evaporating oil is 100 g/mol, this corresponds to approximately (48 x 828 x 1000/100) or 0.4 x 10^6 gmol or 0.4 gmol/m^2.

This mass flux is also $K\Delta P\Delta t/RT$ where K is the mass transfer coefficient, R is the gas constant and T is temperature, RT having a value of 0.024 atm.m^3/gmol.

It is thus possible to deduce that ΔP, the vapour pressure of the oil is

$$\Delta P = 0.4RT/K\Delta t = 0.011 \text{ atm}$$

which is a reasonable value for a fairly volatile crude oil which has been slightly weathered.

Example of Oil Property Change

The mixture described in Figure 3.1 was subjected to isothermal evaporation at 25°C. Figure 3.10 shows that the plot of volume fraction remaining and volume fraction of volatiles remaining is quite linear in the exposure function $\ln((E + 0.02)/0.02)$. The slope is -0.065, the value of the constant C. The value of B is essentially the value of ln E when a F versus ln E curve is exprapolated to an F value of unity. Its value does not strongly influence the correlation. At lower temperatures, the slope is less reflecting the lower vapour pressures. The approximate times for a 1 cm thick slick with a K of 0.003 m/s are also shown. This is a fairly volatile oil with 10% volume distilling before 93°C; thus this 10% is lost very rapidly, i.e. in the first 6 minutes. In practice, evaporative cooling and diffusion limitations would probably delay this fast initial evaporation somewhat.

The oil property changes are given in Figure 3.11. The density increases from 0.828 to 0.90 when 72% (volume) or 78% (mass) remain. This is in general agreement with results of Mackay et al. (1975) who determined that a Norman Wells Oil increased in density to 0.90 from 0.82 when 60% (mass) remain. The viscosity increases from 1.47 cP at 25°C to 40 cP when 58% (mass) remained Mackay et al. (1975) obtained a corresponding experimental viscosity for Norman Wells Oil of 80 cP but that oil had a higher initial viscosity. The solubility drops from its initial 42 mg/l (which consists largely of n-butane and toluene) to 10 mg/l when 20% (volume) is evaporated and to 1 mg/l at 30% evaporated reflecting the loss of toluene. This is in satisfactory agreement with the work of Mackay and Shiu (1975). The vapour pressure also drops rapidly at first from its initial 0.44 atm to a low value of 0.01 atm when 78% (volume) remains and then to 0.001 atm when 68% (volume) remains.

In general, the results appear to be entirely reasonable. Some refinement of the assumed compositions and of the hypothetical properties assigned to the inert component may be necessary to achieve a closer match between experimental and computed properties but this can be done easily by making suitable adjustments to the properties or the equations. The contribution of this development is thus not to give highly accurate properties but is rather to devise a method of calculating these properties by a mathematical procedure which is rigorous and represents the physical reality. Now that the method is developed, refinements are possible to give closer agreement between predicted and actual experimental data for crude oil properties and volatilization rates.

The figures presented in the following pages are representative of the three crude oils whose ASTM distillation curves are presented in Figures 3.3, 3.4 and 3.5. The figures give the fraction of volume remaining versus exposure function $\ln((E + B)/B)$.

In summary, the equations derived here provide a rigorous method of calculating the evaporation characteristics of hydrocarbon mixtures. The input data can be

(i) Actual compositions

(ii) ASTM isobaric distillation curves, either obtained experimentally or inferred from the Nelson compilation.

or (iii) Pan evaporation data, which are essentially isothermal distillation curves.

The most convenient form of the volatility data are regression coefficients B, C and F_I which apply at the given temperature. A simple equation has been proposed but more complex versions are certainly possible and may be desirable in some cases. It would be useful to have available values for these constants for various types of crude oils and petroleum products at relevant temperatures. The equations can be used to give evaporation behaviour in volume, mass or mole quantities (with differing constants) but generally volume quantities are probably preferred. The approach should be useful in calculating evaporation rates of any oil or product at any temperature, spill thickness or wind speed and in estimating the changing properties of the oils such as density, viscosity, pour point, vapour pressure and aqueous solubility. It may thus be useful to those devising oil-spill models and to those responsible for countermeasures development.

```
TEMPERATURE=25.00   DEGREES C
VISCOSITY=     1.47

MOLECULAR WEIGHT        58.       86.      114.      142.      170.      226.       92.      128.      178.      250.
NUMBER OF MOLES      0.23000   0.23000   0.15000   0.13000   0.10000   0.21000   0.01000   0.00500   0.00500   0.29000
MOLE FRACTION        0.16912   0.16912   0.11029   0.09559   0.07353   0.15441   0.00735   0.00368   0.00368   0.21324
MASS FRACTION        0.06411   0.09505   0.08218   0.08871   0.08170   0.22807   0.00442   0.00308   0.00428   0.34841
VOLUME FRACTION      0.09129   0.11973   0.09743   0.10127   0.09100   0.25069   0.00423   0.00250   0.00347   0.23840
DENSITY              0.58175   0.65775   0.69975   0.72575   0.74375   0.75375   0.86575   1.02025   1.02025   1.21075
VISCOSITY            0.08      0.15      0.27      0.49      0.85      2.23      0.22      2.23      2.23    339.77
SOLUBILITY          30.64413   2.77149   0.09870   0.00677   0.00037   0.00019   8.29749   0.25588   0.01041   0.0
VAPOUR PRESSURE      2.39696   0.19934   0.02239   0.00207   0.00015   0.00000   0.04506   0.00037   0.00000   0.0
PARTIAL PRESSURE     0.40537   0.03371   0.00247   0.00020   0.00001   0.00000   0.00033   0.00000   0.00000   0.0

OIL MIXTURE PROPERTIES

DENSITY                          0.82846
API GRAVITY                     39.29817
API GRAVITY AT 15 DEG C         37.72536
TOTAL VAPOR PRESSURE             0.44209
VISCOSITY                        1.47
SOLUBILITY                      42.08539
MEAN MOLECULAR WEIGHT          153.01
APPROXIMATE POUR POINT         -98.18
```

```
1 - N BUTANE
2 - N HEXANE
3 - N OCTANE
4 - N DECANE
5 - N DODECANE
6 - HEXADECANE
7 - TOLUENE
8 - NAPHTHALENE
9 - PHENANTHRENE
10 - INERT
```

Figure 3.1. Synthetic Mixture, Individual Component and Mixture Properties at 25°C.

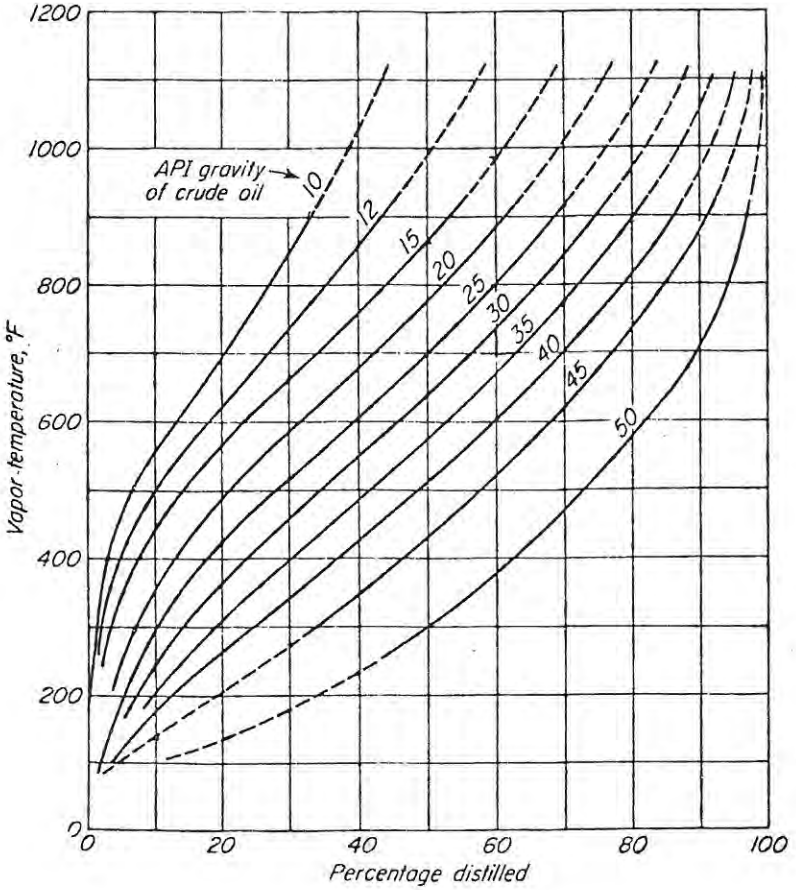

Figure 3.2. Compilation of Isobaric Distillation Curves for Crude Oils (Nelson 1958)

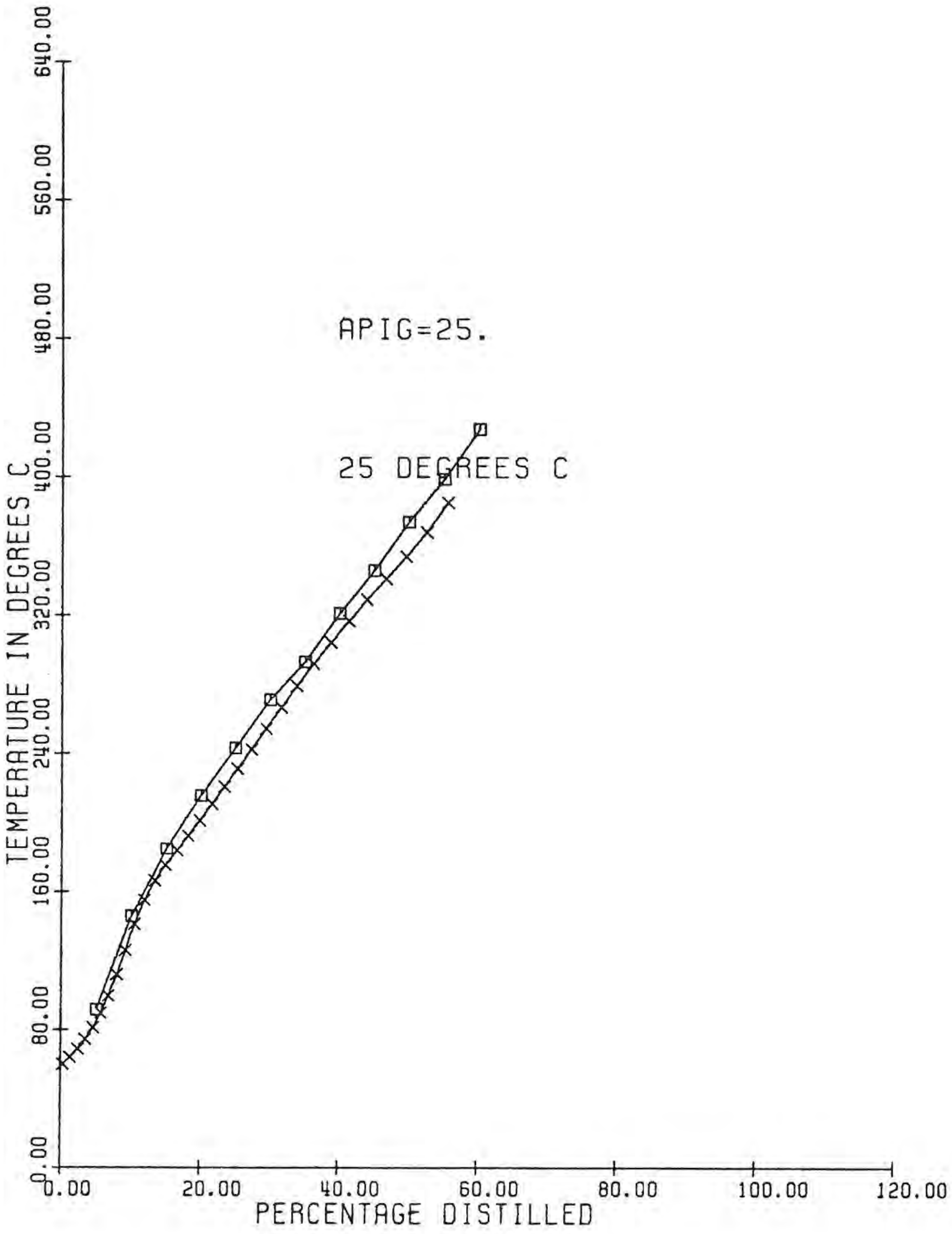

Figure 3.3. Plot of Isobaric Distillation Curve for Crude Oil (APIG=25) with Computed Isobaric Curve Superimposed

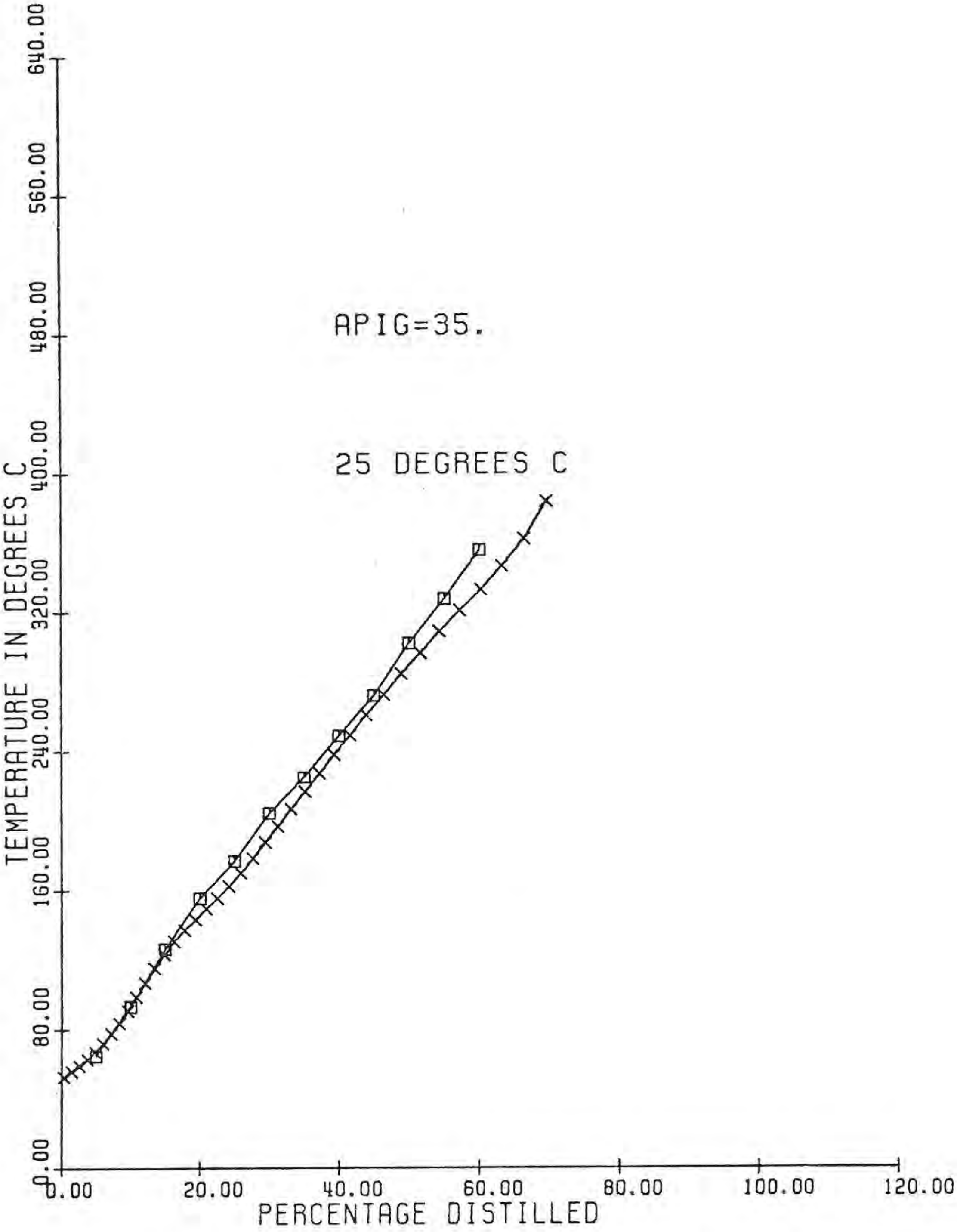

Figure 3.4. Plot of Isobaric Distillation Curve for Crude Oil (APIG=35) with Computed Isobaric Curve Superimposed

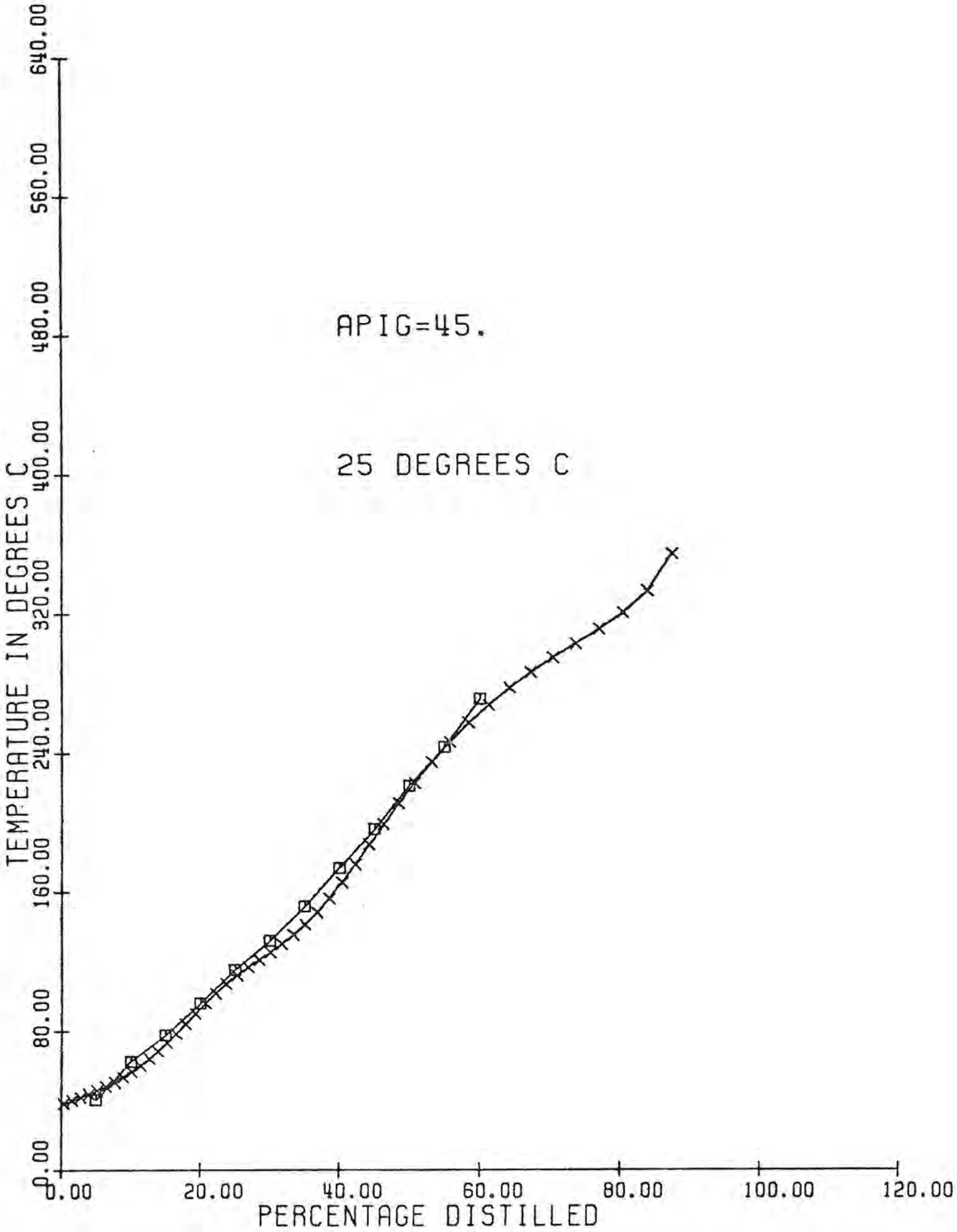

Figure 3.5. Plot of Isobaric Distillation Curve for Crude Oil (APIG=45) with Computed Isobaric Curve Superimposed

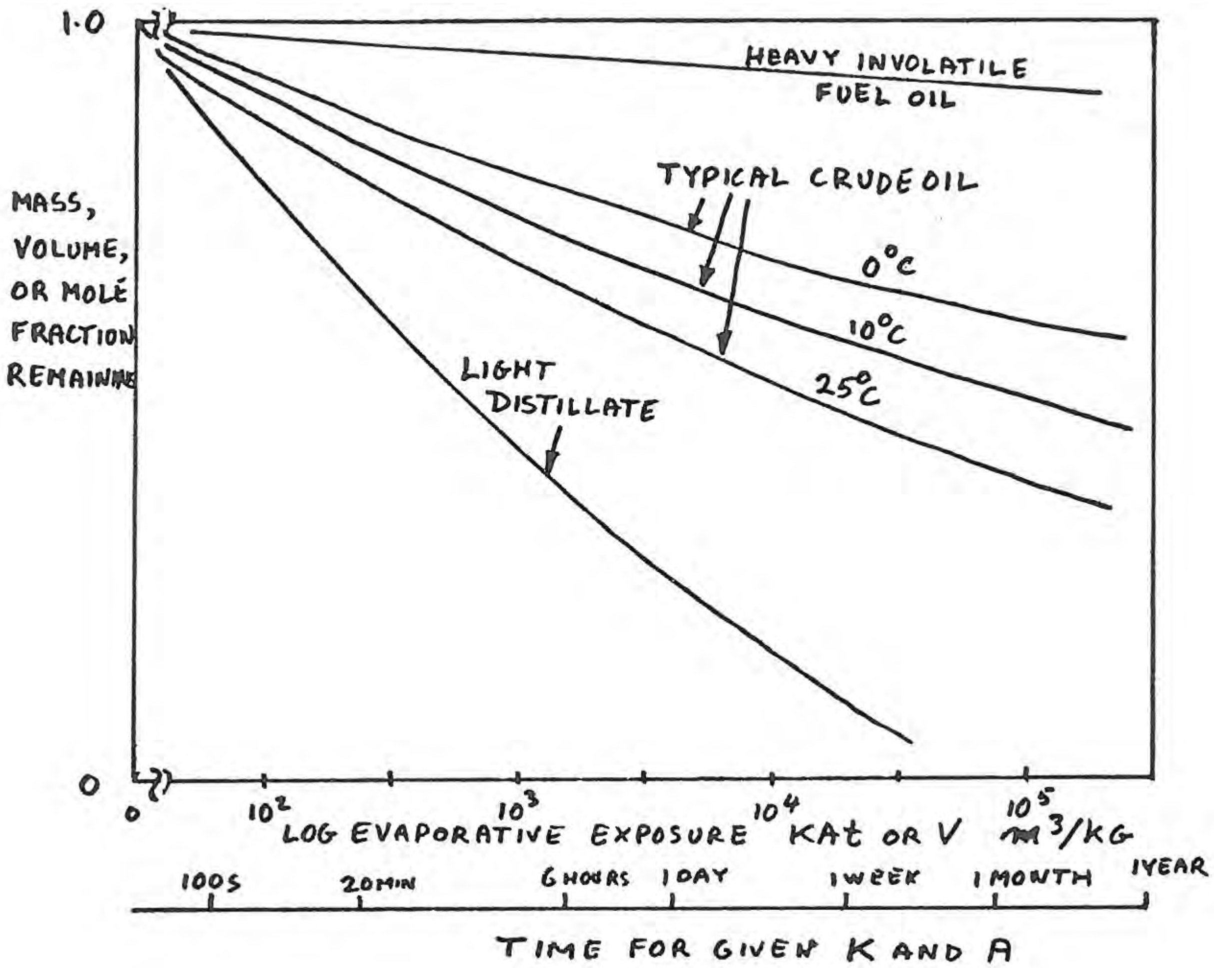

FIGURE 3.6 ILLUSTRATIVE FRACTION REMAINING VERSUS EXPOSURE DIAGRAM

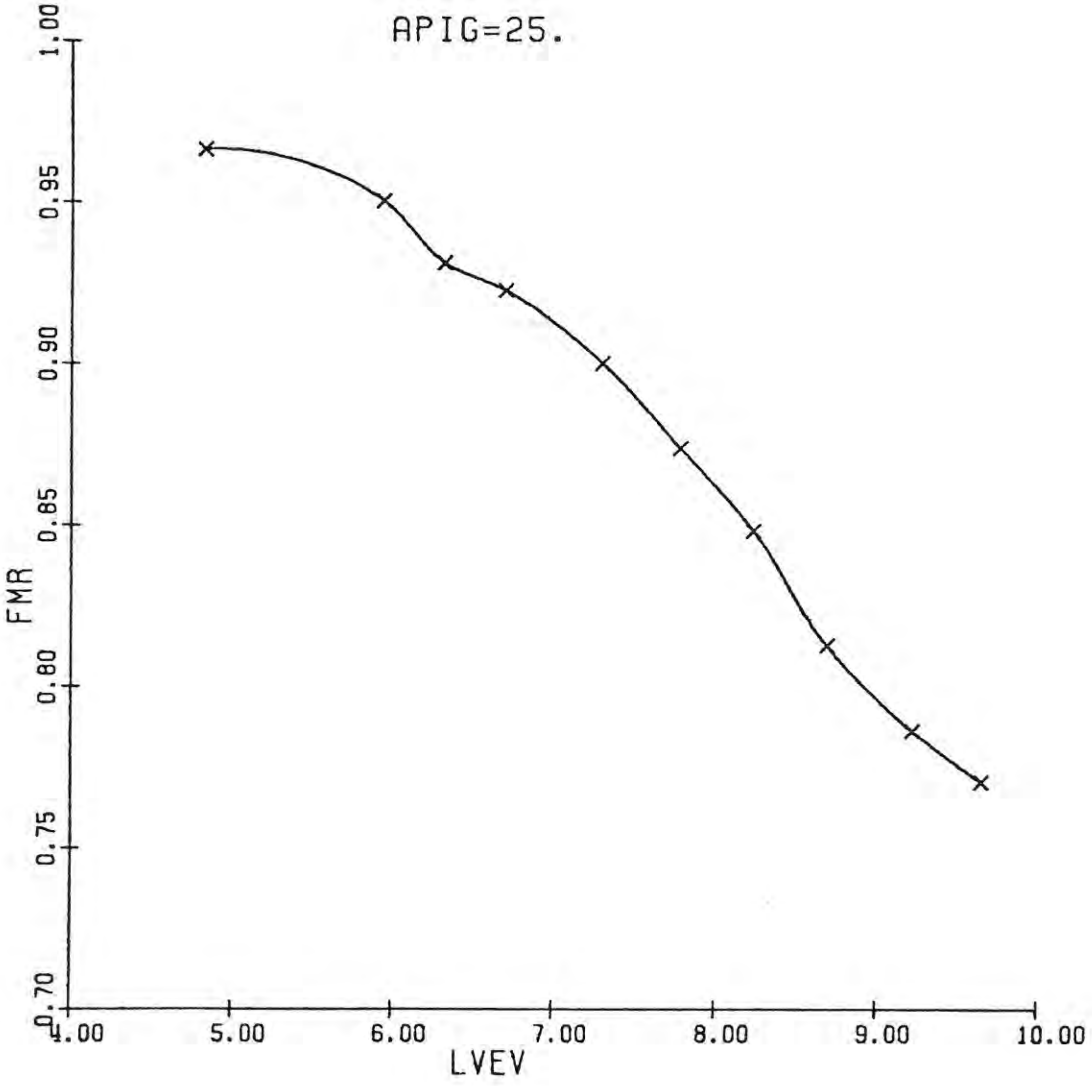

Figure 3.7. Plot of Fraction Remaining versus Exposure

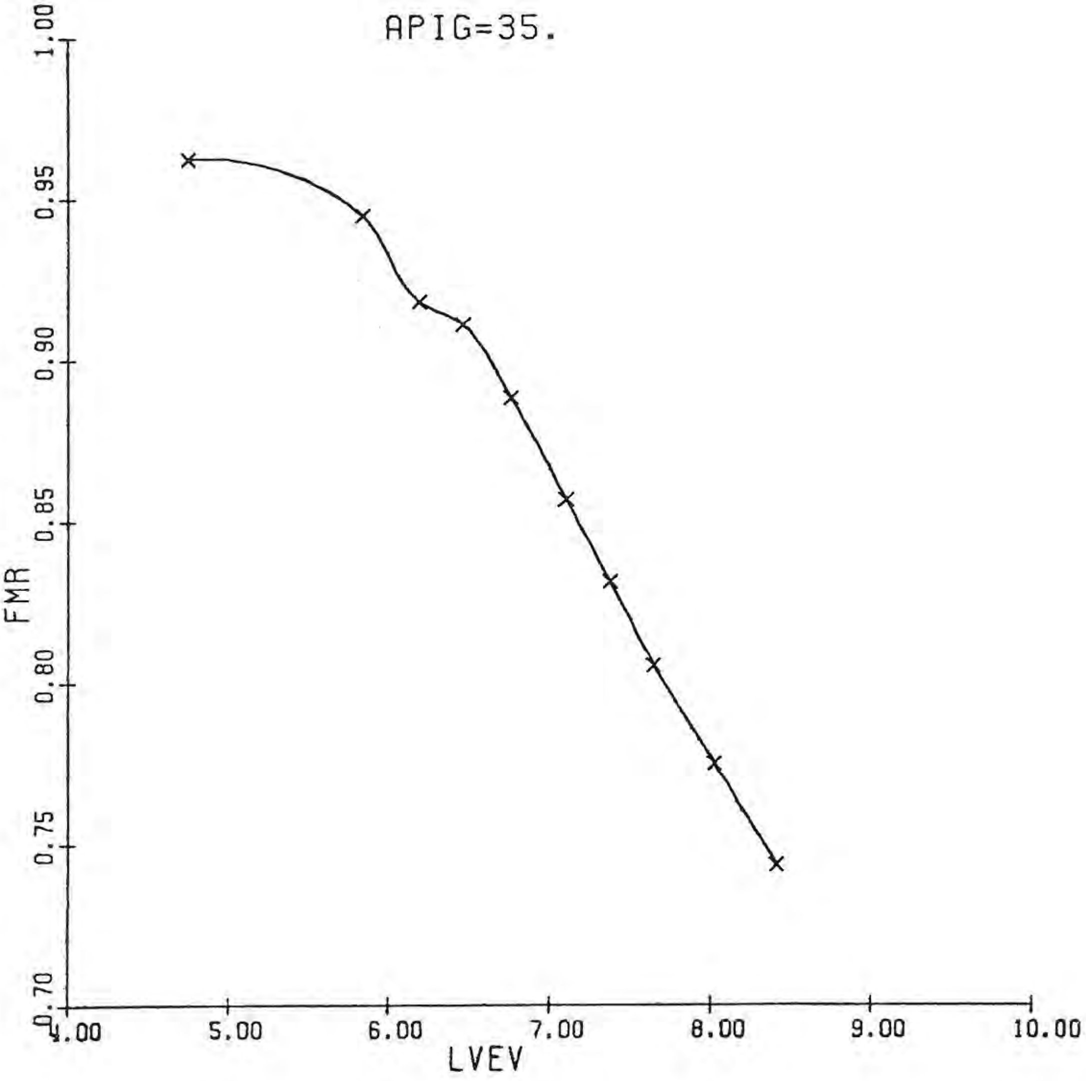

Figure 3.8. Plot of Fraction Remaining versus Exposure

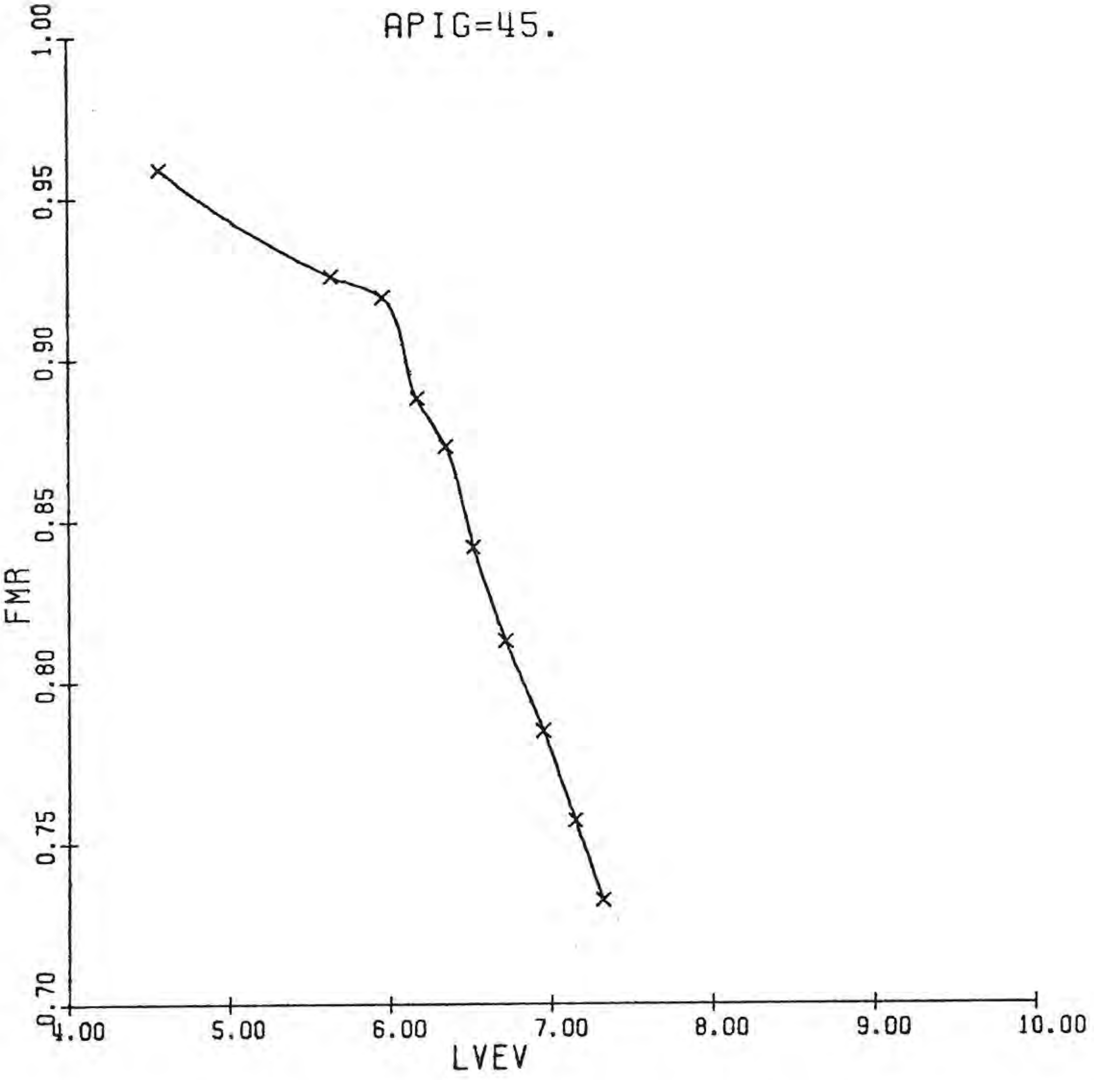

Figure 3.9. Plot of Fraction Remaining
versus Exposure

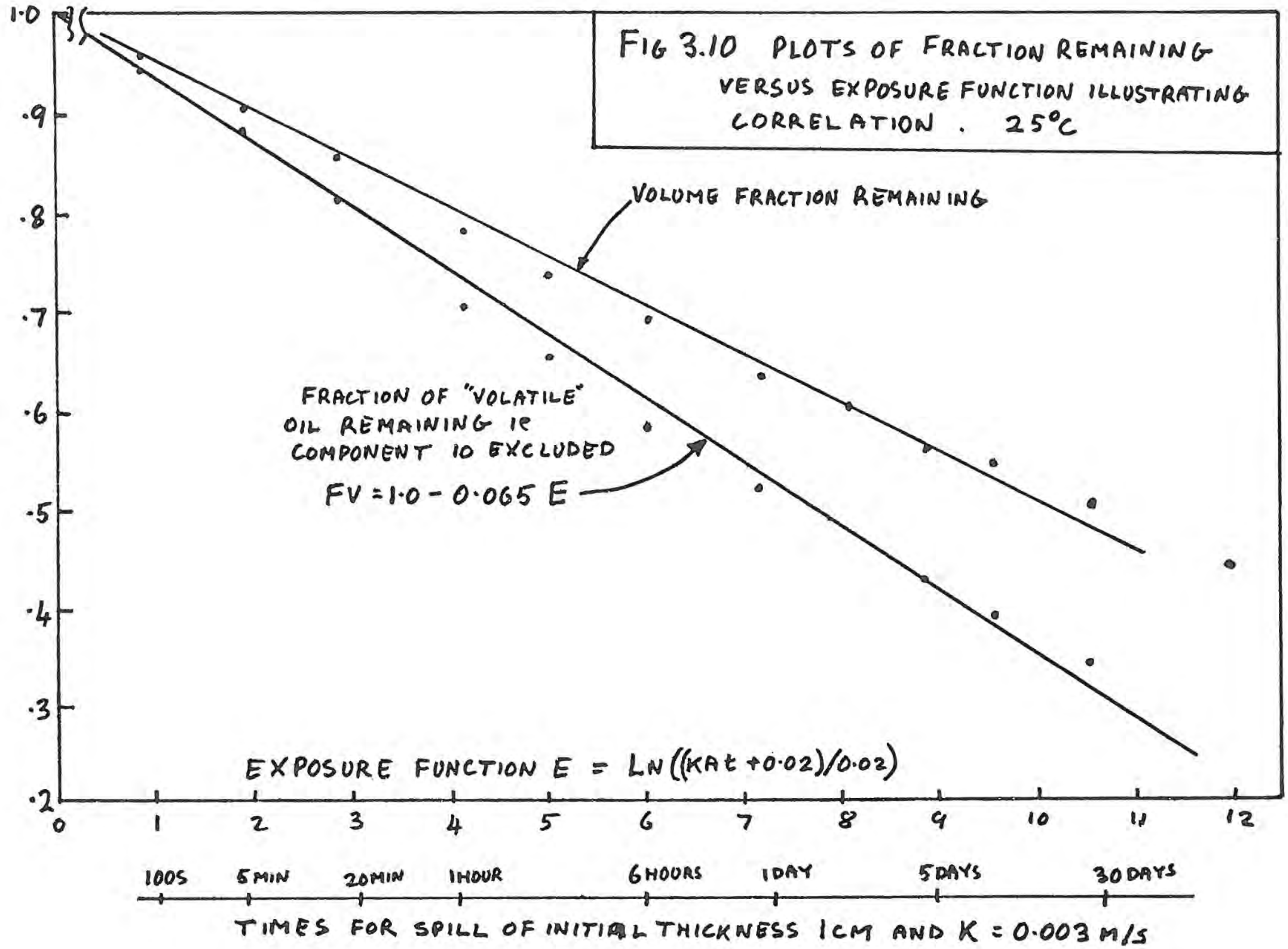

FIG 3.10 PLOTS OF FRACTION REMAINING VERSUS EXPOSURE FUNCTION ILLUSTRATING CORRELATION . 25°C

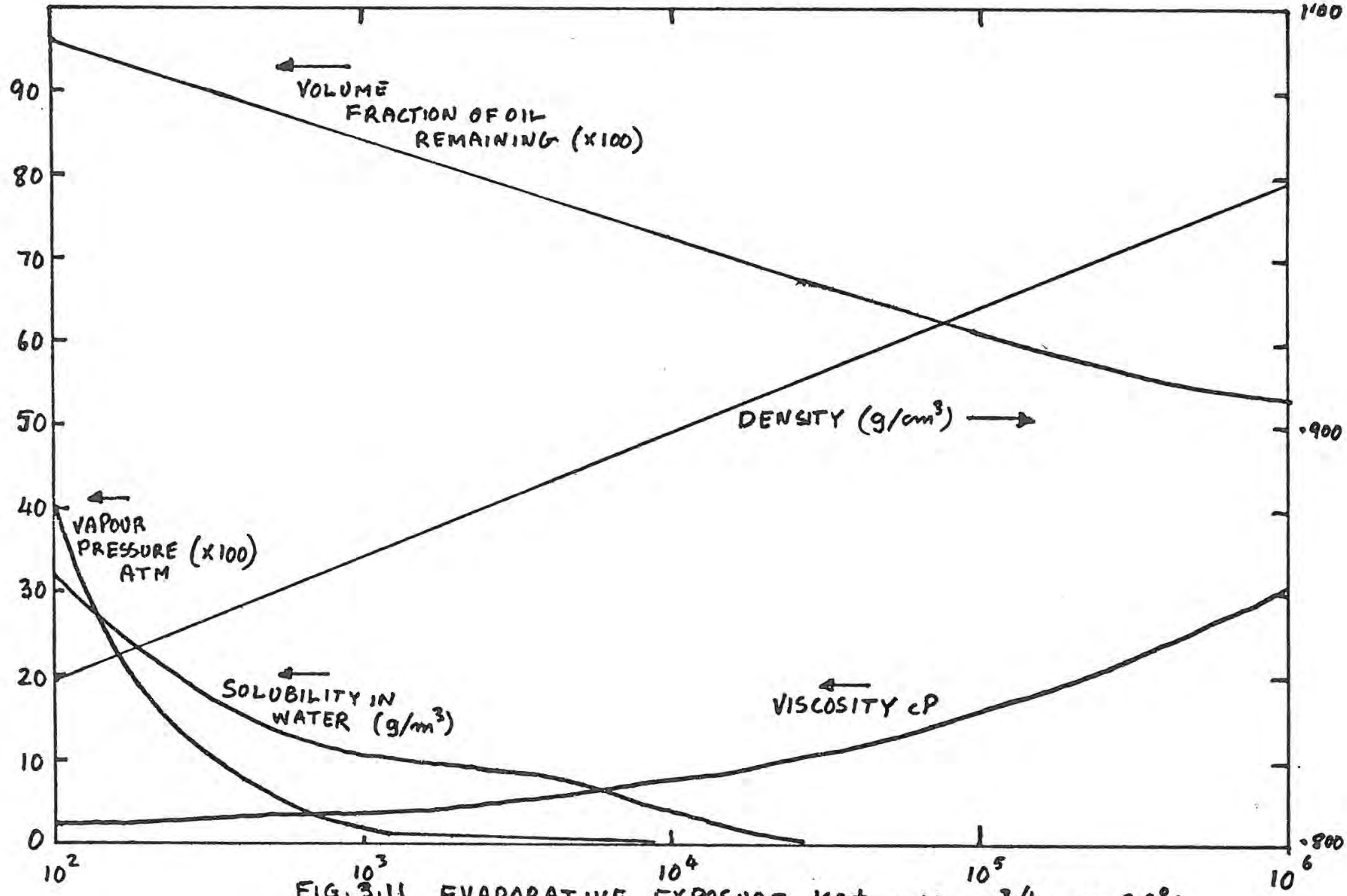

FIG. 3.11 EVAPORATIVE EXPOSURE KAt OR V m³/kg AT 25°C

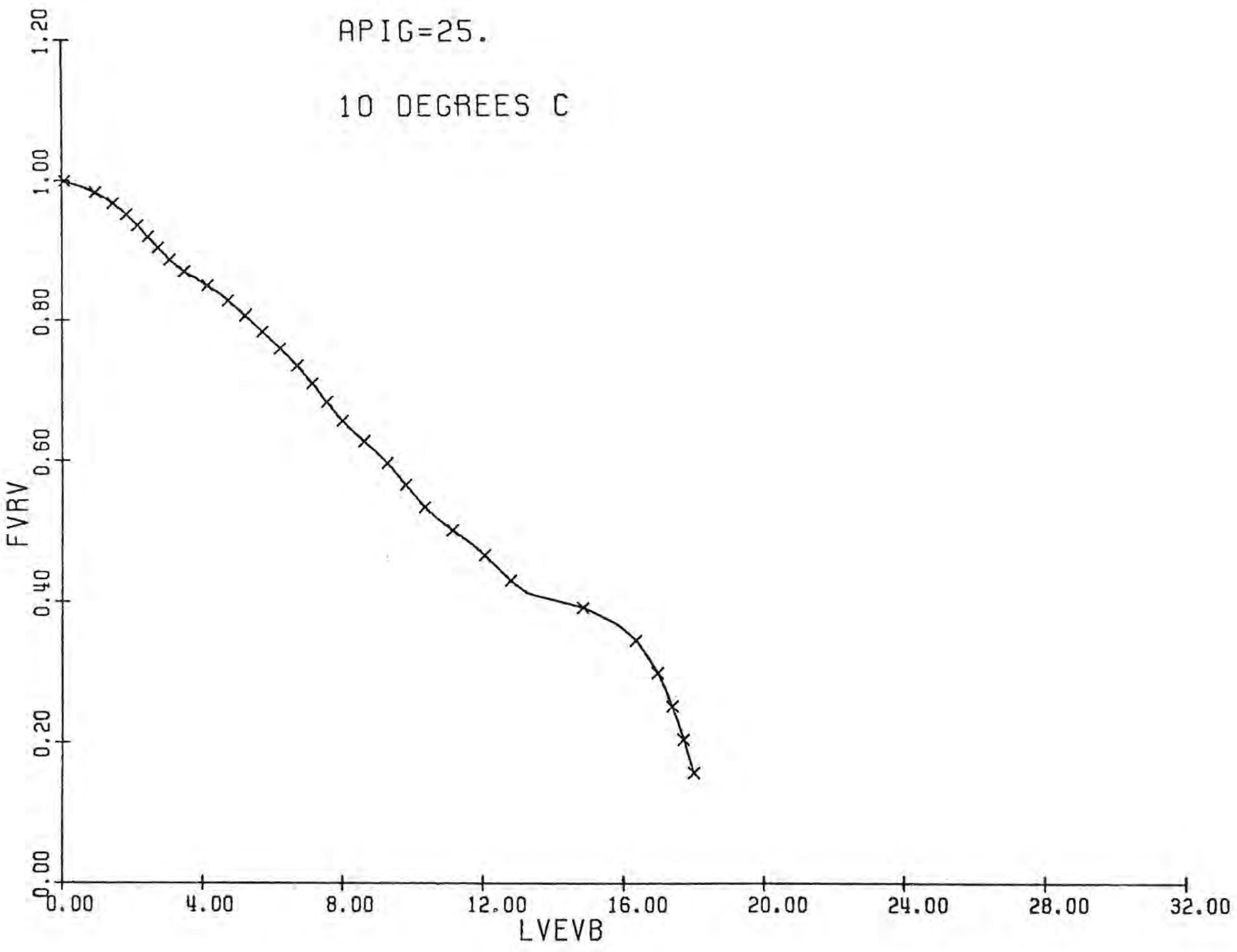

Figure 3.12. Plot of Fraction of Volatiles Remaining versus Exposure Function

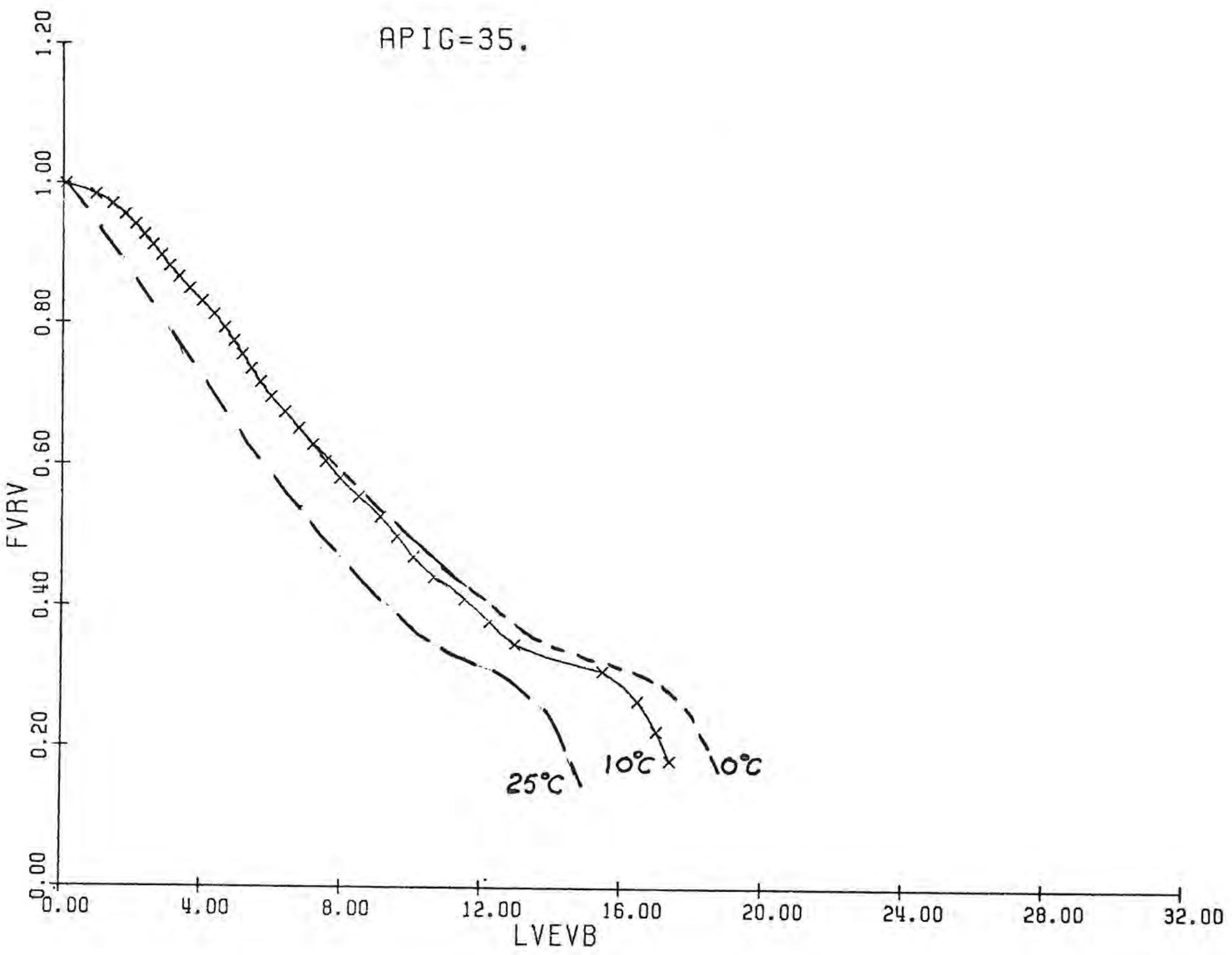

Figure 3.13. Plot of Fraction of Volatiles Remaining versus Exposure Function

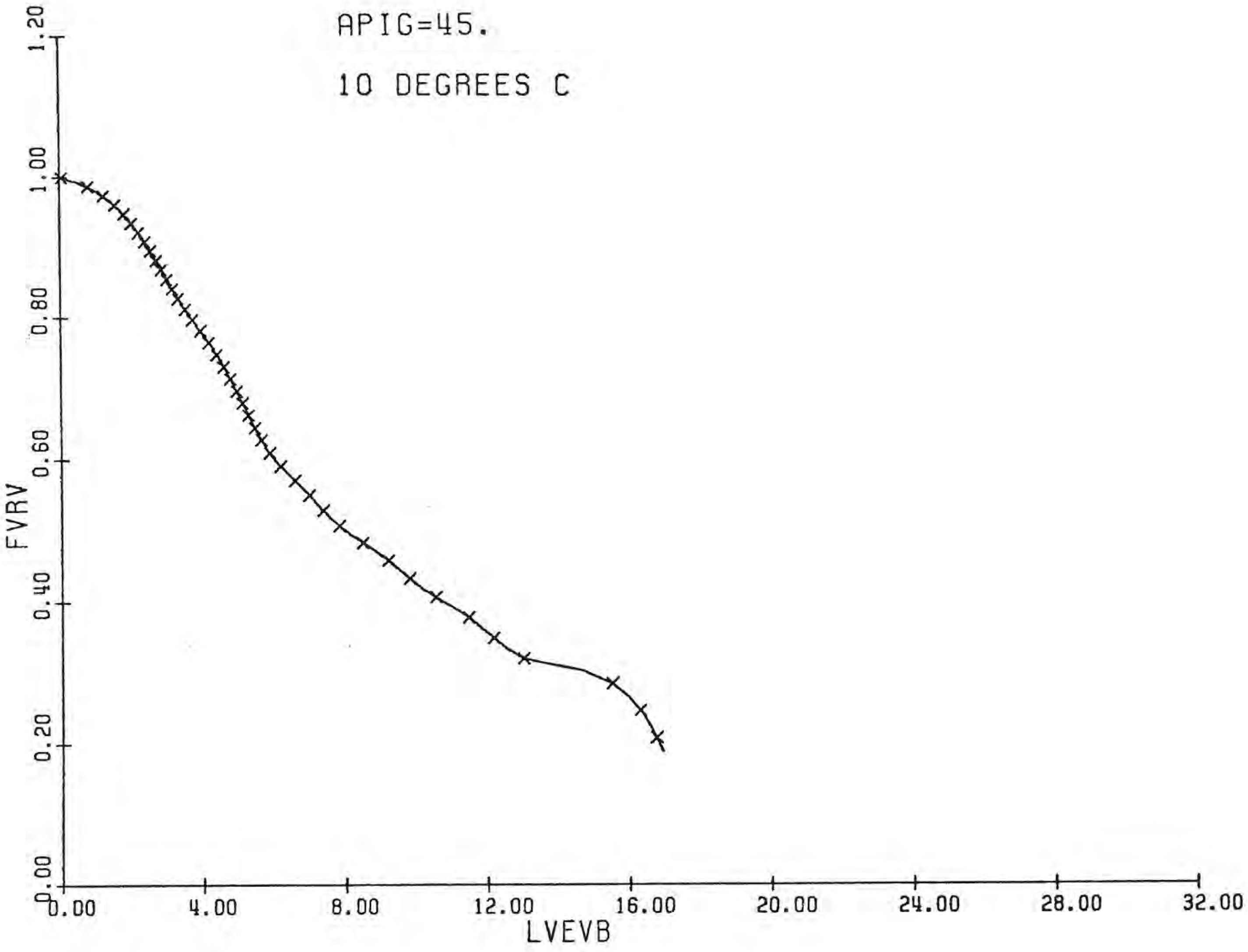

Figure 3.14. Plot of Fraction of Volatiles Remaining versus Exposure Function

Table 3.1. Components of Simulated Mixtures

APIG	Butane	Hexane	Octane	Decane	Dodecane	Hexadecane	Toluene	Naphthalene	Phenanthrene	Inert
15	.10	.06	.15	.13	.10	.40	.06	.005	.005	.85
25	.22	.12	.15	.13	.10	.25	.02	.005	.005	.49
35	.23	.23	.15	.13	.10	.20	.01	.005	.005	.29
45	.36	.36	.15	.10	.10	.23	.005	.005	.005	.10

4. WATER-IN-OIL EMULSION FORMATION

4.1 Introduction

Many oils when spilled on water tend to form water-in-oil emulsions which are usually brown in colour and are inevitably considerably more viscous than the parent oil. Their appearance has led to the colloquial designation of "chocolate mousse". The mechanism of formation and the determinants of stability are in doubt. Small water droplets of diameter 5 to 20 μm apparently become incorporated in the oil as a result of wave turbulence. A possible mechanism is that when larger oil droplets (1 mm to 1 cm diameter) are sheared from the slick by waves or breaking waves, they rise through the water column and coalesce with the slick trapping a small quantity of water between the oil layers. This water forms droplets which may or may not sink and coalesce with the water column beneath. Small water droplets sink very slowly and may thus become trapped in the oil. The concentration of these droplets increases until it may reach 75%, by which time the oil slick is predominantly an assembly of water droplets interspersed with oil. Since the oil can not shear through, but only around, a water droplet, the force necessary to generate a given shear rate or velocity gradient is substantially increased, and is reflected (by definition) as an increased viscosity. This viscosity may exceed the parent oil viscosity by several orders of magnitude thus swamping the effect of viscosity increase attributable to evaporation.

Oils differ in their tendency to form emulsions. Light volatile oils rarely form emulsions, heavy fuel oils usually do, and crude oils vary considerably. It is likely that this difference in behaviour is attributable to the presence or absence of a concentration of a particular component of the oil which induces stability. Several attempts have been made to identify the component but complete identification has not been achieved. The compound (or class of compounds) has obviously a relatively high molecular weight and has the property of accumulating round the water droplet and forming a "skin" or layer which prevents coalescence. In the absence of knowledge of the compounds identity or concentration, the only approach is to undertake laboratory simulation of surface turbulence and observe whether or not emulsions form and remain stable. A blender is the usual apparatus used to mix the oil and water.

Studies of various aspects of this phenomenom have been reported by Mackay (1975), Mackay et al. (1973), Oren and Mackay (1976), Canevari (1969) and Berridge et al. (1969).

In this work, some small-scale experimental studies of emulsion formation were undertaken in which a slick was subjected to simulated sea-surface turbulence and the oil-water content and viscosity changes were monitored. A theoretical model was then assembled to describe the process resulting in equations which may be useful in characterising emulsion formation at sea.

4.2 Experimental

Figure 4.1 is a schematic diagram of the test apparatus. It consists of a glass vessel, 29 cm in internal diameter and 29 cm high. A 0.5 cm thick plexiglass lid was fitted with a rubber gasket and PVC elbows to allow air to enter and exit as shown. The apparatus was operated with 8 litres of water, giving a water depth of 13.3 cm in the tank. The moving air stream was produced by a dry shop vacuum cleaner blower and the air flow was regulated with a valve situated at the blower outlet. The volumetric flowrate to the tank was monitored throughout the experiment using an orifice metre with an orifice of 2.54 cm in a pipe of internal diameter 3.8 cm, the pressure drop being measured on a water manometer. The apparatus is very similar to that used in a dispersant effectiveness test by Mackay et al (1978).

Samples of water were withdrawn from the tank with a 100ml pipette, through a 0.4 cm I.D. stainless steel tube located 3 cm from the tank bottom and 2 cm from the tank wall. The test crude oil samples were pipetted from the water surface, through sampling port "S", using a 50 ml pipette.

Experimental Procedure

In a typical test, 8.0 litres of water were poured into the test tank and allowed to equilibrate to room temperature. For the salt water tests, 3% sodium chloride was added to the water. 125 ml of the test oil were then pipetted onto the water surface, and the oil temperature was allowed to equilibrate with that of the water. A 5 minute contact time was allowed before the blower was started, providing mixing energy to the water surface. The appropriate volumetric flow rate of air was adjusted using the valve on blower outlet.

Samples were withdrawn from the tank at 15 minute intervals for the first hour and a half, 30 minute intervals for the following hour, and 1 hour intervals thereafter. 200 ml water samples were removed through the sampling port, and 7 ml samples of the water-in-oil emulsion were pipetted from the emulsion oil surface.

The water samples were analysed for oil content by infrared spectroscopy. The dispersed oil was extracted from the water sample with two 20 ml aliquots of spectroscopic grade carbon tetrachloride; the resulting carbon tetrachloride solution was then diluted to 50 ml. The concentration of the extracted oil in ppm was measured in a Horiba OCMA-200 oil content analyser. The OCMA-200 uses a non-dispersive infrared (NDIR) analyser, that operates in the range of 3.4 to 3.5 μm of the infrared spectrum.

The viscosities of the water-in-oil emulsions at 20^{o}C were measured using a Ferranti-Shirley viscometer which required only a sample size of 2-3 cm^3.

The oil samples were subjected to water content determination using the Karl Fisher titration method of determining free water and water of hydration in solid or liquid samples. The procedure was adopted from ASTM method E-203-62T.

An Alberta crude oil (density = 0.829 g/cm^3, viscosity = 0.00825 Pa.s (8.25 cP), at a shear rate of 1180.0 sec^{-1} and 20^{o}C) was used as the test crude oil.

4.3 Results

The results of typical tests in fresh and salt water are given in Figures 4.2 and 4.3. During the first ten minutes the dominant process is dispersion of oil droplets into the water, concentrations of 20 to 50 mg/l being obtained on sampling. These concentrations represent finely dispersed oil, not larger (mm) drops which were allowed to rise during sampling. These concentrations appear to be reasonably in accord with those reported in actual experimental spills in which typical oil concentrations in the top metre of the water column are 1 to 10 mg/l. (Cormack 1977, JBF 1976)

It had been expected that these concentrations would increase steadily, possibly approaching a limiting value at which dispersion and coalescence rates were equal. This did not occur. After about 20 minutes the concentration fell and settled out at a steady 10 mg/l after 1 hour. The drop in concentration coincided with a change in the oil appearance, water content and viscosity. The water content increased to 70 to 80% (vol) within 30 minutes and the viscosity increased correspondingly to 100 to 200 cP. The oil tended to gather in a lump of "mousse" and no further dispersion occurred. Indeed the mousse apparently scavenged dispersed oil from the water. Some implications of this behaviour are discussed later.

A plot of viscosity ratio versus water content is given in Figure 4.4 which clearly illustrates the marked increase in viscosity which occurs when the water content exceeds 50% (vol).

4.4 Theoretical.

A mathematical description of the emulsion formation is presently impossible because of the lack of a sound understanding of the physical chemistry of the system. The obvious first approach is to postulate a realistic mechanism and relationship between visocsity and water content.

We can take advantage of the considerable literature on rheological properties of suspensions of rigid particles since it can be assumed that the water droplets behave as rigid particles. This is reasonable in view of the small particle size and the possibility of semi-solid accumulations of wax-like material at the oil-water interface. The rheology of such systems has been reviewed by Jeffery and Acrivos (1976) by Jinescu (1974) and by Thomas (1965). The considerable number of equations relating viscosity to the amount and shape of the dispersed particles has been reviewed by Rutgers (1962). These equations generally reduce at low concentrations to the simple linear relationship first proposed by Einstein (1920). A convenient and well-validated equation applicable over a wide concentration range is that of Mooney (1951) and Mooney and Hermonat (1955).

$$\mu/\mu_o = \exp(2.5W/(1 - K_1W))$$

where μ is the apparent mixture viscosity (here the mousse) μ_o is the parent oil viscosity, W is the fractional water content of the oil and K_1 is a constant.

Figure 4.4 shows the Mooney equations fitted to the experimental data obtained in this study, a satisfactory fit being evident. There is no significant difference between the two curves since the errors in water content and viscosity mask any effect of salinity. It thus appears that the Mooney Equation with K_1 having a value of 0.65 gives an adequate characterisation of the viscosity of emulsions.

Figure 4.5 is a plot of these curves and the data obtained for six crude oils by Mackay (1975). Although the deviations are often considerable the equation gives a reasonable "average" fit to the data. It should be noted that crude oils usually exhibit non-Newtonian; behaviour thus the viscosity ratio depends on the shear rate as well as the water content.

It is interesting to note that it is not until the water content reaches 50% that a noticeable viscosity increase (ie. by a factor of 5 to 10) occurs.

Having established a viscosity-water content equation it is now possible to derive a Kinetic expression to describe the processes of water uptake and release.

We postulate that the rate of water incorporation into the oil (I) depends on sea state S and on the oil viscosity as follows:

$$I = K_i S/\mu \ \mathrm{m^3/m^2.s}$$

Likewise, there will be a coalescence or water removal rate R dependent on the oil composition, its water content, viscosity and slick thickness D as follows:

$$R = K_\tau W/\mu D \ \mathrm{m^3/m^2.s}$$

At any time the net rate of water incorporation will be:

$$d(VW)/dt = A(I - R)$$

where V is the emulsion volume and A its area. Thus D is V/A. Substituting yields:

$$dW/dt = (K_i S/D - K_\tau W/D^2)/\mu$$

$$=(K_i S/D\mu_o)\{1 - K_\tau W/DK_i S\}\{\exp(-2.5W/(1- K_1 W))\}$$

Anyalytical solution of this equation is very complex because D depends on W (i.e. the emulsion swells as water is incorporated). In view of the doubtful basis in physical reality the equation can only be regarded as very approximate, thus only an approximate solution is justified or necessary. A "solution" to this differential equation which has the correct general properties is:

$$\ln \{(\exp(-2.5W/(1-K_1W))(1 - K_2W)\} = -K_i St/D\mu_o = -K_3 t$$

where K_3 is a lumped water incorporation rate constant (s^{-1}) and K_2 is a constant primarily dependent on K_τ the coalescing tendency constant. Direct explicit solution for W as a function of time is impossible except in two special cases.

If K_2 is zero, i.e. the water-in-oil emulsion shows no tendency for coalescence (because of high concentrations of coalescence preventing compounds) the equation becomes:

$$2.5W/(1-K_1W) = K_iSt/D\mu_o = \ln(\mu/\mu_o)$$

$$= K_3t$$

thus $\mu = \mu_o \exp(k_iS/D\mu_o)$

As time elapses, the group (K_iSt/D_o) increases, W increases tending to $1/K_1$ and μ increases tending towards infinity. The rate of increase in W and μ depends on (i) sea state (high sea state promoting a fast increase because of the greater rate of water incorporation), (ii) oil slick thickness D (thin slicks giving a faster increase in W because less water has to be incorporated to give the same value of W) and (iii) oil viscosity μ_o (viscous slicks being slower to incorporate oil).

The second case occurs when K_2 is large i.e. in the range 3 to 10 The term $(1 - K_2W)$ becomes smaller faster than $\exp(-2.5W/(1-K_1W)$, becoming zero when for example W is 0.1 for K_2 of 10.00. The physical interpretation is that when W reaches this value, the rate of water removal equals the rate of incorporation and the viscosity and W stabilize at a constant value. Such oils do not exhibit a "mousse" forming tendency.*

From the derivation, K_2 should depend not only on the content of the "coalescence-preventing" compound but also on slick thickness and possibly also on sea state.

Figure 4.6 is a plot of calculated water contents and viscosities for various values of $K_iSt/D\mu_o$ or K_3t (which is proportional to time) and of K_2. The equation thus has the capability of predicting emulsion formation rates and extents for a variety of oils ranging from those with low K_2 (like heavy fuel oils) which exhibit rapid stable emulsion formation and those of high K_2 values (like light distillutes) which reject water rapidly and thus show little or no emulsion formation tendencies.

---

* Note that when $K_1>K_2$, W tends to $1/K_1$ and when $K_1<K_2$, W tends to $1/K_2$. K_1 is relatively constant at 0.62 to 0.65. If K_2 is less than this W may tend to a physically impossible value greater than unity.

4.5 Discussion

The proposed equation was fitted to the data obtained in the small scale apparatus as illustrated in the lower graphs in Figures 4.2 and 4.3. The fit is clearly adequate, the parameter values being given on the graph. The only available experimental full scale data are those of Cormack and Nichols (1978) who reported water contents for three spills of Ekofisk oil. In the spills at relatively high wind speeds (> 12 knots) the oil incorporated 70 to 80% water within 2 hours. At 2-3 knots the rate of uptake was slower by a factor of 10 to 20. The corresponding fitted values of the constants are presented on Figure 4.7.. The exact dependence of $(k_i St/D\mu_o)$ on wind speed or sea state can not be determined with the present inadequate data but an approximation is possible.

Cormack's data suggest values of K_3 as follows:

Wind speed 2-3 knots $K_3 = 0.0000964 s^{-1}$
12 knots $K_3 = 0.00110$
15-20 knots $K_3 = 0.00130$

An approximate dependence might be

$$K_3 = 0.00001 \text{ (Wind Speed knots)}^2.$$

implying a zero rate at zero wind speed (which rarely occurs), and K_3 values of 0.0001 at 3.1 knots, 0.001 at 10 knots and 0.01 at 31 knots. The "half times" of emulsion formation are approximately the reciprocals of these K_3 values or 2.8 hours at 3.1 knots, 16 minutes at 10 knots and 1.6 minutes at 31 knots. Conditions in the small scale apparatus appear to simulate approximately 10 knots.

This approach may serve to help characterise oils according to their mousse formation tendencies and rates. If the same oil is emulsified at sea and in the apparatus it should be possible to define conditions in the apparatus which will give the same rates of emulsion formation. The orifice plate pressure drop could then be calibrated in units of sea state or wind speed. It may also be useful to gather data for K_1 and K_2 values of a variety of oils and products, K_1 reflecting the viscosity-water content relationship and K_2 the stability of the emulsions. Coupled with K_3 data as a function of sea state, slick thickness etc. it should be possible to use the equations developed here in oil-spill models.

A final conclusion of this work is that the processes of dispersion and emulsion formation are possibly competitive in that a given oil under given temperature and sea conditions is subject to these two processes, either of which can "win" and dominate the spill behaviour. The development of a capability of predicting which process will dominate would be invaluable to those responsible for countermeasures since fast-dispersing slicks give entirely different impacts than emulsified slicks. There are also implications for chemical dispersant application in that it may be essential to apply the dispersant in certain spills prior to emulsification. If on the other hand the spill is going to disperse naturally there is little merit applying dispersants. A knowledge of the likely spill behaviour is thus critically important.

As part of a subsequent study it is suggested that a simple set of equations which describe the process of emulsion formation in finite difference form is as follows.

$$\Delta W = K_A(U + 1)^2(1 - K_B W)\ \Delta t$$

where W is the fractional water content

K_A is a constant

K_B is a constant with a value of approximately 1.33

U is the wind speed

Δt it time

This version is simpler than that presented earlier and may be adequate until more experimental data are available.

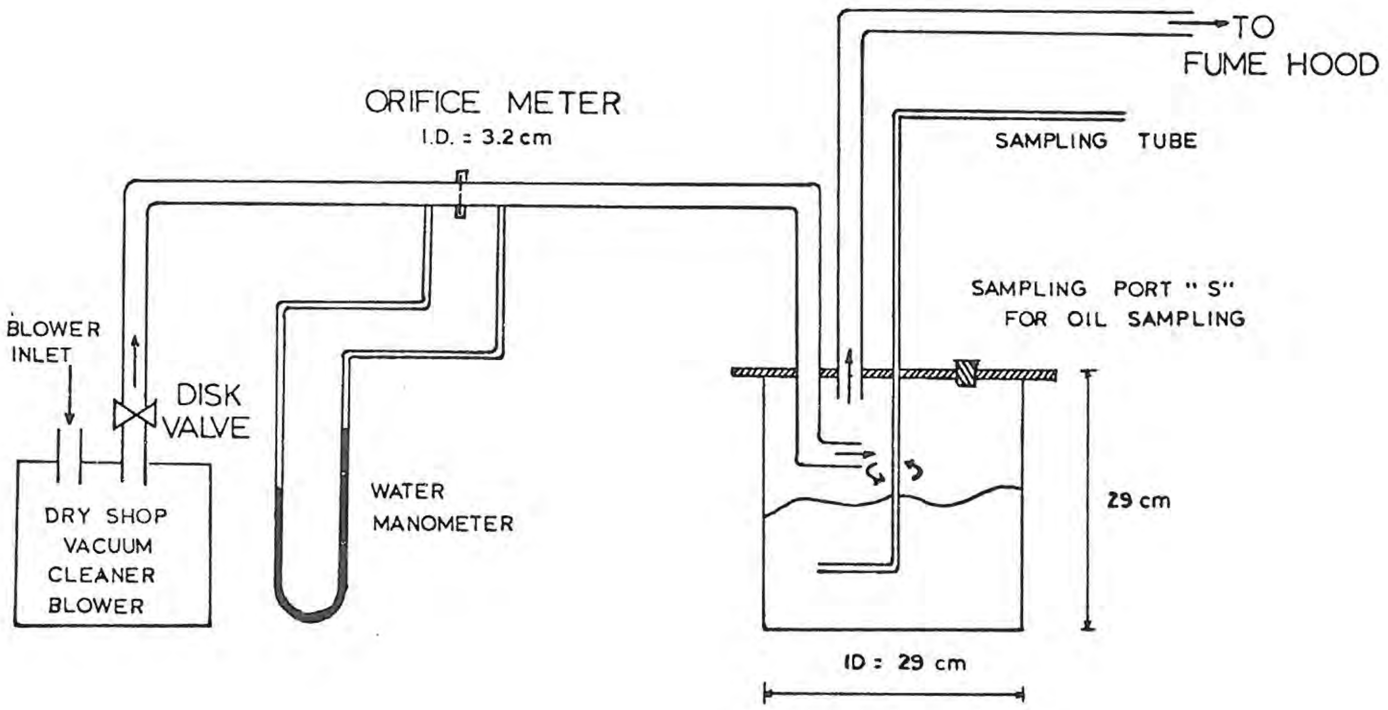

Figure 4.1 Schematic Diagram of the Apparatus

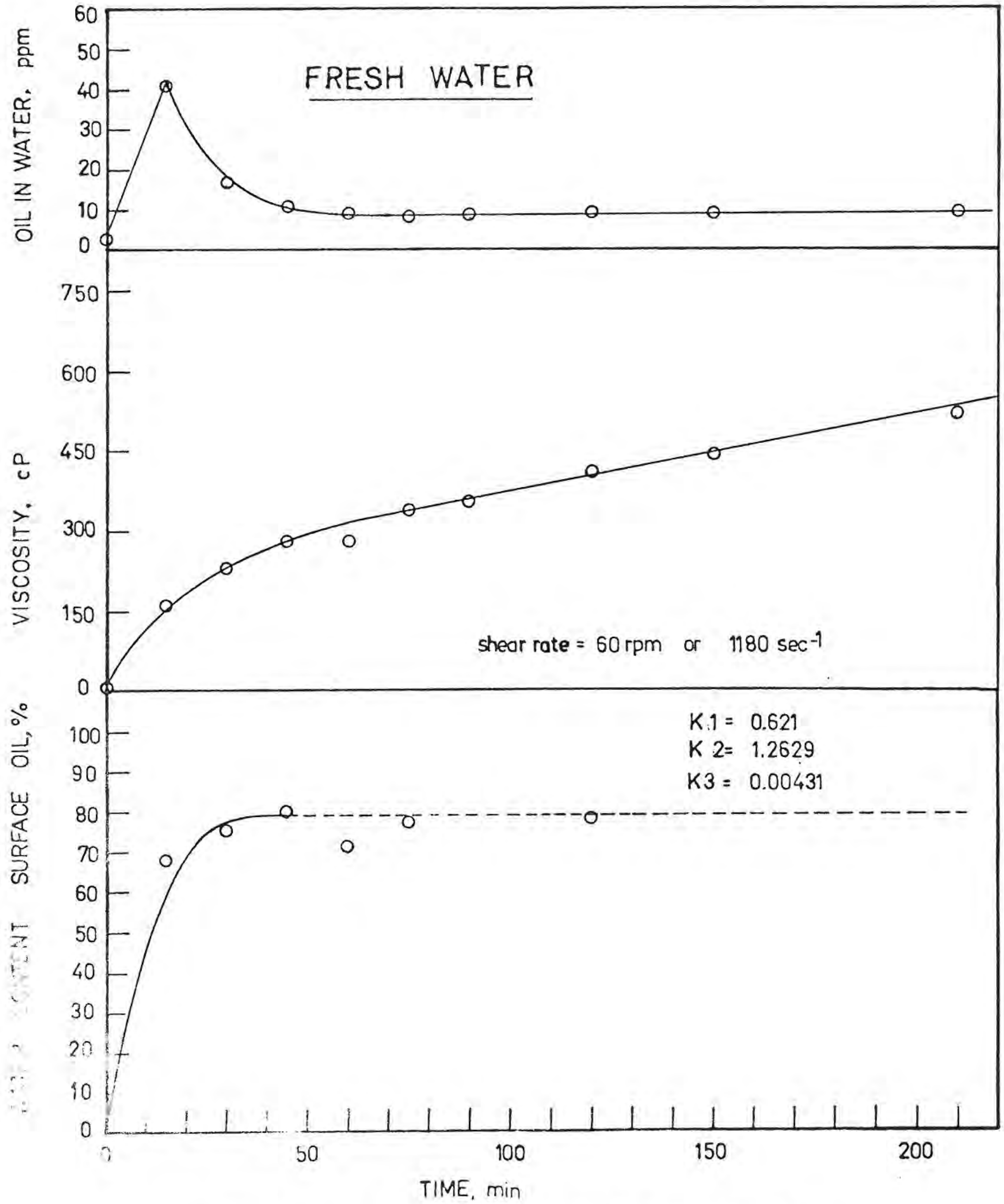

Figure 4.2. Dispersion and Emulsion Formation in Fresh Water

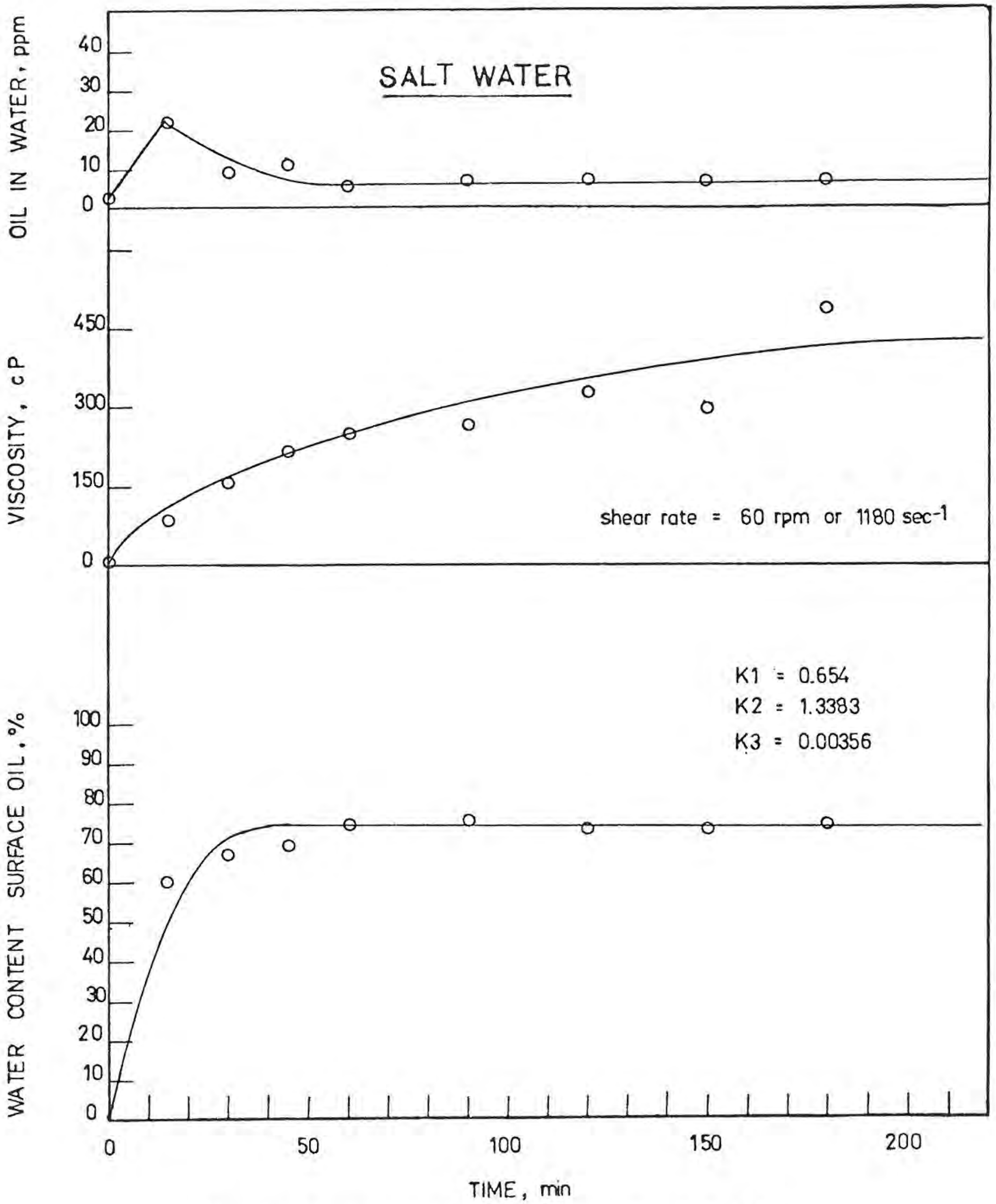

Figure 4.3. Dispersion and Emulsion Formation in Salt Water

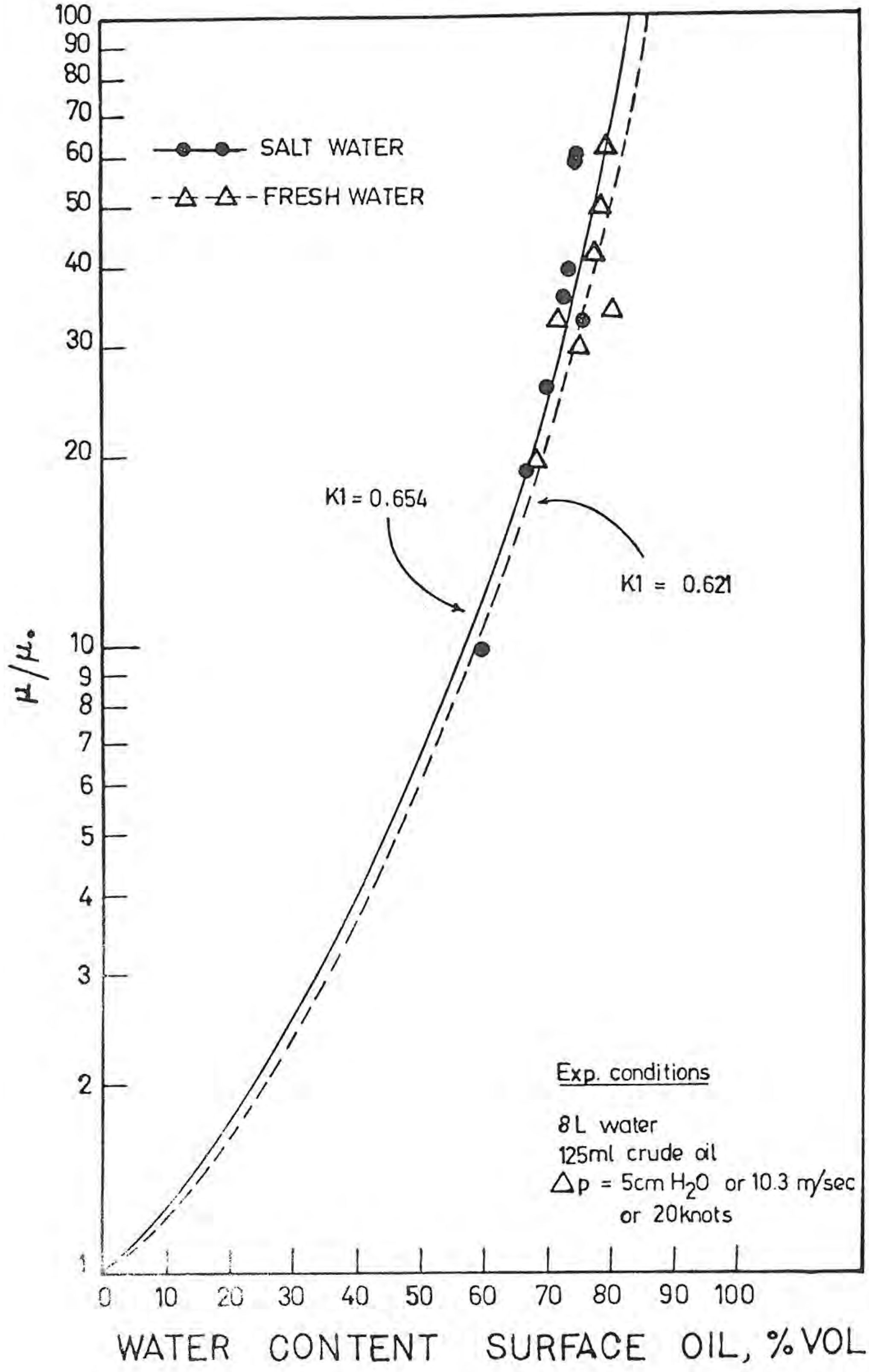

Figure 4.4 Oil Relative Viscosity as a Function of Water Content

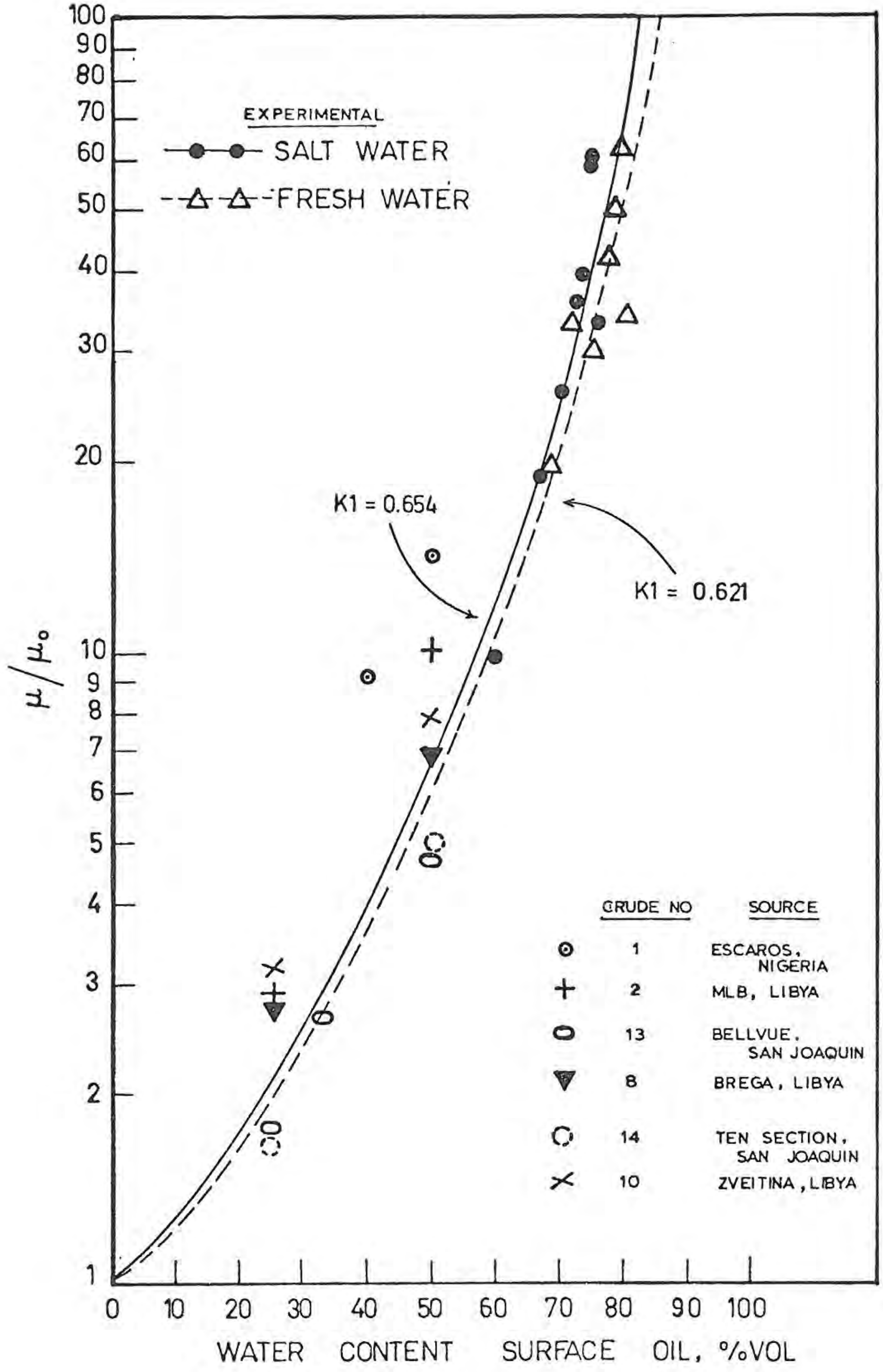

Figure 4.5 Correlation from Figure 4.4 Compared with Data from Mackay (1975)

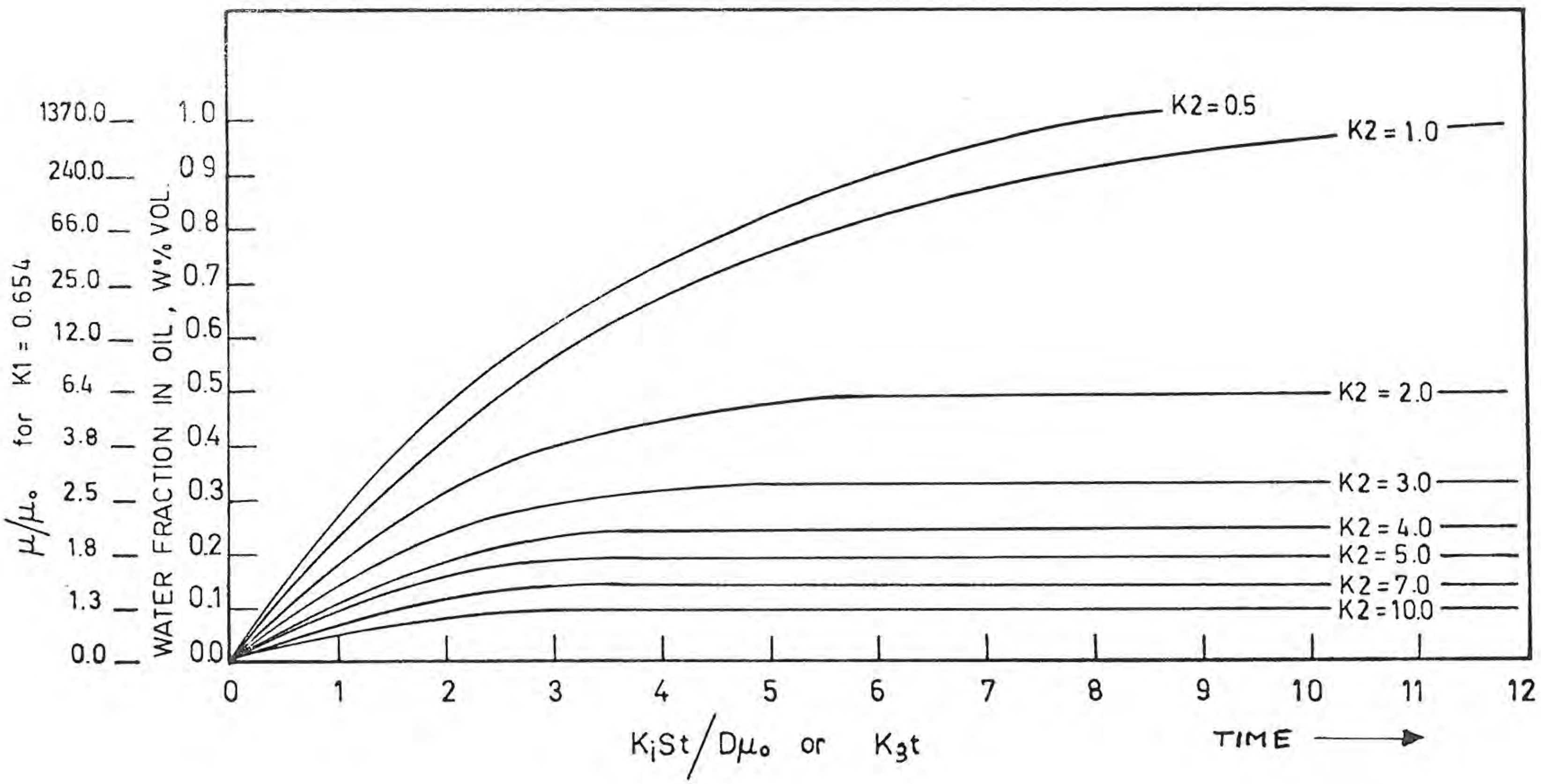

Figure 4.6 Rates of Water Uptake and Viscosity Increase as Correlated by the Equation

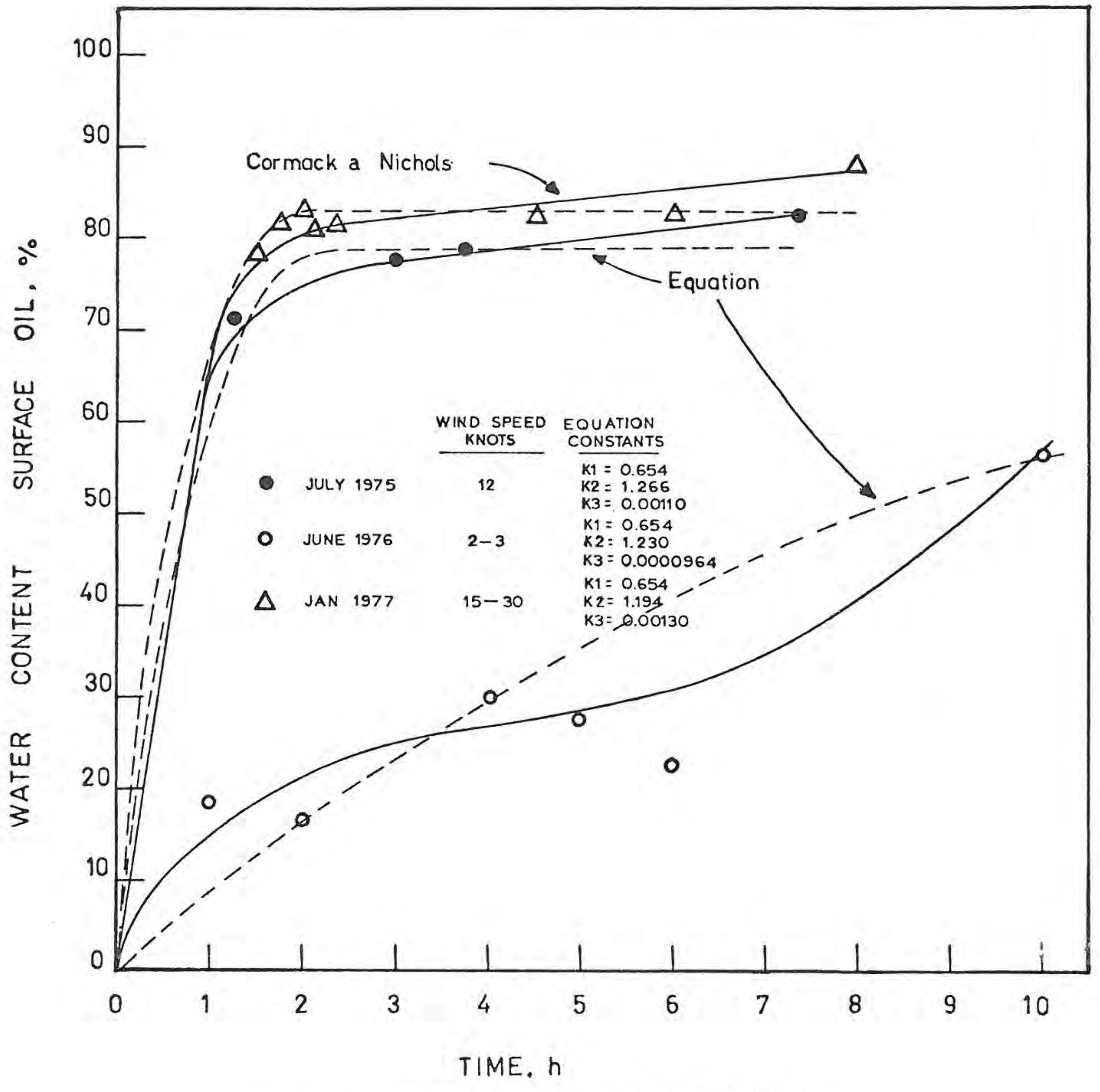

Figure 4.7 Correlation of Cormack's (1978) Data

5. DISPERSION

5.1 Introduction

It is generally accepted that dispersion (also referred to as entrainment or oil-in-water emulsion formation) is both the most important and poorly understood process which occurs to an oil spill. Dispersion largely controls the life time of the oil spill and is, therefore, a significant determinant of whether or not the oil will reach shore, or indeed any given location. It also is probably responsible for determining the extent to which marine biota are exposed (in terms of concentration and time) to oil.

Reviews of the state of knowledge have been compiled by Stolzenbach (1977) and Raj (1977). Some laboratory experimental work has been described by Flow Research Inc. (1978) and by Milgram et al. (1978) under contract from the U.S. Coast Guard. Cormack (1977) has described experimental spills in U.K. waters in which dispersed oil concentrations have been measured. Experimental spills have been undertaken with funding from the U.S. Environmental Protection Agency and the American Petroleum Institute, the first of which has been reported by JBF (1976). Reports from the others are not yet available. These spills have also yielded data on dispersed oil concentrations under actual slicks and on slick lifetime. Leibovich (1975, 1977) has reviewed hydrodynamic aspects of oil behaviour under turbulent sea surface conditions. Blaikely et al. (1977) have suggested dispersion rates as percentages per day for various sea states as part of the 'Slicktrak' model but, although the values are reasonable, it is unclear how they were obtained or what error limits apply. Mackay and Leinonen (1977) suggested a simple first-order equation for dispersion and applied Blaikely's values but this approach is undoubtedly excessively simplistic.

No comprehensive literature review is assembled here, the reader being referred to the excellent and complete review compiled by Raj (1977). A few observations about the dominant mechanisms and the implications for environmental impact are, however, appropriate.

It appears that an oil slick subject to natural sea surface turbulence regimes tends to break up into small oil droplets, some of which have a sufficiently small rising velocity that they are essentially permanently incorporated into the water column where they later dissolve and are degraded microbially. The larger drops with greater rising velocities presumably tend to surface and coalesce with the slick. The mechanisms of formation of these droplets is far from clear. Raj (1977) has suggested that the dominant mechanism is wave-breaking or white-capping in which the water from a breaking wave plunges onto the oil slick driving it under the surface as droplets. Presumably, the thinner the slick the more frequently wave-breaking occurs because of the damping effect of a thick oil slick, and the more likely is the formation of small droplets which become permanently dispersed. It is possible that other mechanisms are operational when oil is dispersed under calmer, non wave-breaking conditions, but this remains a matter of conjecture. Other mechanisms could include rainfall, slick stretching-compression leading to droplet separation, or Langmuir circulations in which slicks may be carried into the water column in down-welling regions.

The principal resistive effect to dispersion is the water-oil interfacial tension which is typically 20 to 30 dynes/cm which corresponds to a significant input of energy for the formation of small droplet surface areas. The issue is not so much the availability of the total amount of energy, since waves contain very large amounts of energy, but rather the availability of the energy in sufficient concentration to permit the new surface to be formed in a small volume. Oil spill dispersants (which are formulations including surface active agents) reduce the oil-water interfacial tension to very low values, and thus facilitate and accelerate the natural dispersion process. In some cases, it may be desirable to assist such chemical dispersion by providing artificial turbulence by breaker boards.

An interesting but probably relatively unimportant process is the formation of near neutrally buoyant water-in-oil-in-water particles, consisting of large, (several mm diameter) water spheres surrounded by a thin oil film which may form and drift for some time in the water column under the slick.

The present lack of understanding of the dispersion mechanism, and our inability to predict rates of dispersion of oil slicks is an important gap in knowledge. Meaningful assessments of the impact of oil spills on marine biota can only be accomplished if there is better knowledge of the concentration and state of dispersion of the oil in the water under various conditions, not only because of the inherent toxicity of such dispersions but also because it is suspected that the major toxic effect of oil may be from the dissolved hydrocarbon and the main dissolution mechanism may be from previously dispersed oil rather than from the slick itself, and also because oil sinking may be mostly of dispersed oil which could be the source of long-term benthic contamination problems.

In this work, we examined the dispersion process at two laboratory scales. The smaller uses a bench scale 6-litre dispersion effectiveness test apparatus (described in the earlier section on emulsion formation), and the larger a 6 m long by 0.6 m wide by 0.6 m deep wind wave tank with artificially induced waves. Caution must always be exercised in extrapolating from such equipment to full scale because of edge effects and hydrodynamic dissimilarities but there is at present little alternative to this approach apart from the very expensive experimental spills mentioned above.

In parallel with the experimental work, a theoretical development has been undertaken which is broadly consistent with the experimental results. The objective is to obtain equations and parameter values which adequately describe the dispersion process for present modelling purposes.

5.2 Experimental

Apparatus

The wind-wave tank used in these experiments is shown in Figures 5.1 and 5.2. It was constructed of 1/8 inch steel plate, 3/4 inch plywood and 1/2 inch plate glass. The back, ends and bottom were constructed of steel, the three right-hand panels were constructed of glass and the remainder was made from plywood. The tank served two purposes. The first of these was to contain water in the bottom 61 cm section. The second was to use the top 61 cm section, in conjunction with the tunnels, to draw air across the surface of the water.

For this purpose, an Aerovent LS-248 fan was situated in the downstream end of the tunnel. This fan was capable of drawing air through the tank at a maximum velocity of approximately 8 m/s. This velocity was reduced by the introduction of plywood "meshes", with different numbers of 2.5 cm I.D. holes, into the tunnel. Flow stabilization was provided by a grid of approximately 3.8 cm diameter cylinders placed with their axes parallel to the direction of air flow.

Waves were generated in the tank by causing a 0.63 cm thick aluminum plate to oscillate back and forward on its axis, attached to the floor of the tank. This paddle was almost the same width as the tank and extended from within 15 cm of the floor of the tank to 15 cm above the water level. It was driven by means of a push rod attached to an off-centre wheel which in turn was driven by a variable speed gear train capable of exerting a torque of 12 inch pounds.

A 15 cm thick pad, made of fibreglass furnace filters wrapped in polyester screening, was placed behind the paddle to absorb the waves generated by the return stroke of the generator.

A grid was drawn on the middle glass panel to allow wave measurements to be made photographically. The vertical divisions of this grid were 1 cm apart and the horizontal divisions were 2 cm apart.

An L-type pitot tube, connected to an inclined manometer, was suspended from the top of the tank. The pitot tube tip was 40 cm above the still water level and 25 cm below the tank roof.

Wet and dry bulb thermometers were also suspended in the air stream.

Procedure

Prior to each run, the water temperature was recorded and the first sample was taken. The wave generator was then set in motion and adjusted to the desired frequency. At this point, the fan was started, if required.

For all of these experiments, the waves were allowed to reflect off the downstream end of the tank. Thus by choosing a harmonic of the fundamental frequency of the tank, it was possible to create large standing waves and simulate actual sea wave profiles, i.e. a large dominant wave with smaller waves superimposed on it. The use of standing waves also minimized surface and bottom drift currents in the tank. Breaking waves were also studied by deliberately selecting a non-harmonic frequency.

At predetermined times during the run, 500 ml samples of the water were collected from the bottom of the tank in 1 litre glass sample bottles with teflon-lined screw caps. Before each sample was taken, 1.5 l of water were allowed to drain from the sample port to ensure a fresh sample.

During each run, five photographs were taken of the waves through the grid on the middle glass panel.

This "froze" the waveform and allowed the dominant amplitude and wavelength to be easily determined.

The frequency of both the dominant wave and the generator were determined by measuring the elapsed time for 10 oscillations to occur with a digital stopwatch.

Analyses

The 500 ml samples were shaken with a known volume of carbon tetrachloride and then decanted into a separatory funnel.

The carbon tetrachloride was then separated from the water and placed in a calibrated Horiba OCMA-200 Oil Analyzer.

This device determines directly the concentration of oil in the carbon tetrachloride by measuring the abosorption of the solution in the 3.4 -3.5 μm range (infrared).

Knowledge of the volume of carbon tetrachloride added to the original sample thus allowed calculation of the original concentration of oil in the sample.

All the glassware used in the analysis was thoroughly rinsed with water, then acetone, and air dried. It was then rinsed with carbon tetrachloride and air dried again.

Disposable polyethylene gloves were worn during all steps of the analysis to prevent skin oils from contaminating the samples.

Oil

The oil used in these experiments was an Alberta crude oil obtained from BP Oil Ltd. To minimize the evaporation of the test oil and thus reduce the accompanying changes in viscosity, density and surface tension, the crude oil was artificially "weathered". This was accomplished by bubbling air through a flask containing 1000 ml of oil until the volume had been reduced to 750 ml. The properties of the 25% weathered oil are given below.

Density = 0.834 g/cm^3
Interfacial tension:* air-water = 67.2 dynes/cm
oil-25% weathered oil = 16.2 dynes/cm
oil-water interface = 28.3 dynes/cm
Viscosity** = 15 cps at 20°C.

---

* Using Fisher Tensiomat

** Using a Cannon-Fenske Viscometer

5.3 Results

Several important qualitative observations were made during the experiments. The first was that the underside of the slick which was originally smooth, formed "bubbles" of oil as time progressed. It was also observed that the slick underwent a stretching motion as the waves passed beneath it. The slick thickened at the crest of the waves and thinned in the trough. Figure 5.3 shows the underside of the slick in a trough early in the run. Figure 5.4 shows the same slick approximately 3 hours later. The top left of this picture shows the underside of the slick in a trough and the top right at a crest. This illustrates the stretching-compression mechanism undergone by the slick during wave passage.

The breaking waves used in runs OS-4-3 to OS-5-4 were created by reflecting waves slightly out of phase. Two types of breaking waves were observed, the plunging breaker (Figure 5.5) and the spilling breaker (Figure 5.6). Both types of breaking waves created an area of foam 10 cm long and the width of the tank. It was also observed that approximately 50% of the waves broke. It was calculated that the breaking portion of the waves covered approximately 10% of the water surface area. Figure 5.7 shows the dispersion of oil by a breaking wave.

The figures give the conditions for each of the runs performed in this study. These runs were designed to investigate four basic parameters, (i) slick thickness, (ii) wave amplitude, (iii) wind over waves, and (iv) breaking waves.

Figure 5.8 shows the concentrations of oil beneath the slick for different slick thicknesses, with the wave conditions held constant. Figure 5.9 illustrates the effect of wave amplitude on dispersion. Figure 5.10 shows the effect of wind over waves of the same amplitude on the dispersion of the slick. Finally, Figure 5.10 depicts the dispersion of oil by breaking waves.

In interpreting these concentrations, it should be noted that the samples were taken from the bottom of the tank, well below the region in which larger oil droplets were present. The concentrations thus represent oil in finely dispersed form, probably 0.1 mm diameter and less, this oil having a very low rising velocity. Considerably higher concentrations, probably in the 1000 to 10000 mg/l (0.1 to 1.0%) range would have been obtained had the water samples been taken near the surface in the vicinity of a breaking wave.

5.4 Discussion

It was noticed that when the water was replaced in the tank after cleaning that the first analysis of oil concentration was unusually high. This occurred in runs OS-1-3, OS-2-5 and OS-4-1. At the beginning of runs OS-6-1 and OS-6-2 some waves broke before a steady wave form was obtained. This explains the unusual results obtained for these runs. The large amount of data scatter seen for the breaking wave experiments is due to the violent action of the waves causing large droplets to be propelled occasionally to the bottom of the tank.

It was observed that during all the runs some oil was dispersed by the sides and reflecting end of the tank. This dispersion took the form of relatively large droplets (1 mm in diameter) and was thus ignored as these droplets rose and coalesced with the slick. Unfortunately, it is impossible to eliminate such "edge effects" in laboratory work of this type.

The accuracy of the analytical technique was judged to be ±0.5 ppm for all runs other than the breaking wave runs, for which the accuracy was ±5 ppm.

The measurement of the wave period was accurate to ±0.01 seconds. The wave amplitude was measured to within ±1 cm and the wavelength was determined to ±5 cm.

Figure 5.8 shows that, in the range investigated, an increase in slick thickness had no significant effect on the dispersion of oil by non-breaking waves. This observation is consistent with a postulation that the mechanism of dispersion by non-breaking waves is by stretching-compression motion of the slick. This also explains the presence of water in-oil-in-water emulsions (bubbles of water surrounded by skins of oil) as the folding of the slick at the crest of the wave could entrap pockets of water in the slick that would be released, with its accompanying skin of oil, when the slick moved to a trough.

Figure 5.9 indicates that as the amplitude of non-breaking waves increases the concentration of oil beneath the slick tends to increase suggesting that the amount of dispersion increases with the degree of turbulence in the water. It should be noted that increasing the wave amplitude by a factor of 5 caused an increase in the equilibrium oil concentration by only approximately 50%. For the runs with the low and high amplitudes the wave steepness ratio was approximately 1/10 and for the waves of medium height the steepness ratio was approximately 1/35.

Figure 5.10 indicates that the presence of wind above the waves had little or no effect on the oil dispersion, at least at the wind velocities tested. This leads to the conclusion that, in reasonably developed seas, the major process contributing to the dispersion of oil is wave state, and that as a first approximation the wind speed can be neglected as a direct factor contributing to turbulence. It must be recognized, however, that it is the wind that creates the waves and thus in the case of a developing sea it may be erroneous to ignore wind as a contributor of turbulence. Wind also causes crest breaking which may enhance dispersion.

Figure 5.11 illustrates that the dispersion of oil by breaking waves is a far more dramatic process than by non-breaking waves. Figure 5.7 shows a photograph of the mechanism by which breaking waves disperse oil slicks. Some of the energy of the breaking wave is imparted to the oil slick causing it to shatter into droplets. Another portion of the breaking energy is converted to turbulent eddys which carry the oil droplets into the water column. Figure 5.11 also suggests that thick slicks being dispersed by breaking waves initially raise the concentration of oil in the water column faster than thinner slicks. However, thin slicks tend to reach a higher ultimate steady-state concentration than thick slicks.

These trends, coupled with the qualitative observation that the thick slicks produced larger oil droplets than the thin slicks, lead to the explanation of this phenomenon,that although thick slicks initially disperse more oil, under breaking waves the larger size of these droplets leads to a lower steady-state concentration than the thin slicks.

It is concluded that there are two separate mechanisms of oil slick dispersion into the water column. First is the stretching-compression mechanism of non-breaking waves that leads to low concentrations of oil beneath the slick. Second is the breaking wave mechanism that results in relatively high concentrations of oil.

The factor that ties these mechanisms together is the amount of turbulence in the water beneath the oil slick. It should be possible to correlate this degree of turbulence with sea states and thereby allow the prediction of rough estimates of disperion rates.

For non-breaking sea conditions, a model based on the stretching-compression mechanism correlated with wave amplitude could be used. For breaking-wave states, an additive combination of the stretching-compression mechanism and the breaking mechanism could be correlated with wave amplitude and the fraction of the slick surface area undergoing breaking. In the next section, such an attempt is made to express these mechanisms in equation form.

5.5 Theoretical

Overall Processes

As a result of the experimental work described earlier, it is suggested that the overall dispersion process can be considered to be that illustrated in Figure 5.12. Oil is dispersed from the slick at the sum of two rates, R_B by a wave breaking mechanism and R_N by a non-wave breaking mechanism. The units for both are $g/m^2.s$. The oil drops lie initially in a well-mixed near-surface layer of depth U m, approximately 30 to 50 cm (the depth of a plunging wave). While in this layer, the larger drops rise and coalesce with the slick. They are thus only temporarily dispersed. Others have a low rising velocity and become permanently dispersed and diffuse vertically down into a less well mixed layer of depth Z m in which the vertical diffusivity is D m^2/s. The concentration of the small or potentially permanently dispersed drops is a constant C_S in the well mixed layer and a variable C in the layer of depth Z, C increasing as time progresses at any given depth. Concentrations are in g/m^3. The rate of diffusion into the less well mixed layer R_D is thus the product of the diffusivity D and the gradient in C at the interface between the layers where Z is zero.

i.e. $$R_D = D(dC/dZ)_{Z=0} = C_S K_1$$

where K_1 is a mass transfer coefficient (m/s).

The oil drops are considered as being of two size classifications. Large drops (arbitrarily > 0.1 mm diameter) rise relatively quickly at a velocity V_L m/s and always coalesce with the slick. They never diffuse vertically downwards into the lower layer. Small drops (arbitrarily < 0.1 mm diameter) have a lower rising velocity V_S m/s and may coalesce or may diffuse downwards. Their fate is thus one of these two competing processes. If the concentration of the large drops is C_L, then the rising flux must be $V_L C_L$ $g/m^2.s$ and similarly for the small drops the rising flux is $V_S C_S$ $g/m^2.s$. These two fluxes add to give a total coalescence rate R $g/m^2.s$

$$R_C = V_L C_L + V_S C_S \quad g/m^2.s$$

Writing a differential equation for this upper layer gives

$$R_N + R_B - R_C - R_D = Ud(C_L + C_S)/dt$$

and when a quasi steady state is reached the right hand side becomes zero.

If it is postulated that F_N and F_B are the volume fractions of the small dispersed oil drops for the two dispersion mechanisms, this equation can be broken down into small and large components.

For small drops

$$F_N R_N + F_B R_B - V_S C_S - R_D = UdC_S/dt$$

Substituting $C_S K_1$ for R_D, separating variables and integrating gives

$$\ln(F_N R_N + F_B R_B - C_S(V_S + K_1)) = - t(V_S + K_1)/U + \text{constant}$$

In reality K_1 is time dependent but assuming for illustrative purposes that it is constant and at the initial condition C_S is zero.

$$C_S = \frac{(F_N R_N + F_B R_B)}{(V_S + K_1)}(1 - \exp(-t(V_S + K_1)/U))$$

at large times the quasi steady state in C_S is

$$C_S = (F_N R_N + F_B R_B)/(V_S + K_1)$$

For large drops

$$(1 - F_N)R_N + (1 - F_B)R_B - V_L C_L = UdC_L/dt$$

$$C_L = (\frac{(1 - F_N)R_N + (1 - F_B)R_B)}{V_L}(1 - \exp(-tV_L/U))$$

and when t is large

$$C = ((1 - F_N)R_N + (1 - F)R_B)/V_L$$

Experimentally, in the wind wave tank there is no diffusion (R_D) possible, thus K_1 is zero. The concentrations measured were C_S, not C_L (which is probably less important). The overall rate constant for the increase C_S with time is thus (V_S/U). V_L can be estimated by observation of large drop rising velocities or it can be calculated from Stokes' Law. The ultimate steady state concentrations are thus $(F_NR_N + F_BR_B)/V_S$. Since V_S is known from the unsteady-state rise in concentration and separate breaking and non-breaking experiments were undertaken, it is thus possible to estimate values for R_NF_N and R_BF_B. The best approach to measuring F_N and F_B, and hence R_N and R_B may be to take "grab" samples of the near-surface water column and subject them to analysis with and without some settling. This was not done in the experiments described here but provision is being made for such analyses in the future.

This set of equations provides a reasonable basis for interpreting the experimental results with the ultimate objective of defining equations and parameters which can be used to describe actual spill behaviour. In preparation for this, it is instructive to postulate equations which may be suitable for describing the dependence of R_N, R_B, F_N, F_B and R_D on slick properties and sea state.

Non-Breaking Wave Dispersion

This is still a rather poorly understood process by which droplets become separated from the oil slick under non-wave-breaking conditions by a stretching-compression mechanism. The dispersion rates are fairly slow and appear to be insensitive to slick thickness.

It is suggested that the following equation applies

$$R_N = k_2x^n \quad *$$

where R_N is the dispersion rate $(g/m^2.s)$, k_2 is a constant dependent on sea state, x is the slick thickness (m) and n is a constant. This has the correct property that when x is zero, R_N is zero. It is likely that thick slicks damp turbulence and thus reduce R_N implying that n is negative. The experimental observations suggest that R_N is fairly insensitive to x thus n is likely to be small. A reasonable value for n is thus -0.25. The dependence of k_2 on sea state can only be suggested very approximately, a reasonable form of dependence being

$$k_2 = k_3S^m$$

where k_3 is a constant, S is sea state and m is a constant to which we arbitrarily assign a value of unity in the absence of information to the contrary.

---

* This equation has the undesirable property that if n is negative R_N becomes infinite when x tends to zero. A better formulation is possibly of the type below in which n can be positive.

$$R_N = K_A/(1 + K_Bx^n)$$

$F_B = 1/(1 + K_B\ \mu^{0.5} x.\gamma)$

F_B is fraction below the critical size

K_B is a constant

μ is viscosity

x is slick thickness

γ is oil-water interfacial tension

The rate of dispersion is then $Fx\ m^2/m^3 s$ and the breakdown into large and small *
drops is as before. Chemical dispersion can be included by reducing γ

Figure 9a WIND-WAVE TANK

SCALE: 1/4" = 10cm

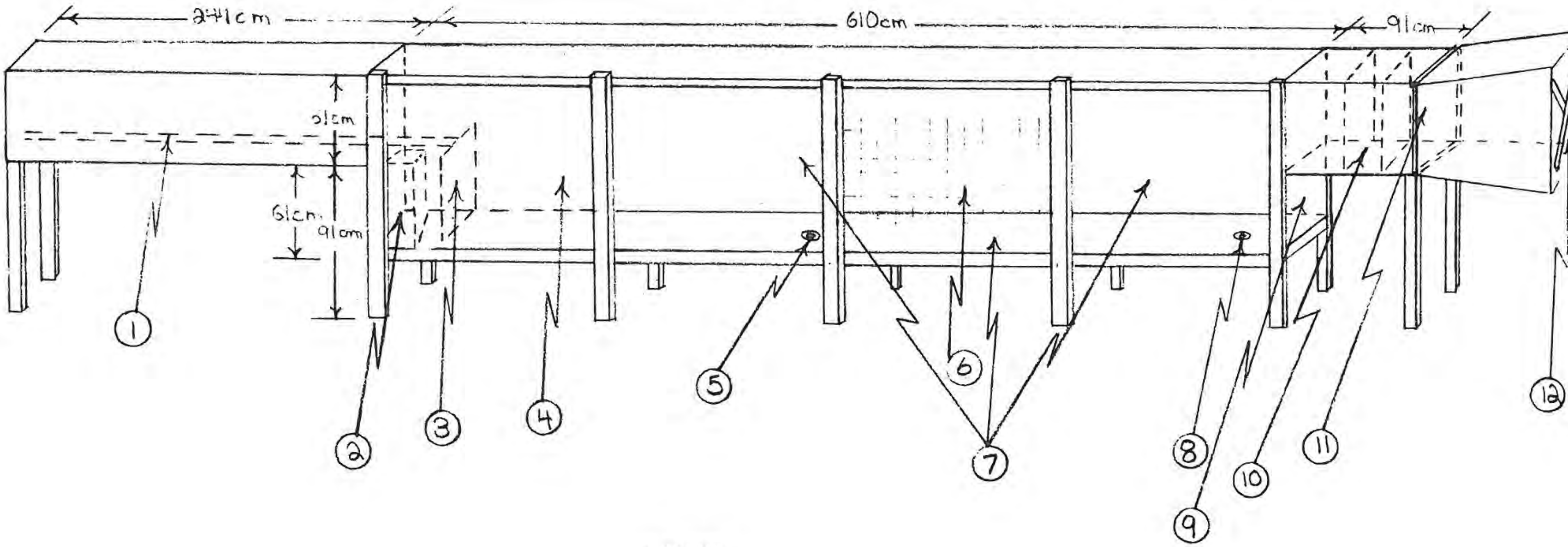

LEGEND

1) Wave Generator Push Rod
2) Wave Absorber
3) Wave Generator Paddle
4) 3/4" Plywood Wall
5) Sample Port "A" and Drain
6) Wave Measurement Grid
7) 1/2" Plate Glass Walls
8) Sample Port "B"
9) Wave Reflecting Wall
10) Air Flow Grid
11) Air Flow Reducing Mesh Plate
12) Aerovent LS-248 Fan

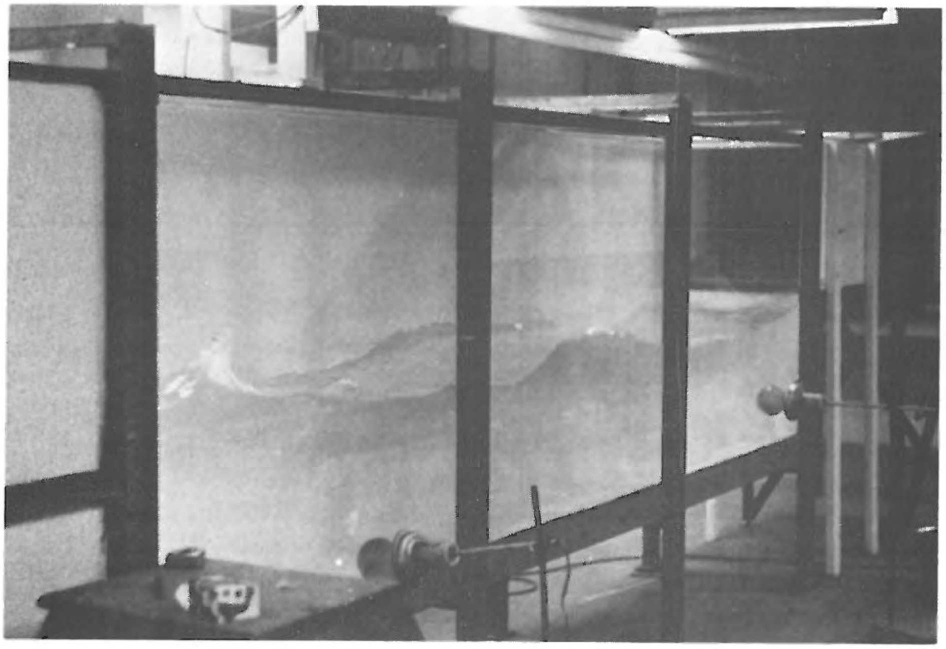

Figure 5.2. Picture of Wind Wave Tank

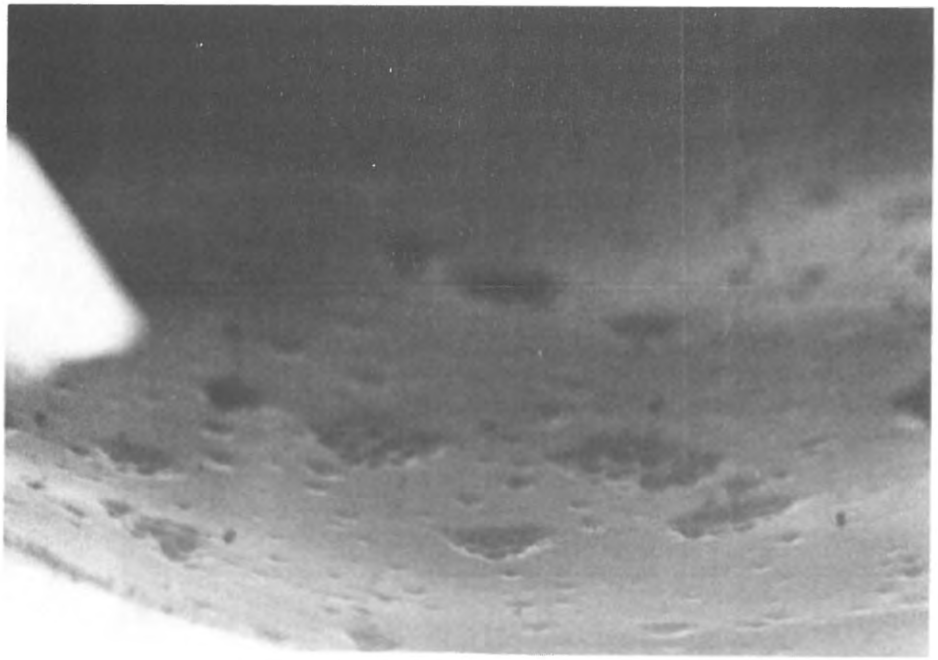

Figure 5.3. Underside of Slick Shortly after Start of Run

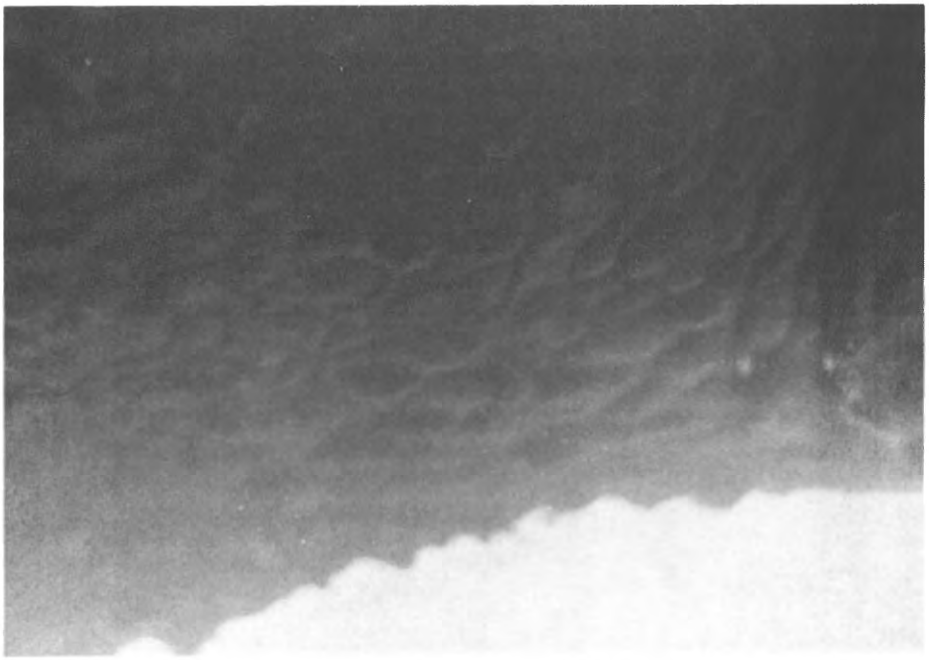

Figure 5.4. Underside of Slick 3 Hours after Start of Run

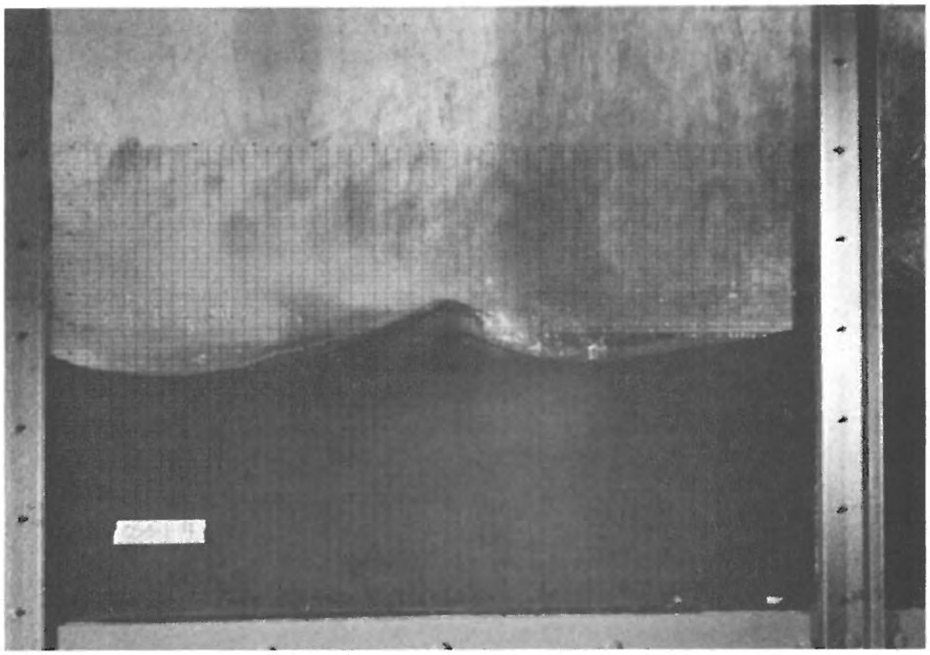

Figure 5.5. Plunging Breaker

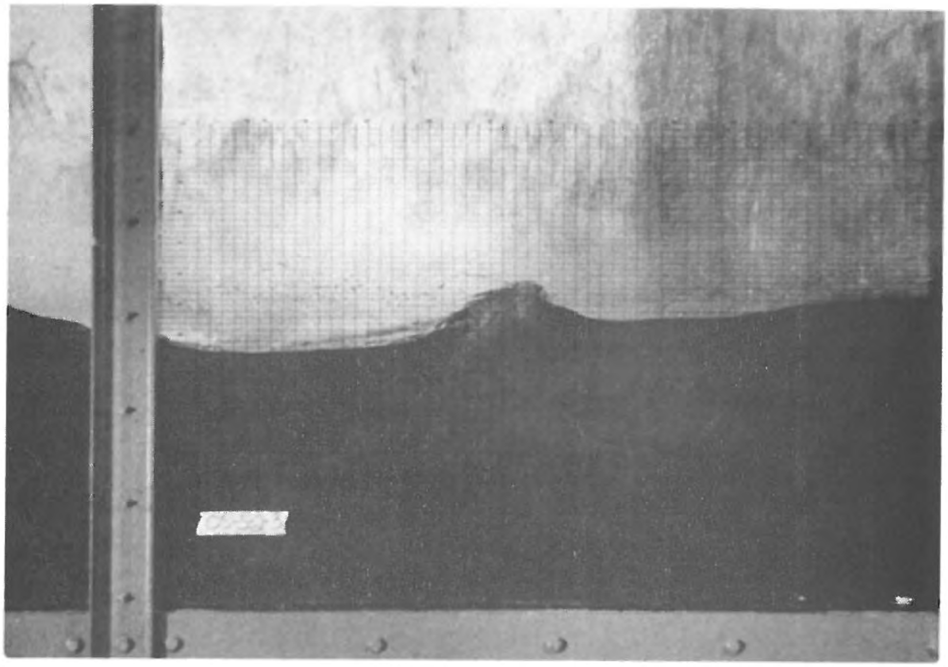

Figure 5.6. Spilling Breaker

Figure 5.7. Dispersion of Oil by Breaking Wave

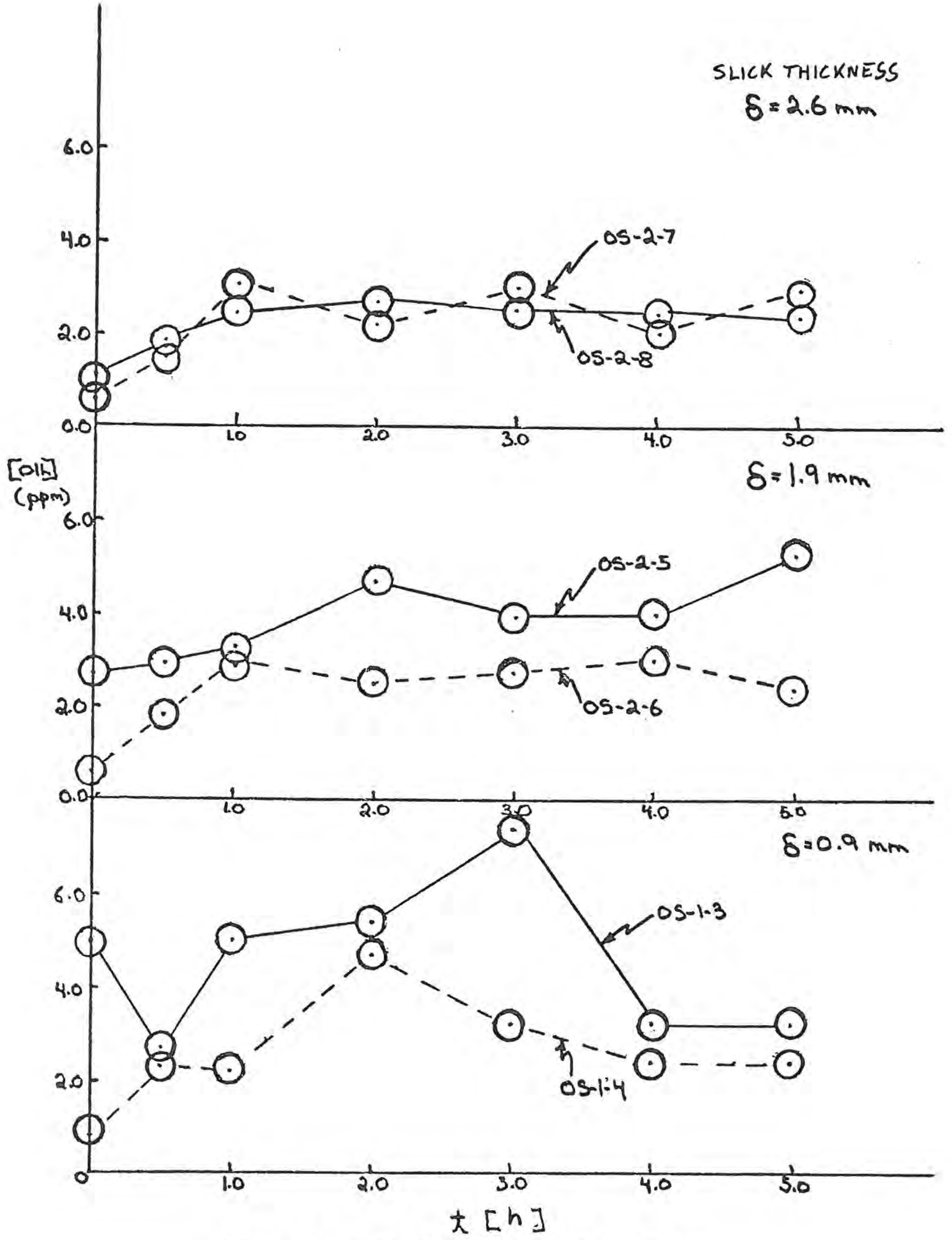

Figure 5.8. THe Effect of Slick Thickness

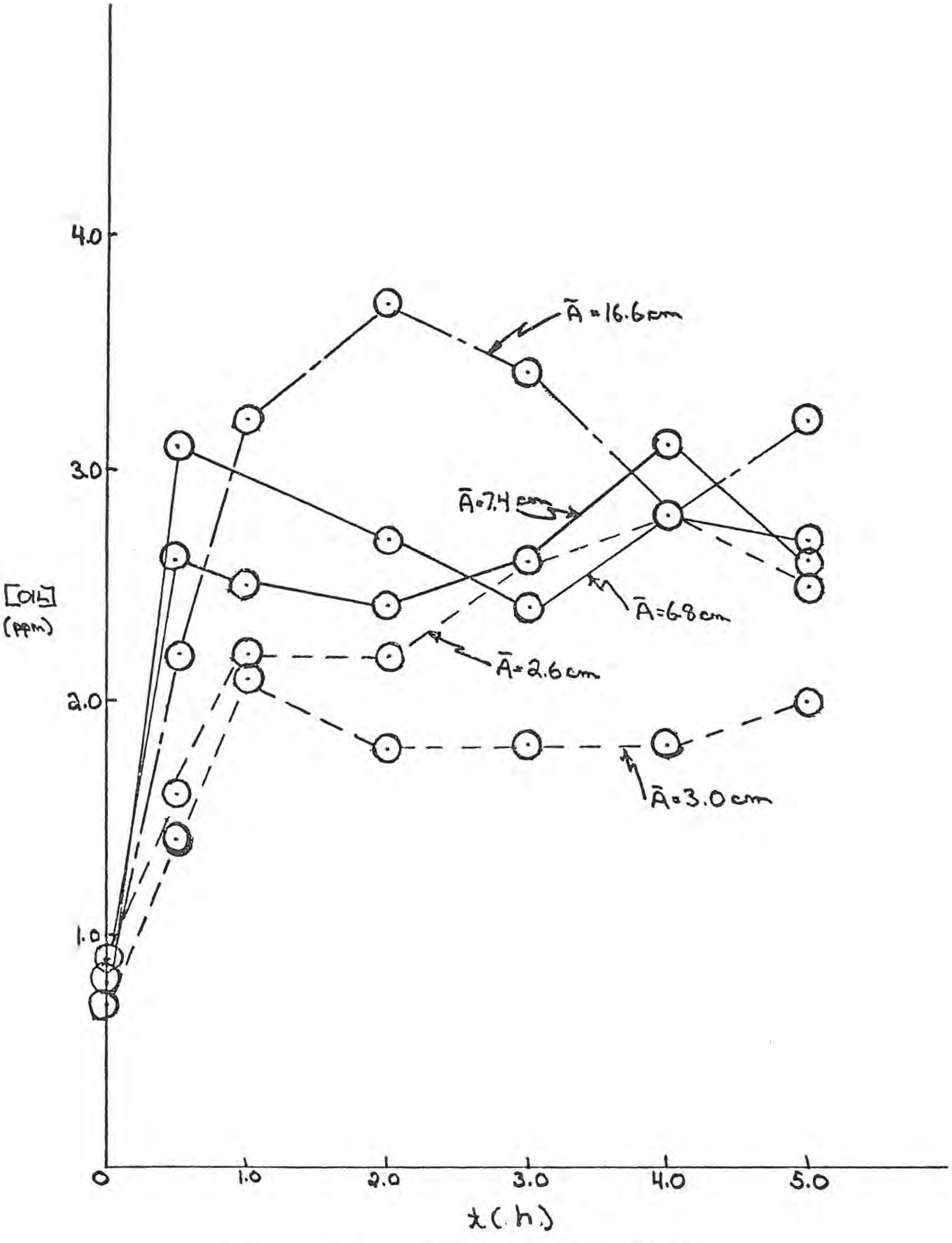

Figure 5.9 The Effect of Wave Amplitude

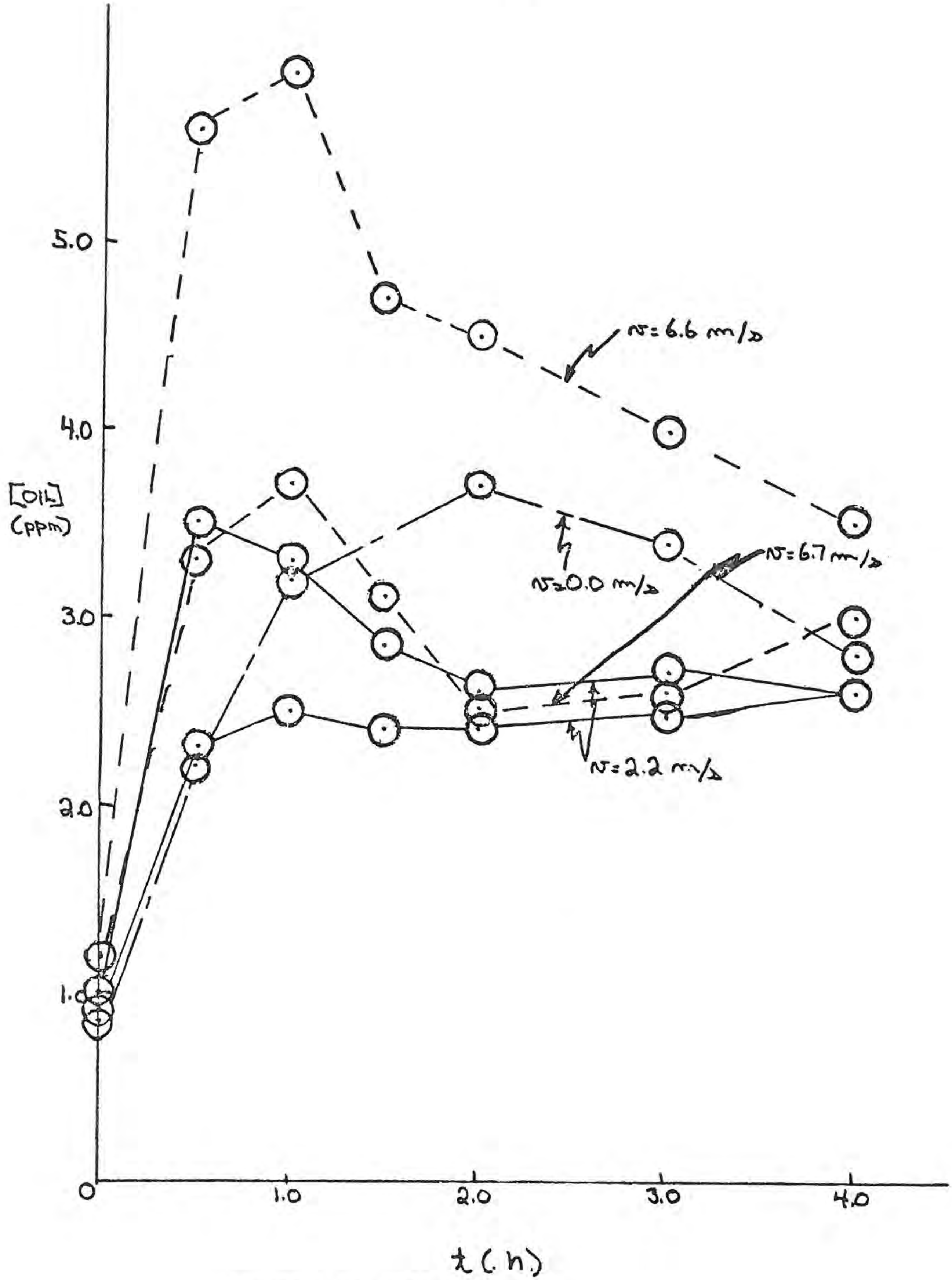

Figure 5.10 Wind Effects

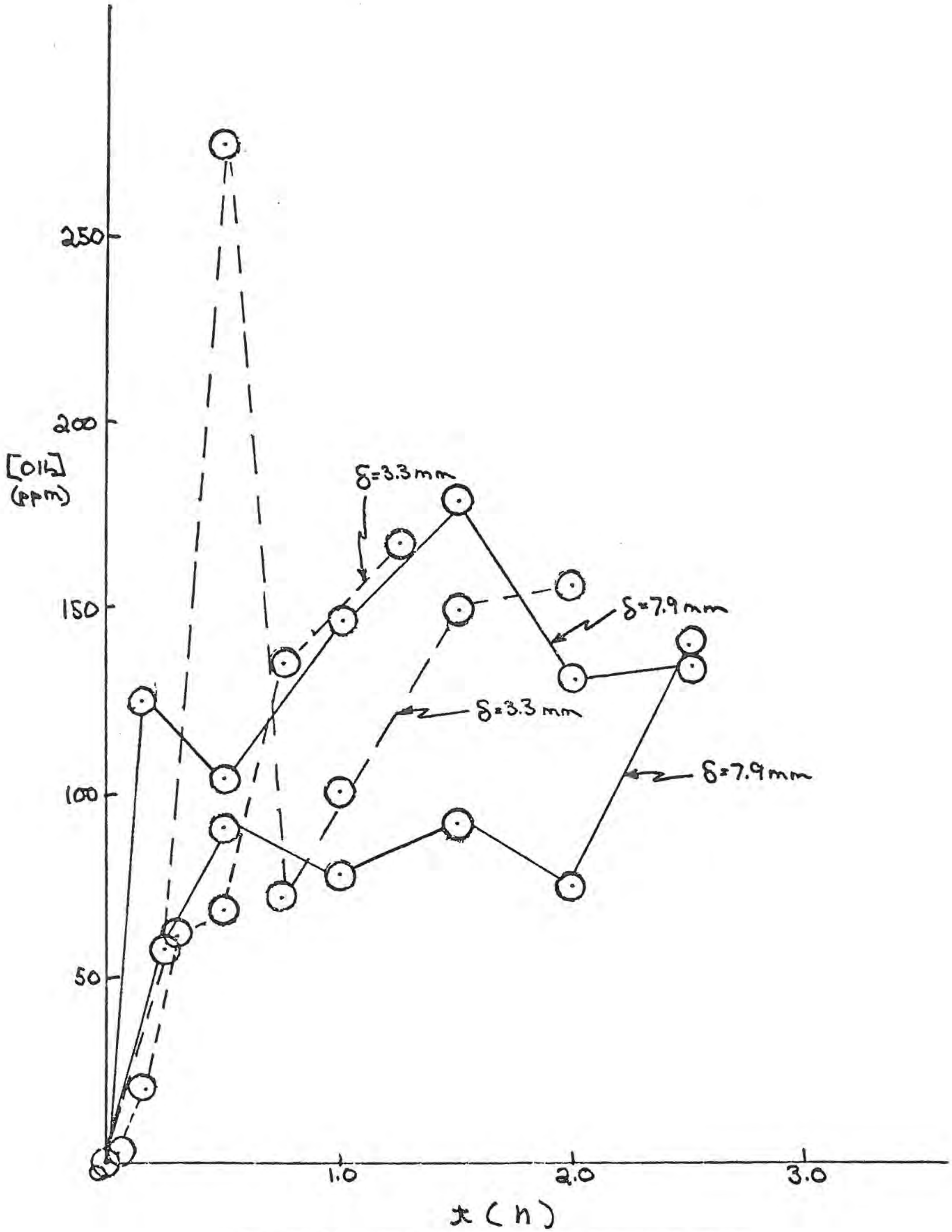

Figure 11. Oil Dispersion by Breaking Waves

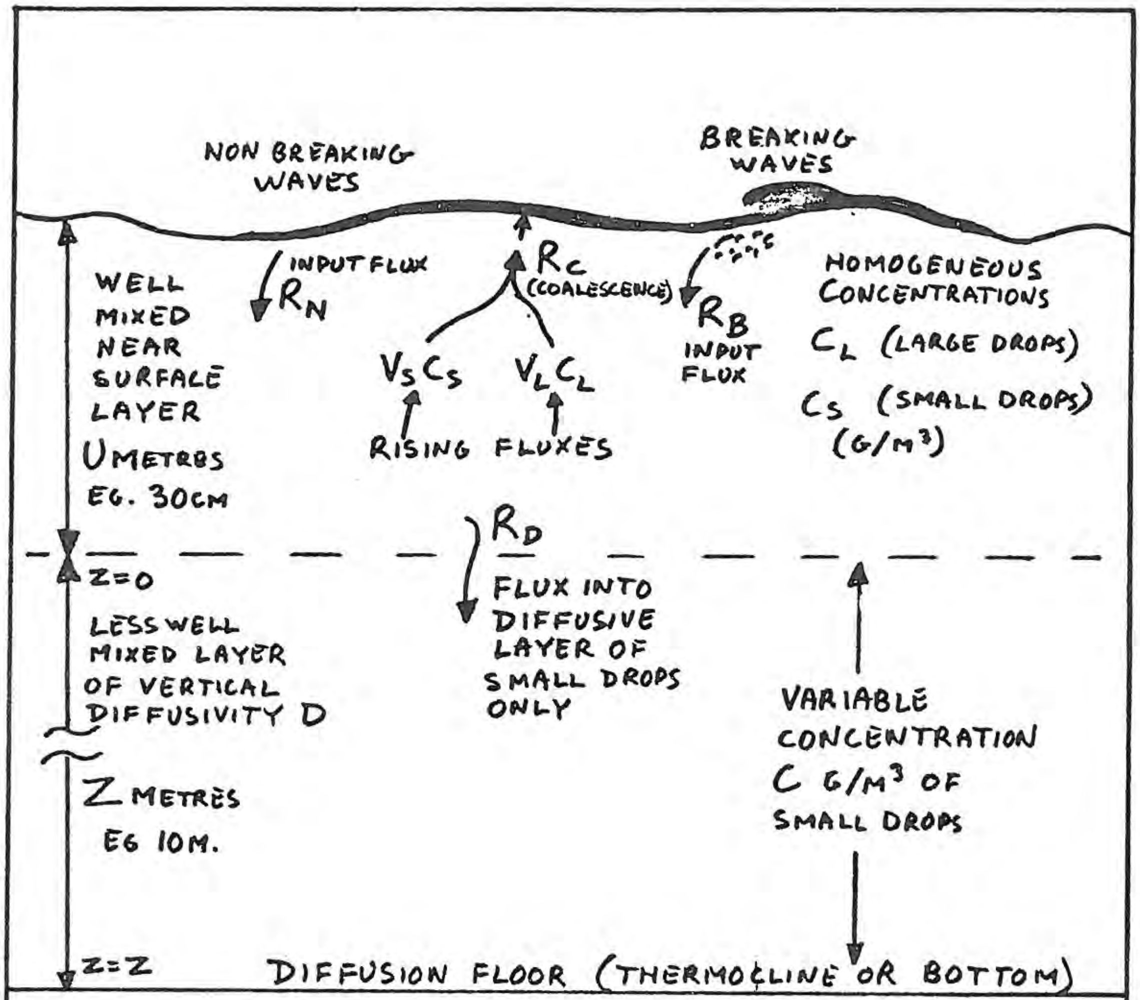

FIGURE 5.12 SCHEMATIC DIAGRAM OF MIXED AND DIFFUSIVE LAYERS UNDER A DISPERSING SLICK

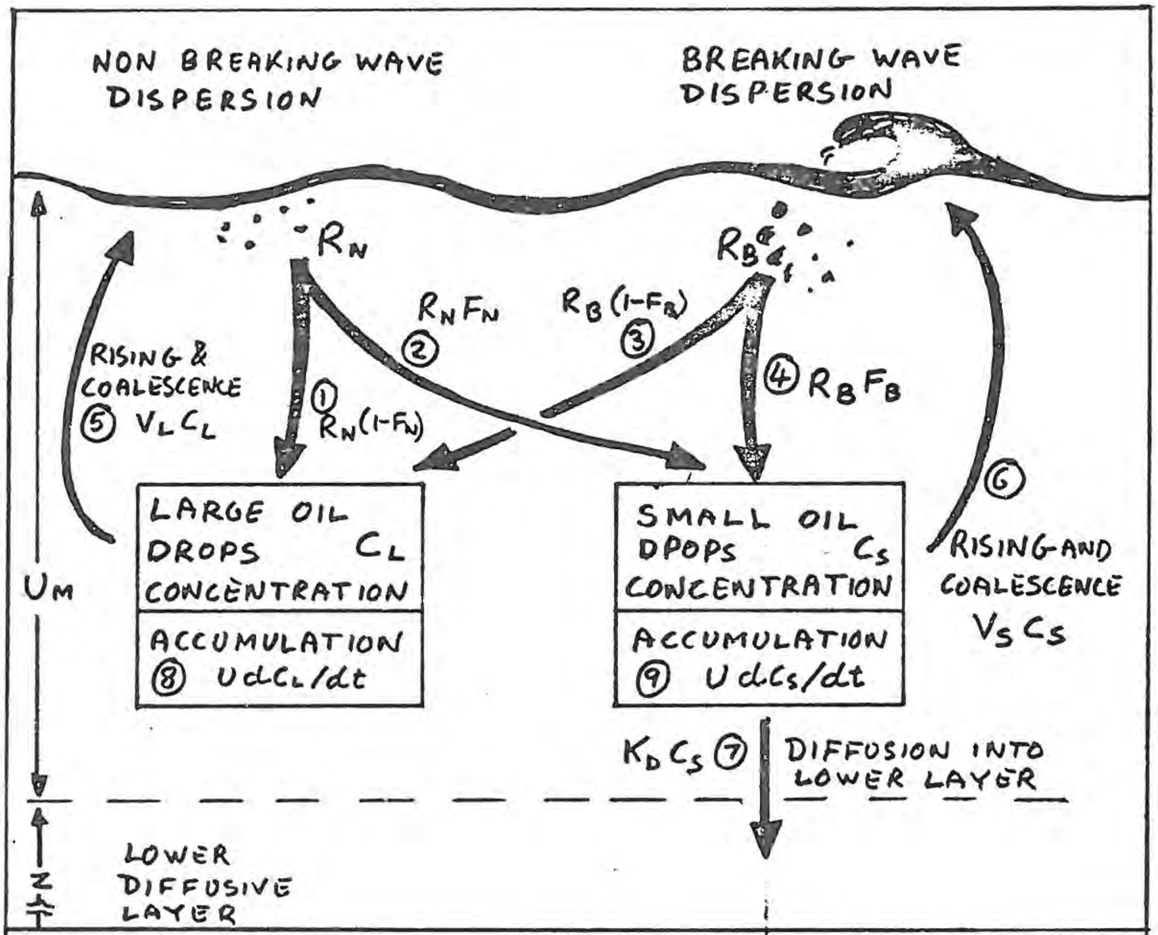

COMPREHENSIVE MODEL (ALL 9 PROCESSES)

$R_N F_N + R_B F_B - V_S C_S - K_D C_S = U dC_S/dt$ (SMALL DROPS)

$C_S = (R_N F_N + R_B F_B)(1 - \exp(-(V_S + K_D)t/U)/(V_S + K_D)\,H$ $(C_S = 0 \quad t = 0)$

$R_N(1-F_N) + R_B(1-F_B) - V_L C_L = U\,dC_L/dt$ (LARGE DROPS)

$C_L = (R_N(1-F_N) + R_B(1-F_B))(1 - \exp(-V_L t/U)/V_L$ " $(C_L = 0 \quad t = 0)$

STEADY STATE MODEL (EXCLUDE PROCESSES ⑧ AND ⑨)

$C_S = (R_N F_N + R_B F_B)/(K_D + V_S)$ $C_L = (R_N(1-F_N) + R_B(1-F_B))/V_L$

NET FLUX FROM SPILL $= K_D C_S$

EXPERIMENTAL TANK MODEL (EXCLUDE ⑦)

AS ABOVE WITH $K_D = 0$

FIGURE 5.13

SUMMARY OF EQUATIONS AND PROCESSES

6. SPILL MODEL

In this section we examine the mechanism by which the various spill processes can be incorporated into a spill-behaviour model. It is envisaged that such a model could be coupled to a spill trajectory model although this may not be necessary or desirable. Work is currently underway to develop this behaviour model but, at the time of writing this report, it is not complete.

The first step is characterization of the oil. Using as input data, an ASTM isobaric distillation curve of the crude oil or product or, alternatively data from wind-tunnel pan evaporation experiments, a 10-component composition is devised (by trial and error) which gives the same volatility behaviour, density, viscosity and aqueous solubility. These properties can be calculated for the original oil and for the oil at any stage of evaporation. It would be useful to assemble these data graphically for the required temperature in the format of Figure 3.3. The evaporation-exposure function should be correlated with fraction volatiles remaining. It may also be desirable to correlate the other properties such as density, solubility and viscosity with the fraction volatiles remaining. This set of calculations may be fairly time consuming, thus for emergency purposes, it is highly desirable that they be done in advance with the results ready for immediate incorporation into a real-time program. Also required is the oil "mousse susceptibility constant" K_2.

Second, data on the ambient conditions are required as follows:

Temperature, wind speed, seastate and wave-breaking frequency. These data can be used to estimate values for the following quantities:

Evaporation mass-transfer coefficient (K in Chapter 3), emulsion formation rate constant (K_3 in Chapter 4), dispersion rate constants for wave-breaking and non wave-breaking conditions (Chapter 5).

In some conditions for water column concentration calculations, information will be required on the structure of the water column, such as depth to a bottom or a diffusion floor.

Third, data are required on the volumes and durations of the oil spill, for example:- 10 m^3 per hour for 2 days.

Fourth, it will be necessary to specify some computation variables such as time increment or frequency of printout.

The main program should be designed to accept these data then print them out for verification purposes. Also printed out should be all constants used in the program such as AK, BK and CK, the spreading parameters.

Discussion

The program as outlined above could possibly be rendered more efficient by altering the time increments as the computation proceeds. The process of dissolution from the oil slick is not included because it is believed to result in negligible mass loss from the spill. If it is desired to calculate under-slick oil concentrations, it may be desirable to include a dissolution calculation. The program has relatively modest computer capacity requirements since it does not store any substantial quantities of data. It should therefore be programmable on a mini-computer with say 16K capacity. There are a number of advantages to such an approach, including the possibility that the program could be run interactively, inserting wind or temperature changes as desired. This could have significant advantages in environmental emergency situations and for educational purposes such as spill response training programs.

With further development, it should also be possible to include in the program the capacity to remove oil (for example, by an oil recovery device) or to disperse it chemically at any desired rates. The implications of such remedial measures could thus be tested.

If the dispersion rate is made oil viscosity dependent, it should be possible to simulate the competitive processes of emulsion (mousse) formation and natural dispersion and predict which process will dominate.

The development of a program which could be coupled to this program and would be capable of generating water column oil concentrations is discussed in a separate report. Such a program is complex because of the poorly understood diffusive properties of the water column in both horizontal and vertical directions. An additional complication (and mitigating factor) is that wind-induced drift of the oil will tend to move the oil relative to the water column, thus causing enhanced dilution rates.

At the present stage of model development, it is believed that the best approach is to devise separate programs for (i) trajectory prediction or analysis in real time or for environmental impact assessment, (ii) oil spill behaviour models, as described here, and (iii) models capable of computing water column concentrations. In addition, there is also a role for site specific models, for example, for rivers or tidal regions with unique current behaviour.

7. CONCLUSIONS AND RECOMMENDATIONS

The work described here has resulted in the formulation of equations in finite difference form, suitable for inclusion in oil-spill models for the processes of spreading, evaporation, water-in-oil emulsion formation and dispersion. There remains a need to obtain further data on these processes to refine the equations and permit more accurate prediciton. Some specific suggestions follow.

Spreading

Area measurements from experimental and accidental spills should be compiled to refine the values of the three spreading constants. It seems likely that these constants depend on oil viscosity, interfacial tension and wind speed. These dependencies should be quantified. The prediction of slick shape may be useful in certain circumstances and should be explored, possibly as a simple expression of the major and minor ellipsoidal axes.

Evaporation and Property Change

Experimental verification of this approach for a series of crude oils and petroleum products is desirable, as is establishment of a tabulation of compositions yielding volatility and other properties of various oils and products. The inhibiting effect of emulsion formation on evaporation should be explored since it is presently not included in this approach. The relationship between weathered oil volatility and ignitability should be examined since this may elucidate the conditions under which oil may or may not be burned.

Emulsion Formation

Further verification of the water content-viscosity correlation would be useful, including the effect of temperature. The situation which prevails when the emulified water freezes is not understood and should be investigated. Values of the susceptibility factor K_2 should be sought for various oils and products and the chemical compounds responsible for stability should be identified with a view to relating K_2 to their concentration. Values for K_3 the formation rate constant are known only very approximately at present. The dependencies of K_3 on oil thickness, viscosity and on sea state should be elucidated.

Dispsersion

Considerable further experimental work is necessary to validate and calibrate the equations proposed here. Obvious approaches are to determine dispersion rates and resultant oil particle sizes for various oils under various turbulence conditons. This topic remains the most difficult and important gap in knowledge about oil spills.

Modelling

It is recommended that continuing efforts be devoted to developing separately (i) trajectory models, (ii) behaviour models and (iii) water column concentration models. Every opportunity should be used to attempt to verify these models in order to establish their accuracy and inadequacies.

REFERENCES

American Petroleum Institute Technical Data Book - Petroleum Refining, Washington, D.C. 2nd Ed. (1970).

Berridge, S.A., Thew, M.T. and Loriston-Clarke, A.G., Proc. Symp. on Scientific Aspects of Pollution of the Sea by Oil, Inst. Petrol, London (1969).

Blaikley, D.R., Dietzel, G.F.L., Glass, A.W., van Kleef, P.J., Proc. Joint Conf. on Prevention and Control of Oil Spills, New Orleans, Amer. Petrol. Inst., Washington, 45 (1977)

Blokker, P.C., Proc. 4th International Harbor Conf., Antwerp (1964).

Canevari, G.P., Proc. Joint Conf. on Prevention and Control of Oil Spills, New York, Amer. Petrol, Inst. (1969).

Cormack, J.A., and Nichols, J.A., "Investigation of Factors Affecting the Fate of North Sea OIls Discharged at Sea", Part I Ekofisk Crude Oil July 1975-February 1978, Report LR 273 (OP) (1978) and Part II The Ekofisk Blow-out, April-May 1977, Report LR 272 OP) (1978). Published by Warren Spring Laboratory, Herts., U.K.

Cormack, D., and Nichols, J.A., Proc. Joint Conf. on Prevention and Control of Oil Spills, New Orleans, Amer. Petrol. Inst., Washington, 381 (1977).

Einstein, A., Kolloid. Z 27, 137 (1920).

Fay, J.A., Proc. Joint Conf. on Prevention and Control of Oil Spills, Washington, D.C., publ. by Amer. Petrol. Inst., 463 (1971).

Goodwin, S.R., Mackay, D., and Shiu, W.Y., Can. J. Chem. Eng. 54 290 (1976).

Hollinger, J.P., "The Determination of Oil Slick Thickness by Means of Multi-frequency Passive Microwave Techniques", prepared for the U.S. Coast Guard, NTIS Report No. NRL Memorandum Report 2953 (1974).

Hoult, D.P., "Oil Spreading on the Sea", in Annual Review of Fluid Mechanics, Vol. 4, M. Van Dyke, W.G. Vincenti, and J.F. Wehausen (eds) 341 (1972).

J.B.F. Scientific Corp., "Physical and Chemical Behavior of Crude Oil Slicks on the Ocean", Pub. 4290. Publ. by Amer. Petrol. Inst., Washington, D.C. (1976).

Jeffrey, P.G., Proc. Joint Conf. on Prevention and Control of Oil Spills, Washington, D.C., Amer. Petrol. Inst., 469 (1973).

Jeffrey, P.G., and Acrivos, A., A.I.Ch.E.J., 22, 417 (1976).

Jinescu, V.V., Intern. Chem. Eng., 14, 397 (1974).

Leibovich, S., J. Petrol. Tech. 311, March (1977).

Leibovich, S., Ocean Engng. 3 29 (1975).

Leinonen, P.J., Ph.D. Thesis, Dept. of Chem. Eng. and Appl. Chem., Univ. of Toronto (1976).

Leinonen, P.J. and Mackay, D., "Mathematical Model of the Behaviour of Oil Spills on Water with Natural and Chemical Dispersion", prepared for Fisheries and Environment Canada and published as Economic and Technical Review Report No. EPS-3-EC-77-19 (1977).

Lin, J.T., Gad-el-Hak, M., Liu, H.-Ta., "A Study to Conduct Experiments Concerning Turbulent Dispersion of Oil Slicks", U.S. Dept. of Transportation, U.S. Coast Report No. CG-D-54-78 (1978).

Mackay, D., Charles, M.E., and Phillips, C.R., "The Physical Aspects of Crude Oil spills on Northern Terrain - Final Report", Pub. ALUR 74-75-84, Dept. of Indian and Northern Affairs (1975).

Mackay, D., and Matsugu, R.S., Can. J. Chem. Eng. 51, 434 (1973).

Mackay, D., Nadeau, S., and Ng, C., "A Small Scale Laboratory Dispersant Effectiveness Test" presented at the ASTM Meeting, and accepted for publication in the Proceedings (1977).

Mackay, D., and Shiu, W.Y., J. Chem. Eng. Data 22, 4, 399 (1977).

Mackay, D., and Shiu, W.Y., Can. J. Chem. Eng. 53, 239 (1975).

Mackay, G.D.M., "Emulsions of Water in Crude Oils" paper presented at 77th General Meeting, Canadian Inst. of Mining and Metallurgy, Toronto (1975).

Mackay, G.D.M., MacLean, A.Y., Betancourt, O.J. and Johnson, B.D., J. Inst. Petrol. 59, 164 (1973).

May, W.E., Wasik, S.P., and Freeman, D.H., Anal. Chem., 50, 997 (1978)

Milgram, J.H., Donnelly, R.G., Van Houten, R.J., Camperman, J.M., Unpublished report to the U.S. Coast Guard (Personal Communication from R. Griffiths, USCG) (1978).

Mooney, M., J. Colloid. Sci., 6, 162 (1951).

Mooney, M., and Hermonat, W., J. Colloid Sci., 10, 121 (1955).

Nadeau, J.S., and Mackay, D., "Evaporation Rates of Complex Hydrocarbon Mixtures under Environmental Conditions", a Report prepared for and published by Environmental Protection Department of Imperial Oil Limited.

Nelson, W.L., Petroleum Refinery Engineering, McGraw-Hill, New York (1958).

Oren, J.J., and Mackay, G.D.M., Inst. Petrol. Pub. No. 1P76-005 London (1976).

Raj, P.P.K., "Theoretical Study to Determine the Sea State Limit for the Survival of Oil Slicks on the Ocean", U.S. Dept. of Transportation, USCG Report No. CG-D-90-77 (1977)

Reed, R., Sherwood, T.K., and Prausnitz, J.M., "The Properties of Gases and Liquids", 3rd Ed. McGraw-Hill, New York (1977).

Rutgers, R., Reolog. Acta, 2, 305 (1962).

Stolzenbach, K.D., Madsen, O.S., Adams, E.E., Pollack, A.M., and Cooper, C.K., "A Review and Evaluation of Basic Techniques for Predicting the Behavior of Surface Oil Slicks", Ralph M. Parsons Laboratory for Water Resources and Hydrodynamics, Report No. 222, NOAA, U.S. Dept of Commerce.

Thomas, D.G., J. Colloid. Sci., 20, 267 (1965).

Wood, B., M.A.Sc. Thesis Dept. of Chem. Eng. and Appl. Chem., Univ. of Toronto, (1971).

Yang, W.C., and Wang, H., Water Research, 11, 879 (1977).

Zwolinski, B.J., and Wilhoit, R.C., "Handbook of Vapor Pressures and Heats of Vaporization of Hydrocarbons and Related Compounds", API44-TRC Publ. in Science and Engin., Pub. No. 101 (1971).

Mackay, D., and Shiu, W.Y., Bull. Environ. Contam. and Toxicol., 15, 101 (1975).